Experimental research on wall-hollow core slab connections

Requested by: Suomen Betonitieto Oy

| Requested by	Suomen Betonitieto Oy PL 11 00131 Helsinki
Order	26.2.2003 Arto Suikka
Contact person at VTT	Matti Pajari VTT BUILDING AND TRANSPORT Puumiehenkuja 2 A, Espoo P.O.Box 1806 FIN–02044 VTT, Finland Tel. + 358 9 456 6677 Fax + 358 9 456 7027 Http://www.vtt.fi/rte/

Task   **Experimental research on wall-hollow core slab connections**

1 BACKGROUND

When multi-storey concrete buildings are made of bearing wall elements and prestressed hollow core slabs, the ends of the slab elements, together with the jointing concrete or mortar, transfer the loads from the upper wall element to the lower one. Simultaneously, the slab ends are subjected to a negative bending moment until they crack. To avoid unfavourable cracking modes of the slab end, different types of connection have been proposed and used in different countries.

Recent tests [1] have shown that when the wall elements are heavily loaded, the clamping effect is so strong that the slab ends tend to crack vertically outside the wall, see Fig. 1.
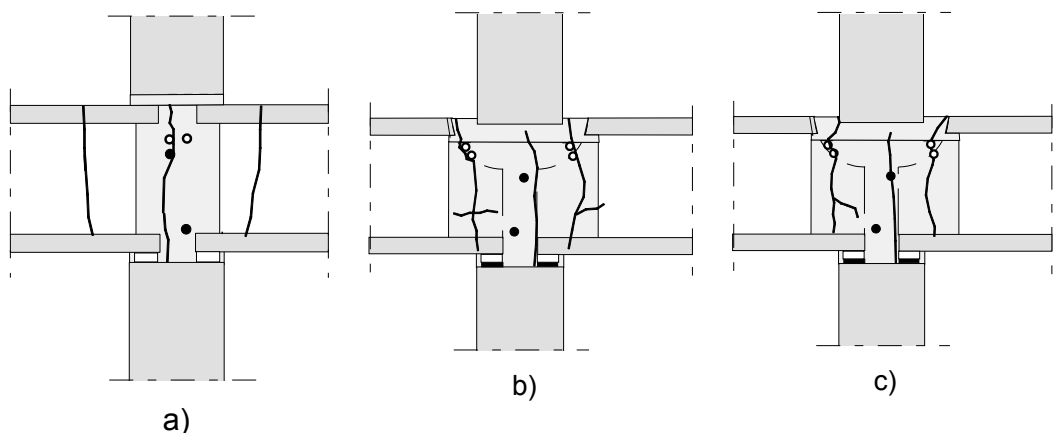
Fig. 1. Cracking pattern in the connection before failure [1].

Due to the lack of shear reinforcement in the slabs this may mean a considerable reduction in the shear resistance. In the previous tests [1] the load on the wall was increased until the connection between the upper and lower wall element failed. The slabs were also loaded, but because they did not fail, only a lower limit for their shear resistance was obtained. Therefore, a new test series was planned to clarify the shear resistance of the slabs when the wall load is kept at a constant, high level.

2 TEST ARRANGEMENTS

2.1 Principles in test planning

Six load tests were performed, see Fig. 2. Three tests (B1, B2 and B3) simulated a Finnish BES connection, three tests (N1, N2 and N3) a connection with notched slab ends. The latter connection type is widely used in Sweden.

In this report, the grouted and vertically compressed slab end is called clamped end, the opposite end is called simply supported.
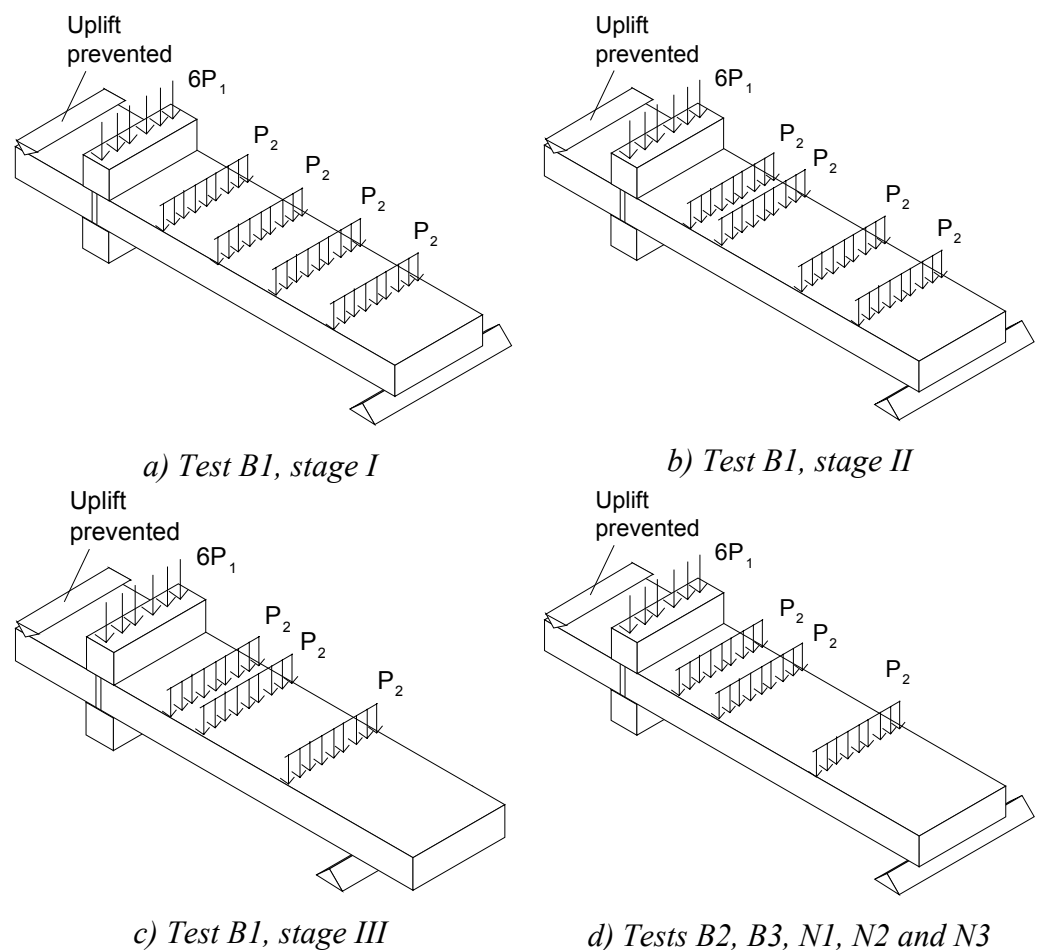

a) Test B1, stage I

b) Test B1, stage II

c) Test B1, stage III

d) Tests B2, B3, N1, N2 and N3

Fig. 2. Overview on test layout. P_1 is kepth constant ($6P_1$ = 1.6 MN) while P_2 is increased until failure.

In Fig. 2.a the planned loading arrangements are illustrated. However, in the first test B1 the simply supported end of the slab failed, first locally, and then, after rearrangement of the loads as shown in Fig. 2.b, globally. Therefore, a third test layout illustrated in Fig. 2.c was used to make the slab fail at the clamped end. The loads for the remaining five tests are shown in Fig. 2.d.

The loads on the slabs were distributed along the span in order to create a typical rotation at the slab end and to simulate realistic cracking at the connection.

2.2 Test specimens, loads and measurements in load tests

In all figures of this report the measures are given in millimetres unless otherwise specified.

Each test specimen was made of one short (1.0 m) and one long (8.0 m) prestressed hollow core slab element extruded by Parma Oy in Forssa factory. All elements were taken from the same bed and same casting lot. The joints of the slab elements were reinforced and the elements were grouted together in laboratory. The slab elements were 320 mm in depth. They were provided with four hollow cores and 11 12.5 mm strands (A_p = 93 mm^2/strand, 0.2% yield limit = 1630 MPa, nominal values given by the manufacturer of the slabs). They were cast on 7th of March 2003 and delivered to VTT on week 11. The nominal and measured cross-sectional data of the slabs as well as data about strands are given in Appendices D and G, respectively.

The notches in slabs in tests N1 – N3 were made before hardening of the concrete using a special screw. For the planned and actual notches, see App. A, Fig. 1 and App. B, Fig. 1, respectively.

In N-tests the upper wall element was simulated by a concrete beam, in B-tests by a a steel beam. The steel beam in the latter tests was justified by the fact that the slab end would in any case crack vertically due to the negative bending moment, see the previous results [1], and after the cracking the material or design of the upper structure would not affect the shear resistance of the slab.

In all tests the lower wall was simulated by a rigid steel body onto which the test specimen, provided with a steel plate below the connection, was placed. This simplification was also justified by the previous tests [1] in which the first cracks in the lower wall appeared at a considerably higher wall load than that applied in the present teststs (=1.6 MN).

The concrete beams were cast on 10 – 12th and delivered to VTT on 25th of March 2003. Their design is depicted in Fig. 16.

A concrete collar simulating the joint concrete and incorporating the tie reinforcement was cast around the clamped end of the test specimen.

The design of the test specimens and location of loads are shown in Figs 3 – 15. The arrangements in different stages of assembling, loading and demolition

are also illustrated in photographs of Appendices A and B. The reinforcing steel was of type A500HW with nominal strength 500 MPa.
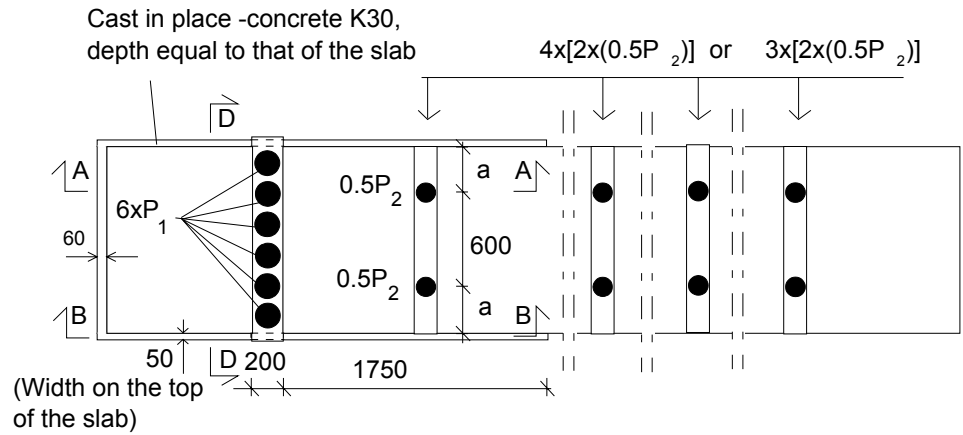

Fig. 3. Plan view on loading arrangements and cast-in-situ collar outside the slab elements. Sections A – A, B - B and D – D are presented in Figs 8, 9, 11, 12, 14 and 15.
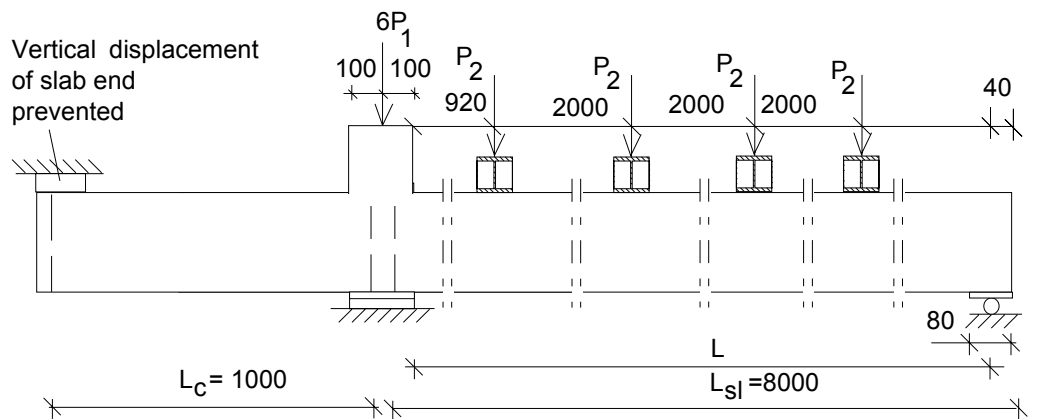

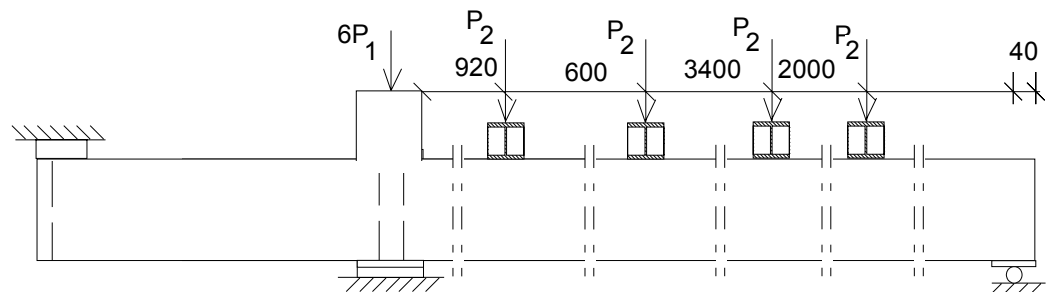*Fig. 4. Location of loads in test B1.I. See also Fig. 3.*

Fig. 5. Location of loads in test B1.II. See also Fig. 3.

Fig. 6. Location of loads in test B1.III. See also Fig. 3.

Fig. 7. Location of loads in tests B2, B3, N1, N2 and N3. See also Fig. 3.

Fig. 8. Tests B1 … B3. Arrangements at clamped end, section A – A, see Fig. 3. For the steel beam above the connection see Fig. 10.
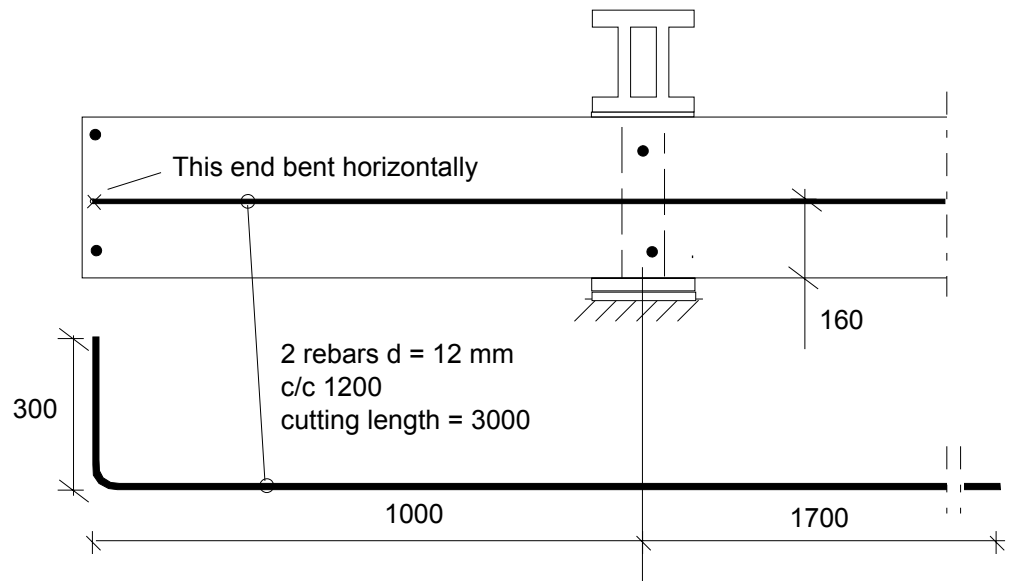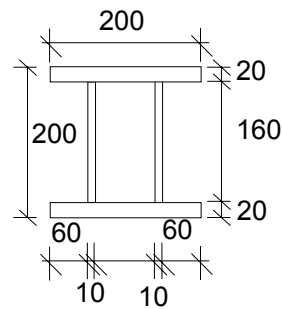
Fig. 9. Tests B1 ... B3. Arrangements at support, section B – B, see Fig. 3.

Fig. 10. Steel beam simulating upper wall in tests B1, B2 and B3. Weight of the beam was 1.7 kN and length 2.0 m.
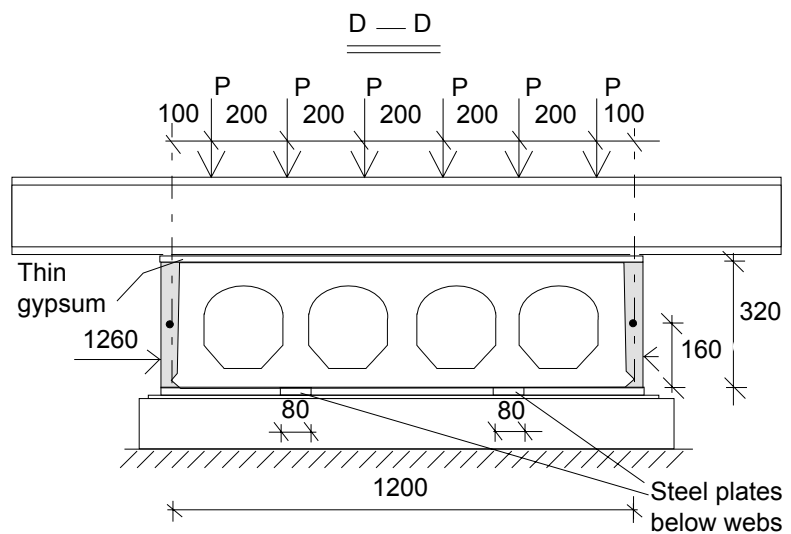

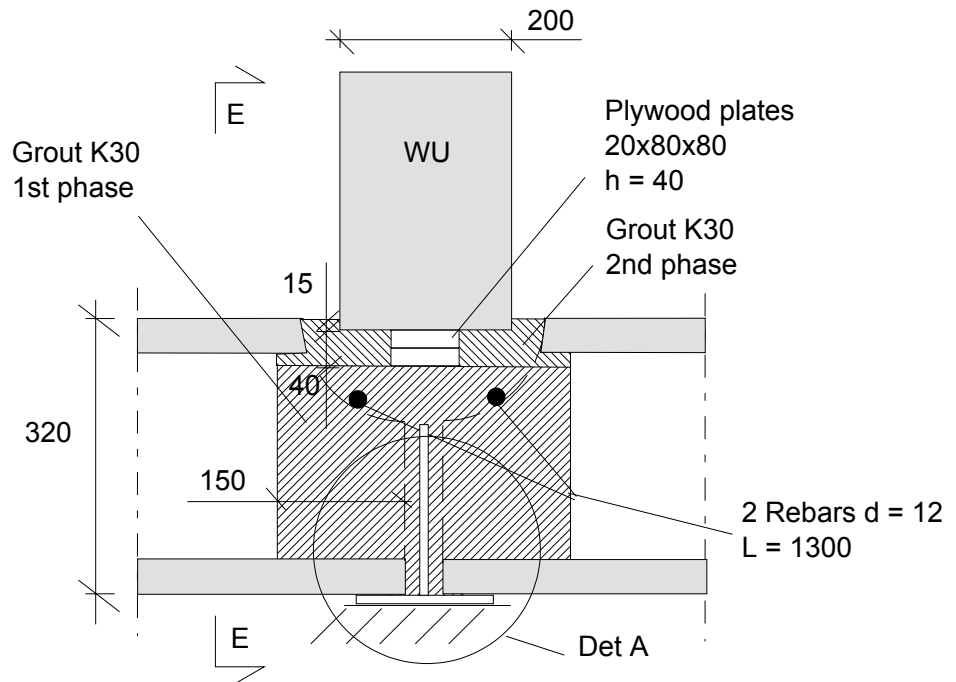*Fig. 11. Tests B1 ... B3. Arrangements at support, section D – D, see Fig. 3.*

Fig. 12. Tests N1 ... N3. Arrangements at support, section A – A, see Fig. 3. For element WU see Fig. 16.
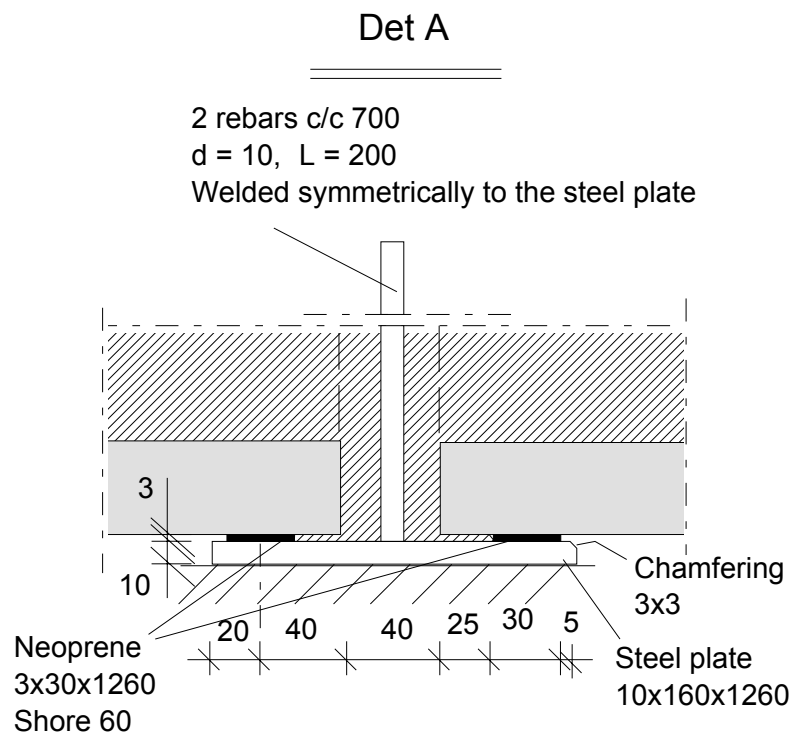
Det A

Fig. 13. Tests N1 ... N3. Arrangements at support, Det A, see Fig. 12. The steel plate is only 160 mm wide in order to prevent direct contact with the soffit of the slab when the slab end is rotated.
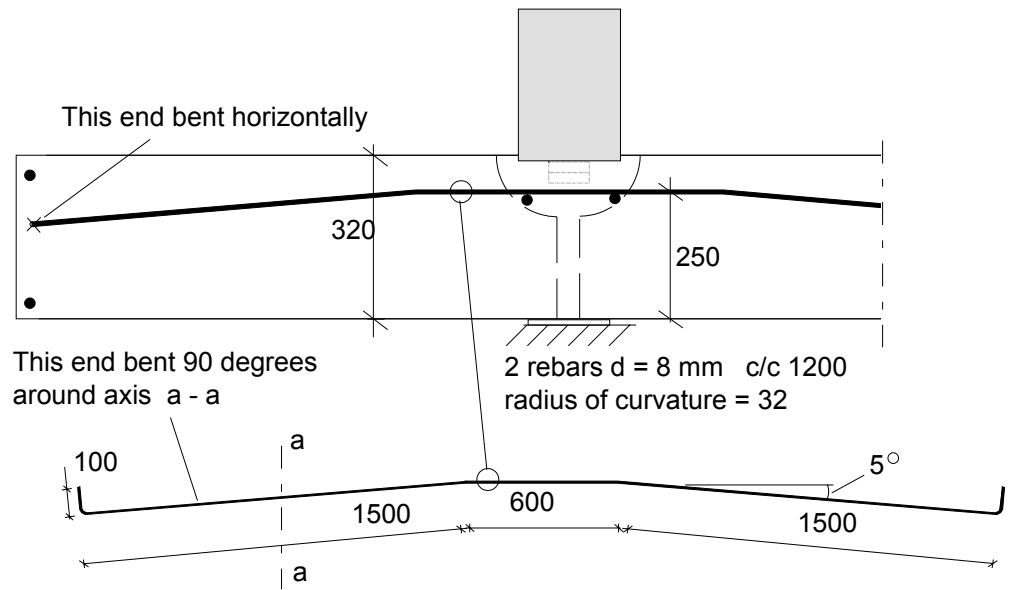
This end bent horizontally

320

250

This end bent 90 degrees
around axis a - a

2 rebars d = 8 mm   c/c 1200
radius of curvature = 32

100

a

5°

1500

600

1500

a

Fig. 14. Tests N1 ... N3. Arrangements at support, section B – B, see Fig. 3.

D — D

P   P   P   P   P   P
100 | 200 | 200 | 200 | 200 | 200 | 100
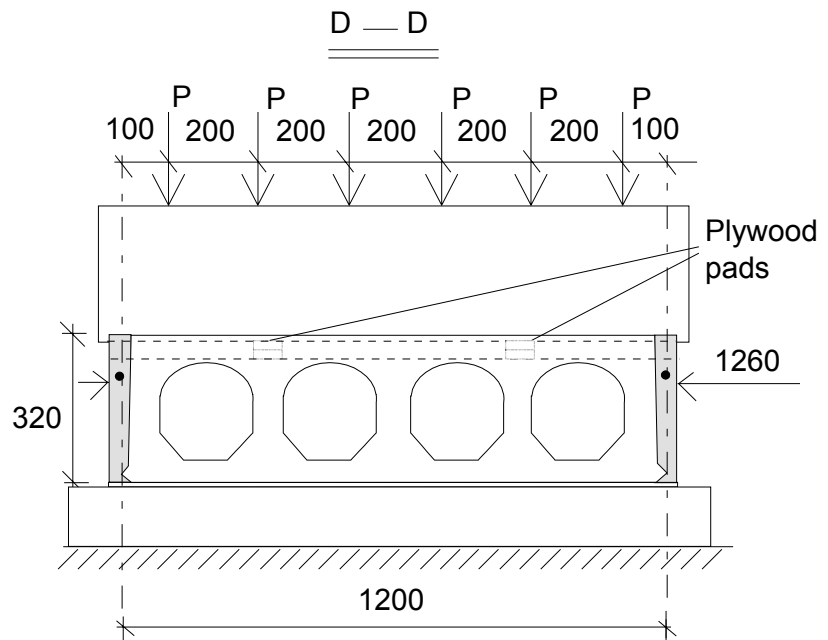
Plywood
pads

1260

320

1200

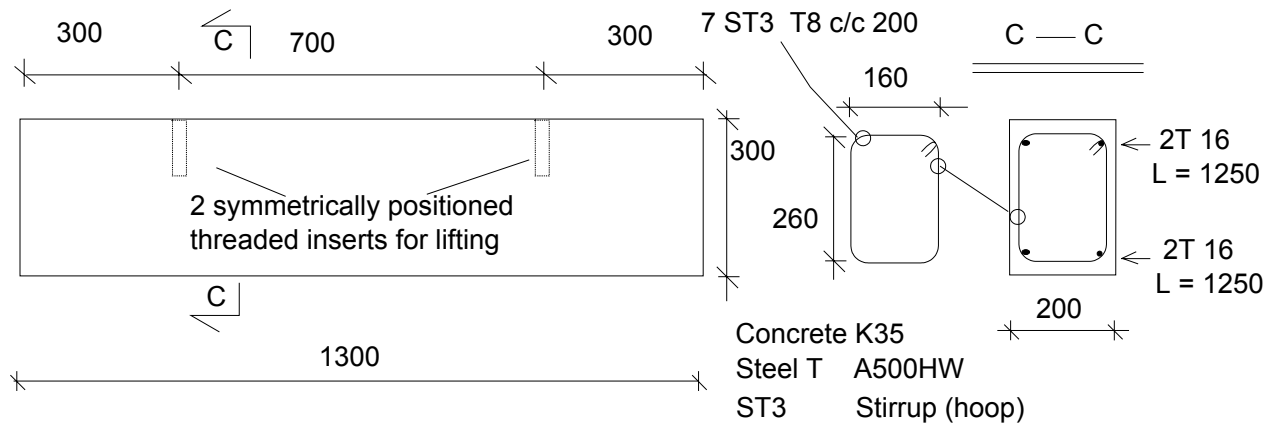*Fig. 15. Tests N1 ... N3. Arrangements at support, section D – D, see Fig. 3.*

Fig. 16. Upper beams WU in tests N1, N2 and N3, see Fig. 12. T x refers to a reinforcing bar with diameter = x.

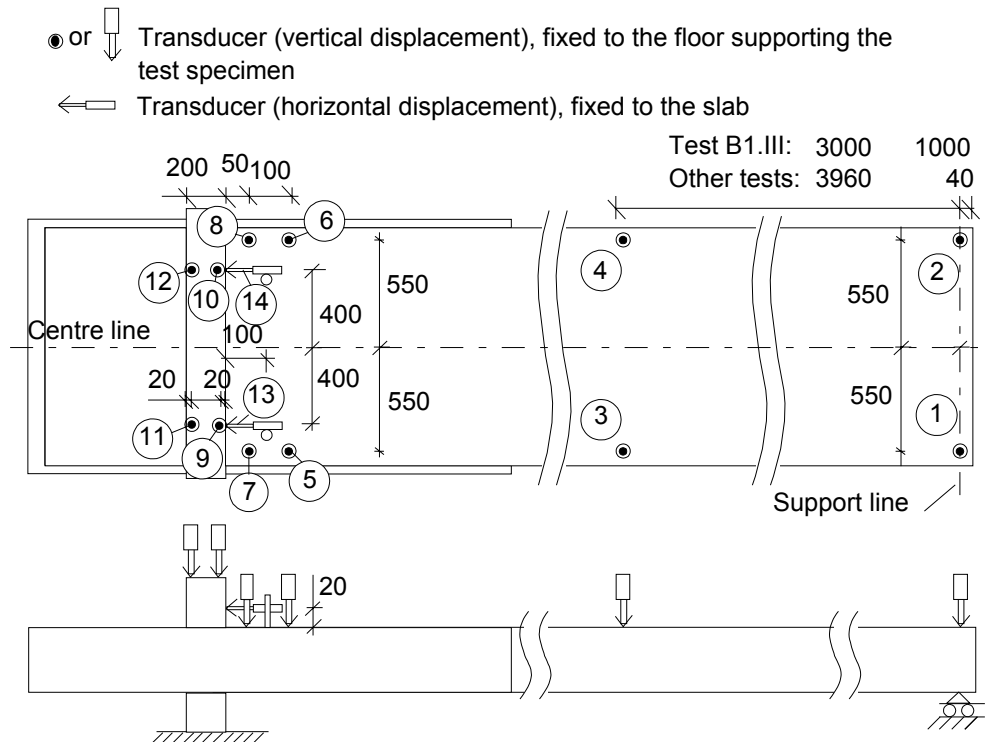Location of transducers for measuring displacements is shown in Fig. 17.

Fig. 17. Location of transducers 1 – 14 (not in scale) for measuring displacements. Plan and elevation.

In test B1.I the actuators were vertical when the loading was started. In other tests the actuators were slightly inclined before loading, see App. F. The aim was to stabilize the assembly of spreader beams on the deflecting slab.

The inclination of actuators in tests B2, B3, N1, N2 and N3 is illustrated in Fig. 18. Since there are two forces pushing the slab to the left and only one to the right, there is a compressive horizontal force H in the slab between the connection and the first load $P_{2,1}$. H is reduced by the deflection of the slab,

because the slab moves to the right and because the lower end of two actuators out of three act on a point (point A in Fig. 18) which moves to the right due to the curvature of the slab.
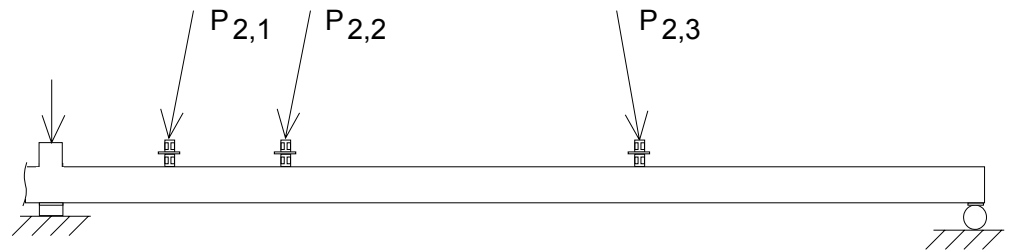

Fig. 18. Inclined loads in tests B2, B3, N1, N2 and N3.

At failure, the sum of the horizontal forces affecting the connection was less than 1.0 kN, as shown in App. F. Such a compressive force is 0.8% and 1.9% of the nominal yield force of tie reinforcement in tests B1 - B3 and N1 - N3, respectively. It has a negligible effect on the observed shear resistance.

3 MEASUREMENTS BEFORE LOAD TESTS

The length, weight, cross-sectional geometry and slippage of the strands were measured before assembling the test specimens. The results are given in App. D.

Two tensile tests on the tie bars, i.e. the reinforcing bars specified in Figs 9 and 14, one on each bar thickness, were carried out to determine the mechanical properties of the steel. The results are given in App. D.

The strands were made of seven indented wires. Their measured geometrical properties are given in Appendix F.

All measured properties were typical of normal production.

4 RESULTS OF LOAD TESTS

4.1 Loading strategy

At first the load on the connection was increased to $6P_1 = 1.6$ MN. This load level was maintained throughout the test. Thereafter, the loads P_2 on the slab were increased to a value of $P_2 = P_{2,c}$ which exceeded the load that made the slab end crack due to the negative moment at the support. Thereafter the loads P_2 were reduced to 0. The load cycle $\approx 0 \rightarrow P_{2,c} \rightarrow \approx 0$ was repeated for two more times. Finally the loads P_2 were gradually increased until failure.

4.2 Total loads vs. actuator loads

The total vertical load F_1 on the connection is obtained from

$F_1 = 6P_1 +$ weight of upper wall + weight of loading equipment

$= 6P_1 + 1.7$ kN $+ 3.6$ kN $= + 6P_1 + 5.3$ kN   in test B1, B2 and B3,

$= 6P_1 + 2.0$ kN $+ 3.6$ kN $= + 6P_1 + 5.6$ kN in tests N1, N2 and N3

and the total line load F_2 on a slab from

$F_2 = P_2 +$ weight of loading equipment

$= P_2 + 0.6$ kN

where P_1 and P_2 are the measured actuator forces.

4.3 Observed failure mode and shear resistance

The observations made during the tests are given in Tables 1 and 2. Photographs in Appendices A and B give more detailed information about the cracking and failure modes. It should be noted that the loading arrangements in tests B2, B3, N1, N2 and N3 were the same but differed in tests B1.I, B1.II and B1.III from each other and from the other five tests. For this reason, V, i.e. the shear force next to the support is used as a load parameter instead of P_2.

When calculating the shear forces from the loads, the bending moment due to the tie reinforcement has been ignored. In the ultimate shear force the error due to this approximation is of the order of -0.7 and -0.5% ($-2.1 \ldots - 1.5$ kN) in B-tests and N-tests, respectively. In other words, the error is negligible and ignoring it is on the safe side.

Table 1. Observations made during test B1. V is the shear force at the connectioned slab end due to self weight and imposed load including the weight of the loading equipment.

	$P2$ kN	V kN	
B1.I	24.5	70	First flexural crack next to the connection
	62.4	146	First flexural cracks in the span
	90.2	201	Outermost web at the simpy supported end failed in shear. Deflection of slab large, actuators so much inclined that stability of the spreader beams could not be guaranteed, 90% of the flexural resistance in use.
B1.II	0	21	The second line load was moved 1.4 m closer to the connection.
	105	250	The simply supported slab end failed and fell roughly 3 – 5 cm down onto a temporary support. The strength of the connection at the opposite end may have been reduced due to this impact.
B1.III	0	19	The simply supported slab end was lifted, the support moved below the outermost load and the loading was continued with three line loads.
	109	222	Shear tension failure of the slab close to the connection

Table 2. Load at first cracking due to negative bending moment ($P_{2,cr,connection}$), load at first flexural cracking in the span ($P_{2,cr,span}$), failure load ($P_{2,u}$), shear force next to the connection at failure (V_u) and failure mode.

Test	$P_{2,cr,connection}$ kN	$P_{2,cr,span}$ kN	$P_{2,u}$ kN	V_u kN	Failure mode
B1.III				222[1]	Shear tension failure
B2	20 - 25[2]	95	140.2	302	Shear tension failure
B3	30	95	145.1	312	Shear tension failure
N1	19	90	135.2	292	Shear tension failure (shear-anchorage failure)
N2	18	86	138.1	298	Shear compression or anchorage failure
N3	19	86	137.3	296	Shear compression or anchorage failure, rupture in tie bar on North side next to connection

[1] Resistance reduced by the failure at the opposite end of the slab
[2] First crack at 10 kN, but this crack did not make the slab end rotate

The observed failure modes next to the connection are illustrated in Fig. 19. The observed shear resistance as well as the contribution of different loads to the ultimate shear force are given in Table 3. The observed shear resistance is of the same order as or higher than that observed in shear tests on similar simply supported slabs without cast-in-situ concrete. It seems that in the present tests the cast-in-situ concrete fully compensated for the negative effects of the unfavourable cracking at the slab end.

The failure of the simply supported slab end in tests B1.I and B1.II is discussed later together with the results of reference tests.

A lower limit of 250 kN for the shear resistance of test specimen B1 was obtained in test B1.II. The shear resistance 222 kN observed in test B1.III does not represent the real resistance because the slab was subjected to a heavy impact caused by the abrupt failure of the simply supported slab end in test B1.II. When this brittle and sudden shear tension failure took place, the simply supported end fell suddenly to a support lying approximately 3 - 5 cm below the soffit of the slab. This impact obviously reduced the resistance of the opposite end. Otherwise it is difficult to explain the low shear resistance, lower than that in test B1. For this reason, the resistance observed in test B1.III is rejected from further considerations.
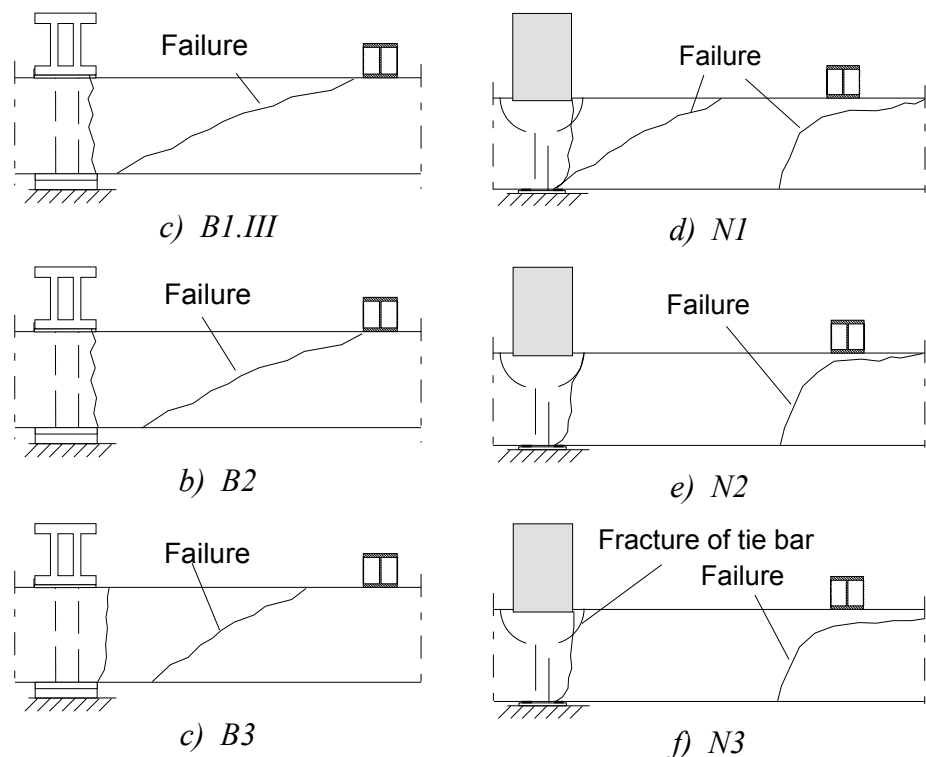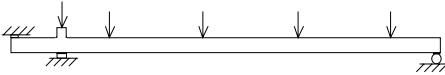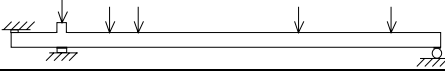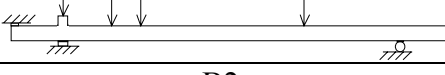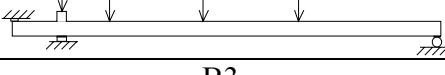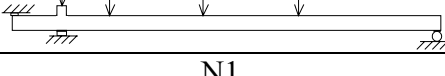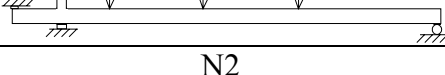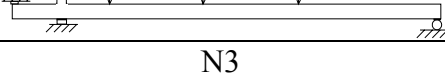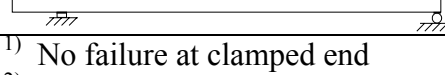

Fig. 19. Main flexural crack due to negative bending moment and failure crack(s).

Table 3. Shear force at failure next to support due to actuator force ($V_{p,u}$), loading equipment ($V_{p,eq}$), self weight of slab ($V_{p,g}$) and all loads(V_u) as well as shear force at the simply supported end due to all loads ($V_{u,end2}$).

	$V_{p,u}$ kN	$V_{p,eq}$ kN	$V_{p,g}$ kN	V_u kN	$V_{u,end2}$ kN
B1.I	180.4	1.2	19.8	201[1]	201[2]
B1.II	229.2	1.3	19.8	250[1]	212[3]
B1.III	203.2	1.2	17.9	222	
B2	281.3	1.2	19.8	302	
B3	291.1	1.2	19.8	312	
N1	271.1	1.2	19.9	292	
N2	276.9	1.2	19.6	298	
N3	275.3	1.2	19.7	296	

[1] No failure at clamped end
[2] Failure of one web at simply supported end
[3] Failure at simply supported end

4.4 Load-time and load-displacement relationship

The measured load-time and load-displacement relationships are depicted in Figs 20 - 65. V_p, the shear force due to the actuator loads P_2, is used as the load parameter.
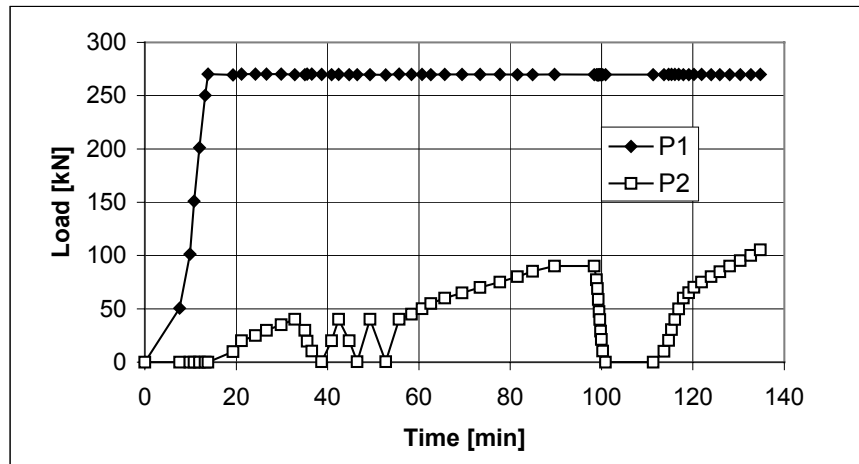
4.4.1 B1

Fig. 20. Load – time relationship in tests B1.I and B1.II.
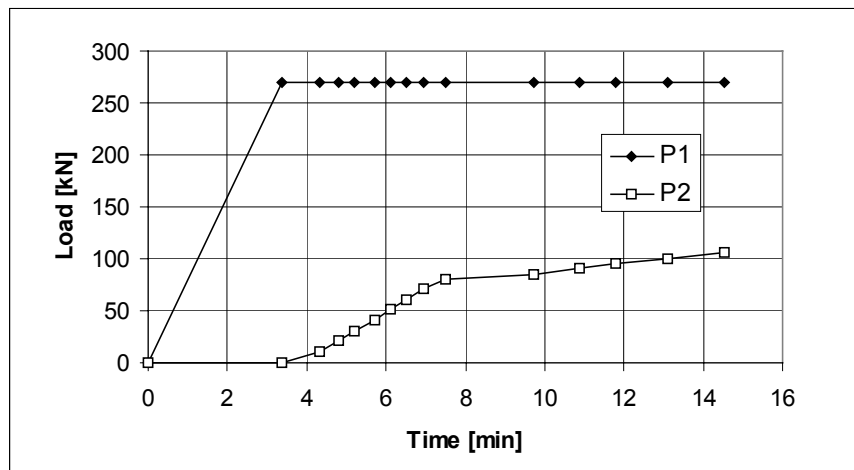

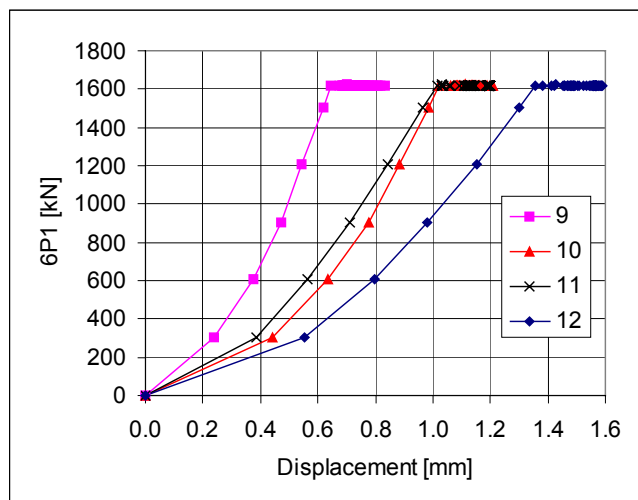*Fig. 21. Load – time relationship in test B1.III.*

Fig. 22. Vertical displacement of connection measured by transducers 9 – 12 in tests B1.I and B1.II.
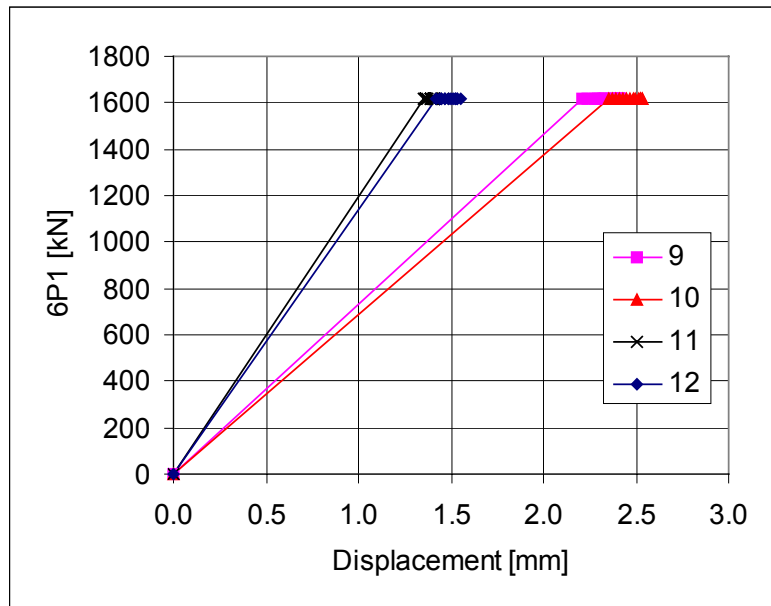
Fig. 23. Vertical displacement of connection measured by transducers 9 – 12 in test B1.III.
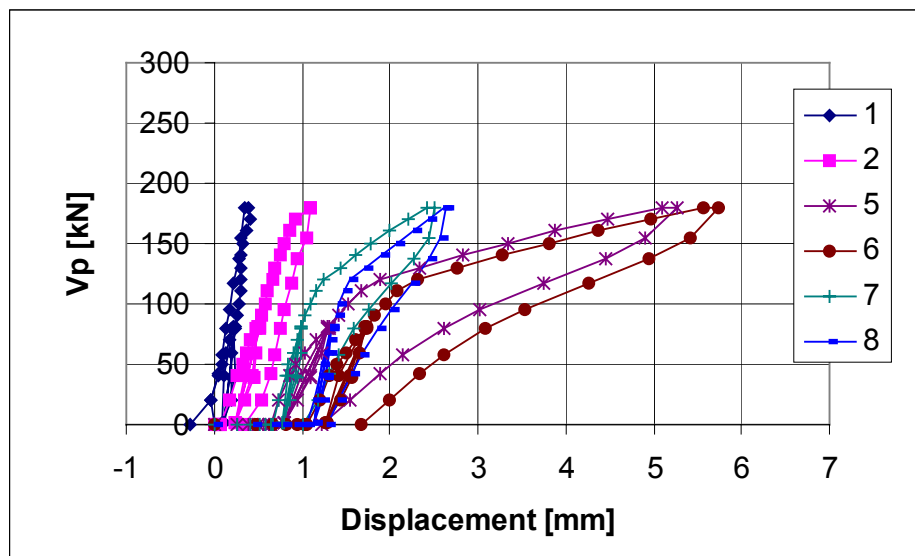

Fig. 24. Vertical displacement of slab measured by transducers 1 – 2 and 5 – 8 in test B1.I.
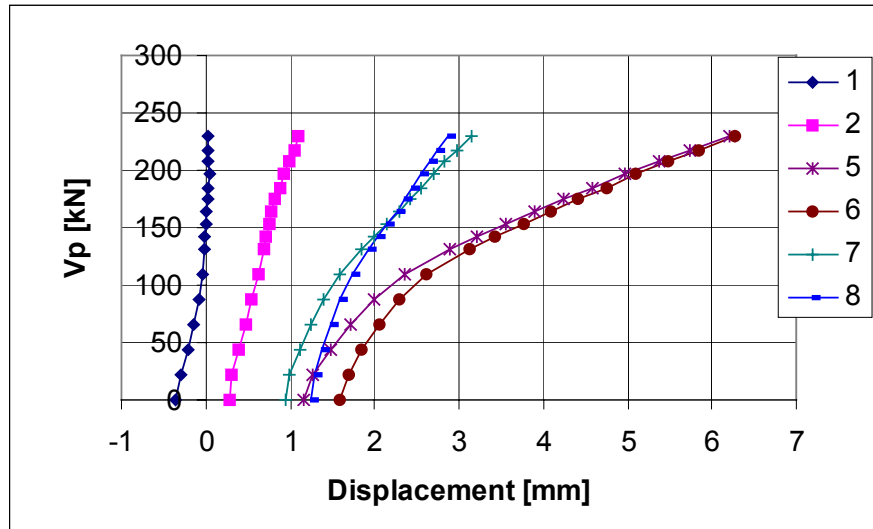
Fig. 25. Vertical displacement of slab measured by transducers 1 – 2 and 5 – 8 in test B1.II.

Fig. 26. Vertical displacement of slab measured by transducers 1 – 2 and 5 – 8 in test B1.III.

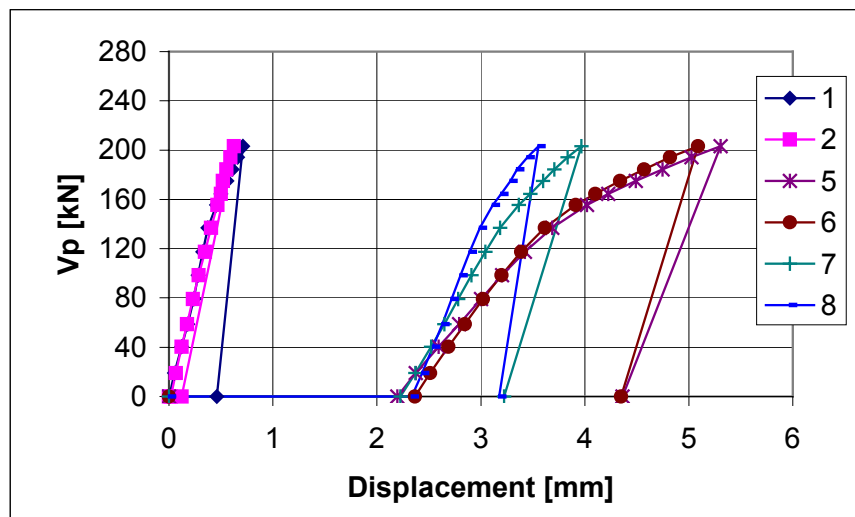*Fig. 27. Vertical displacement of mid-slab measured by transducers 3 and 4 in test B1.I.*

Fig. 28. Vertical displacement of mid-slab measured by transducers 3 and 4 in test B1.II.

Fig. 29. Vertical displacement of mid-slab measured by transducers 3 and 4 in test B1.III.

Fig. 30. Width of flexural crack at slab end next to the connection measured by transducers 13 and 14 in test B1.I.

Fig. 31. Width of flexural crack at slab end next to the connection measured by transducers 13 and 14 in test B1.II.

Fig. 32. Width of flexural crack at slab end next to the connection measured by transducers 13 and 14 in test B1.III.

Fig. 33. Rotation of slab end next to the connection, calculated from displacements measured by transducers 5 - 8 in test B1.I.

Fig. 34. Rotation of slab end next to the connection, calculated from displacements measured by transducers 5 - 8 in test B1.II.

Fig. 35. Rotation of slab end next to the connection, calculated from displacements measured by transducers 5 - 8 in test B1.III.

4.4.2 B2

Fig. 36. Load – time relationship in test B2.

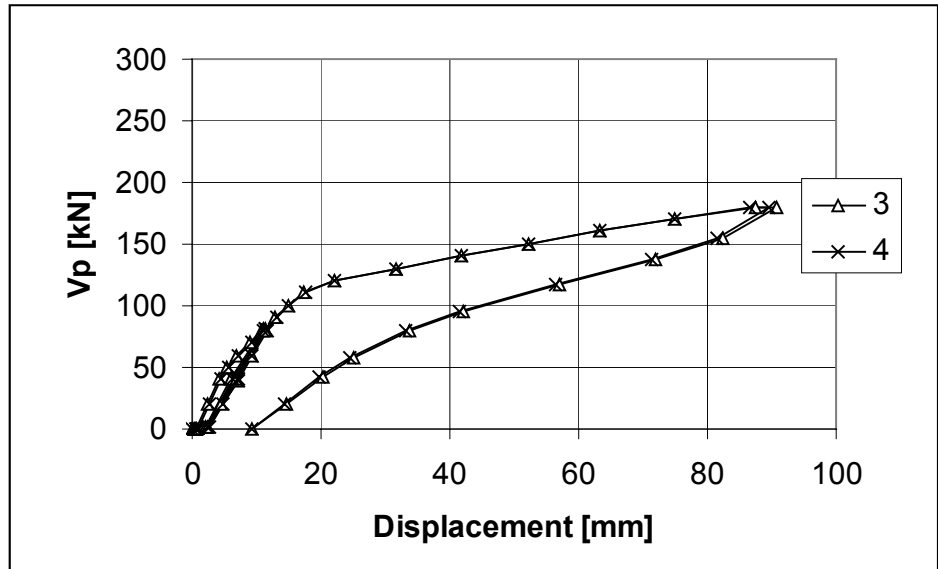*Fig. 37. Vertical displacement of connection measured by transducers 9 – 12 in test B2.*

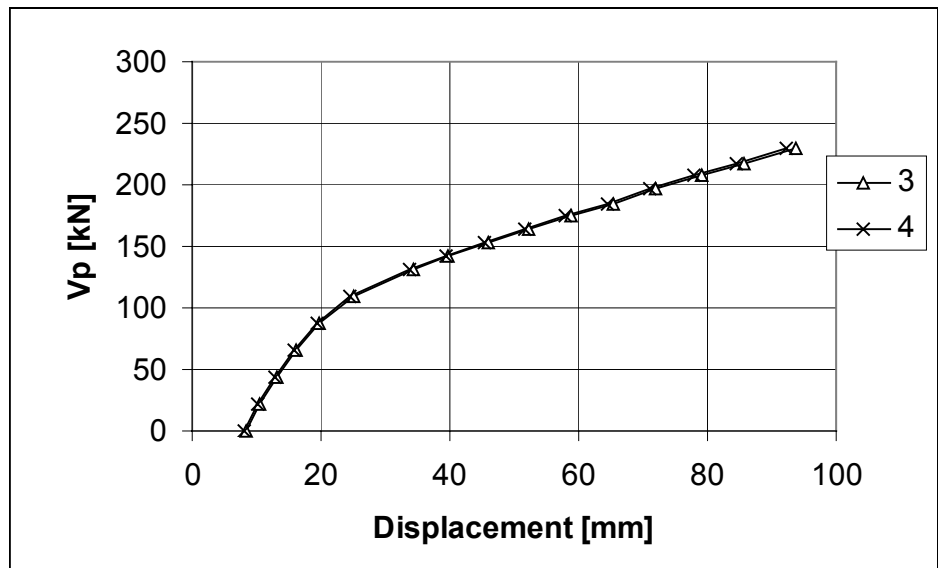*Fig. 38. Vertical displacement of mid-slab measured by transducers 3 and 4 in test B2.*
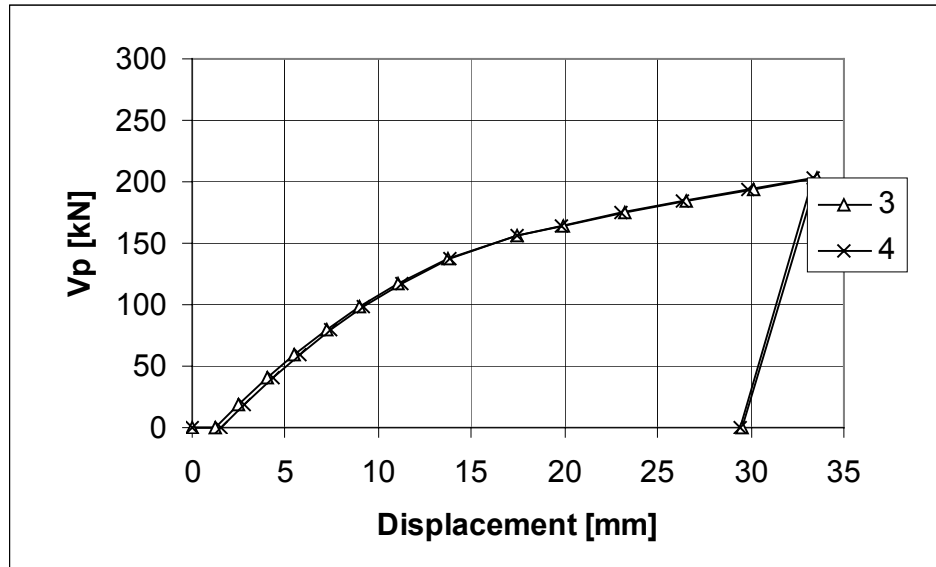
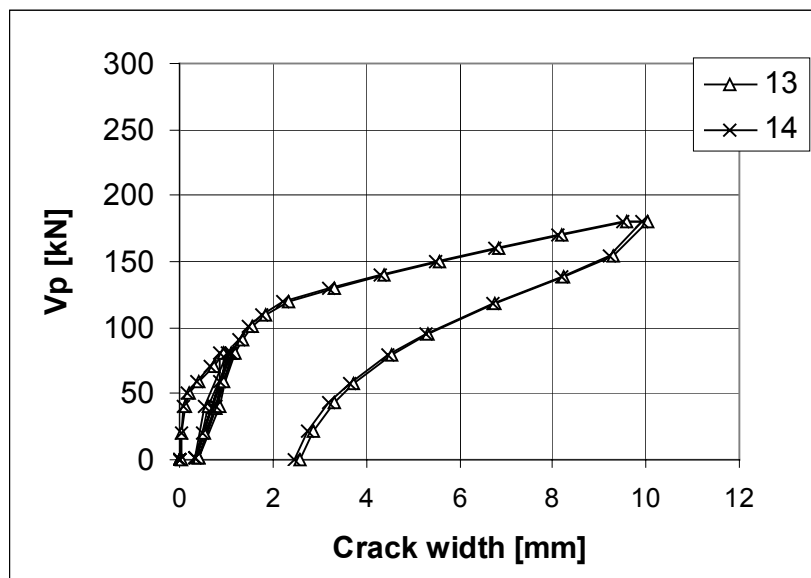*Fig. 39. Vertical displacement of slab measured by transducers 1 – 2 and 5 – 8 in test B2.*

Fig. 40. Width of flexural crack at slab end next to the connection measured by transducers 13 and 14 in test B2.

Fig. 41. Rotation of slab end next to the connection, calculated from displacements measured by transducers 5 - 8 in test B2.

4.4.3 B3
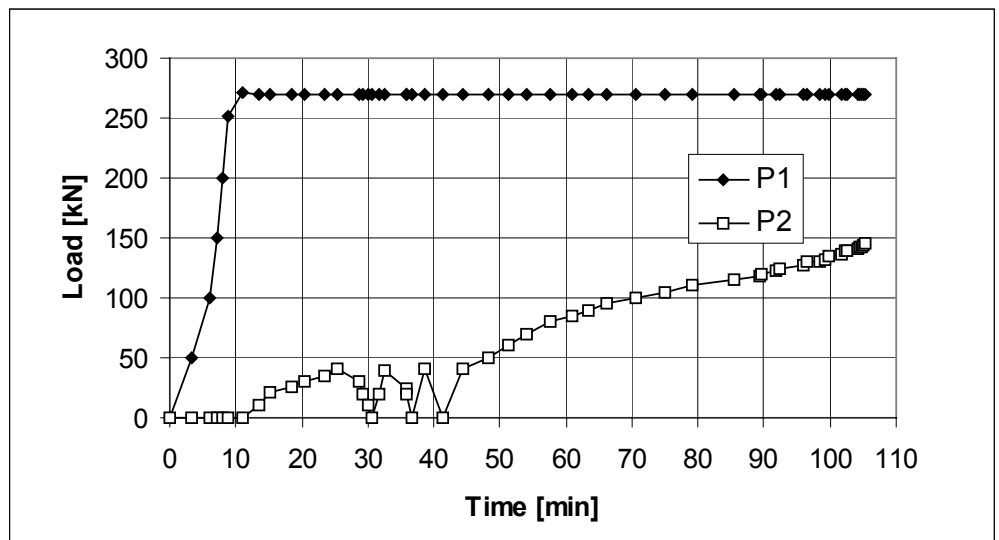
Fig. 42. Load – time relationship in test B3.
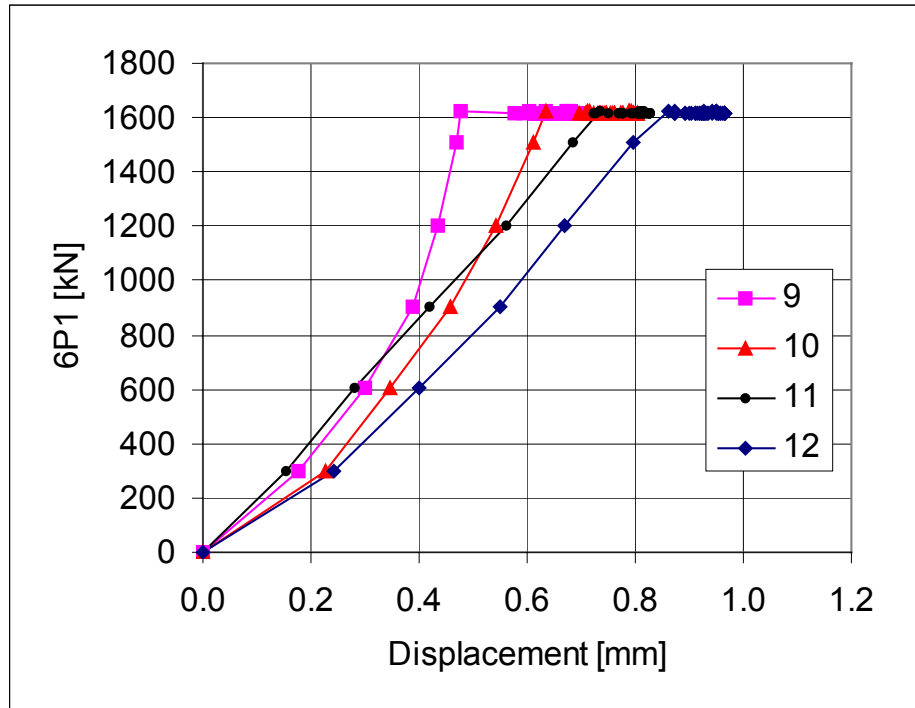
Fig. 43. Vertical displacement of connection measured by transducers 9 – 12 in test B3.
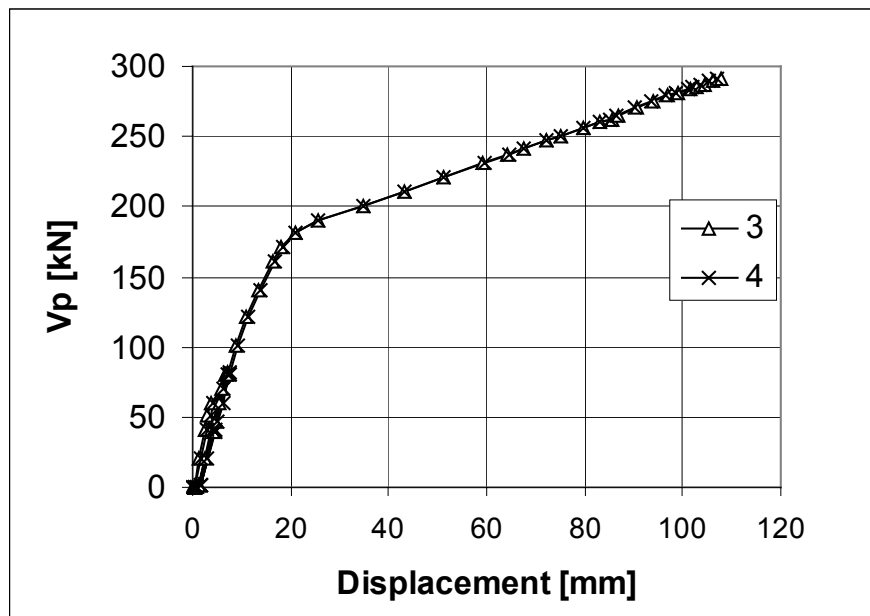
Fig. 44. Vertical displacement of mid-slab measured by transducers 3 and 4 in test B3.
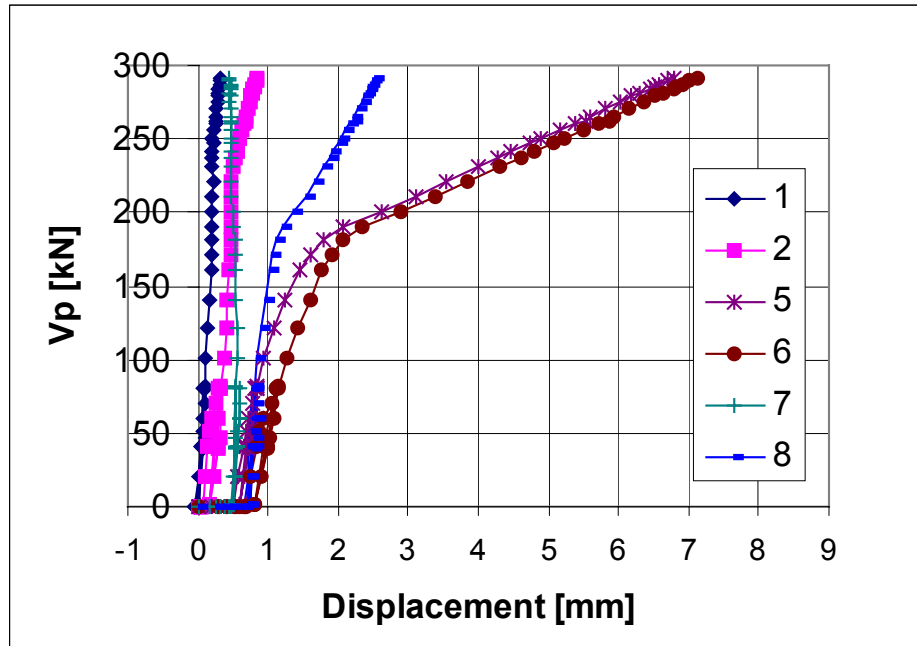
Fig. 45. Vertical displacement of slab measured by transducers 1 – 2 and 5 – 8 in test B3.
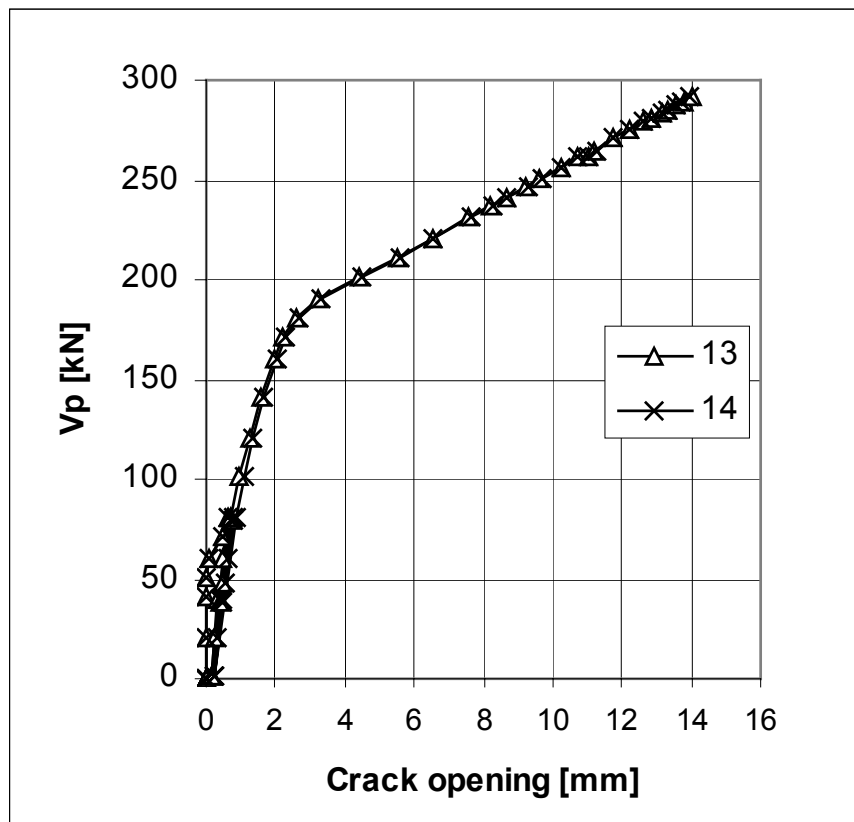
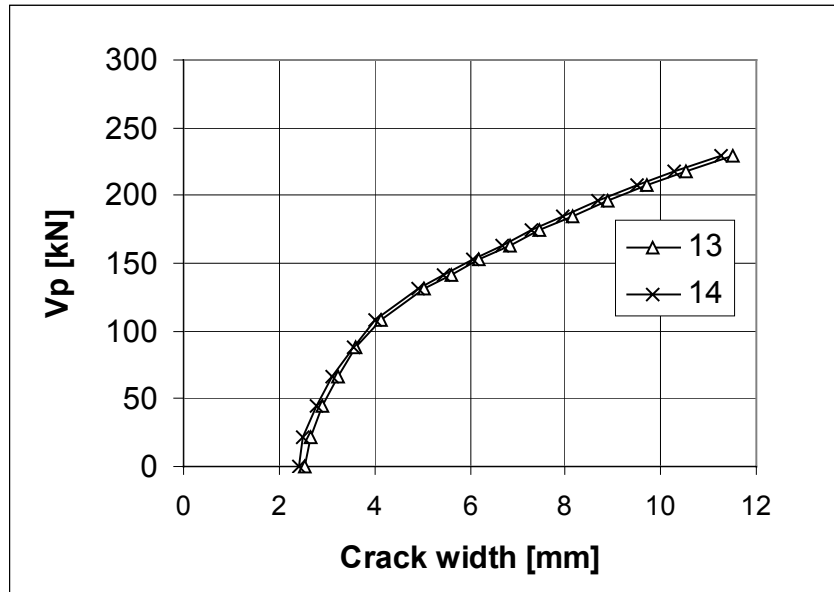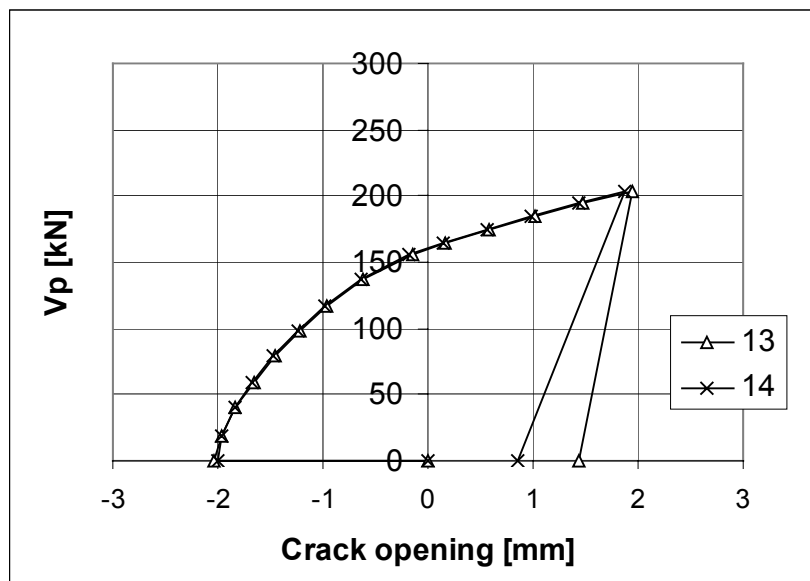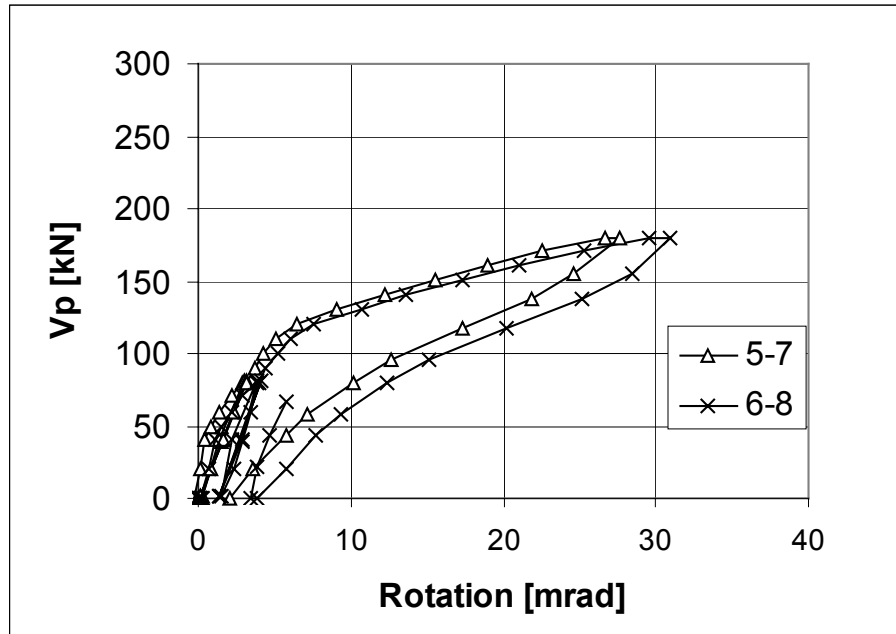*Fig. 46. Width of flexural crack at slab end next to the connection measured by transducers 13 and 14 in test B3.*
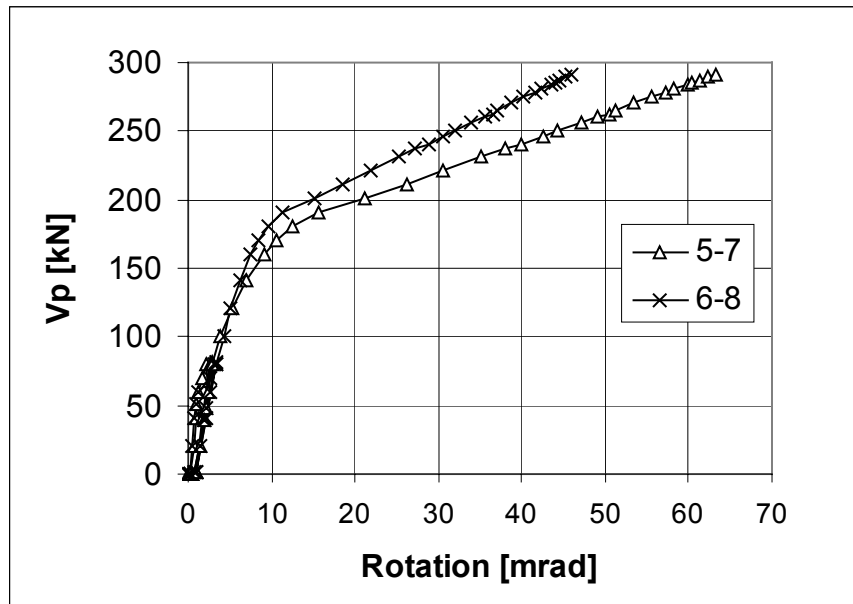
Fig. 47. Rotation of slab end next to the connection, calculated from displacements measured by transducers 5 - 8 in test B3.

4.4.4 N1
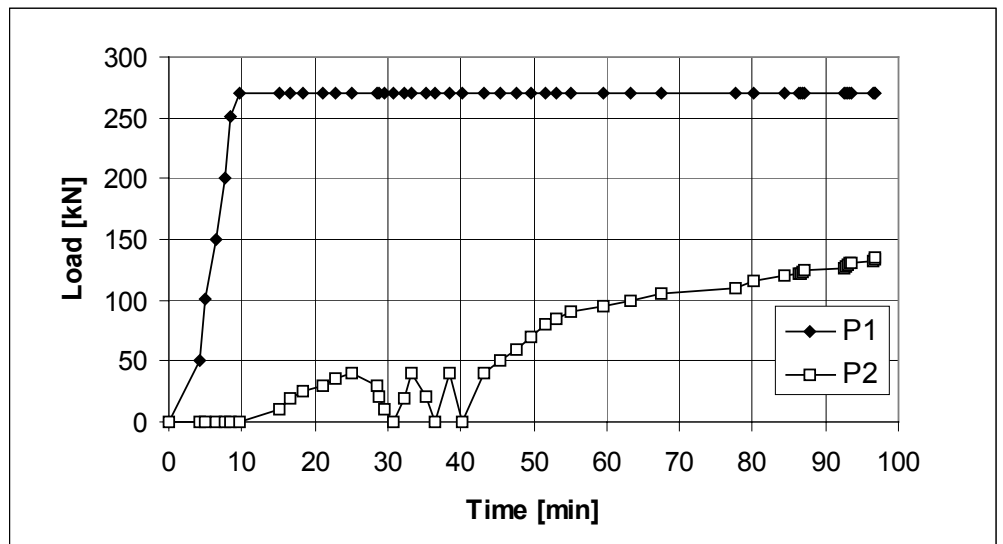
Fig. 48. Load – time relationship in test N1.
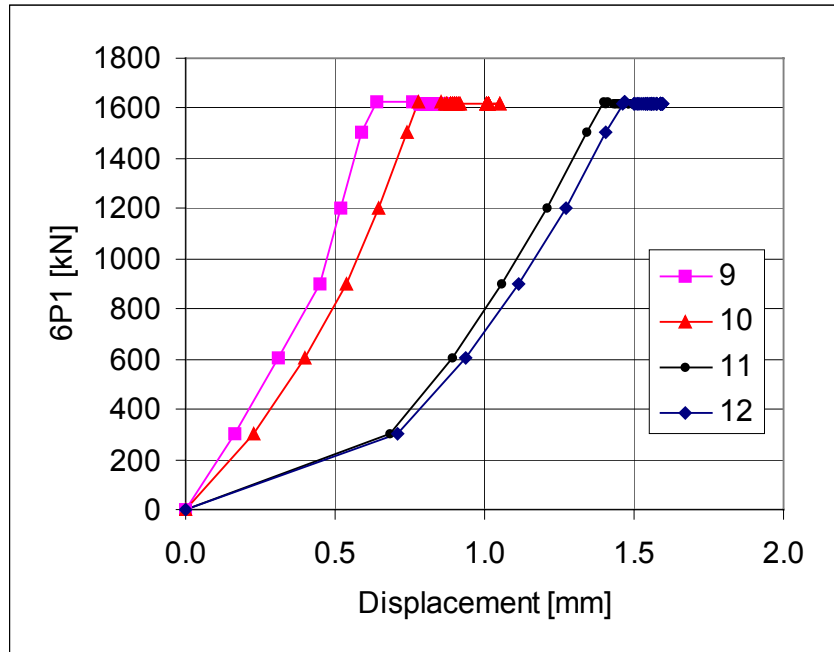
Fig. 49. *Vertical displacement of connection measured by transducers 9 – 12 in test N1.*
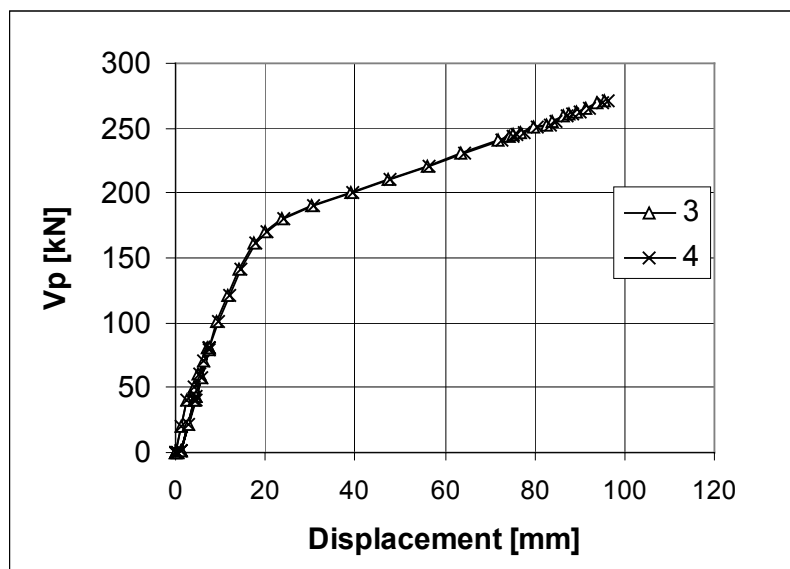
Fig. 50. *Vertical displacement of mid-slab measured by transducers 3 and 4 in test N1.*
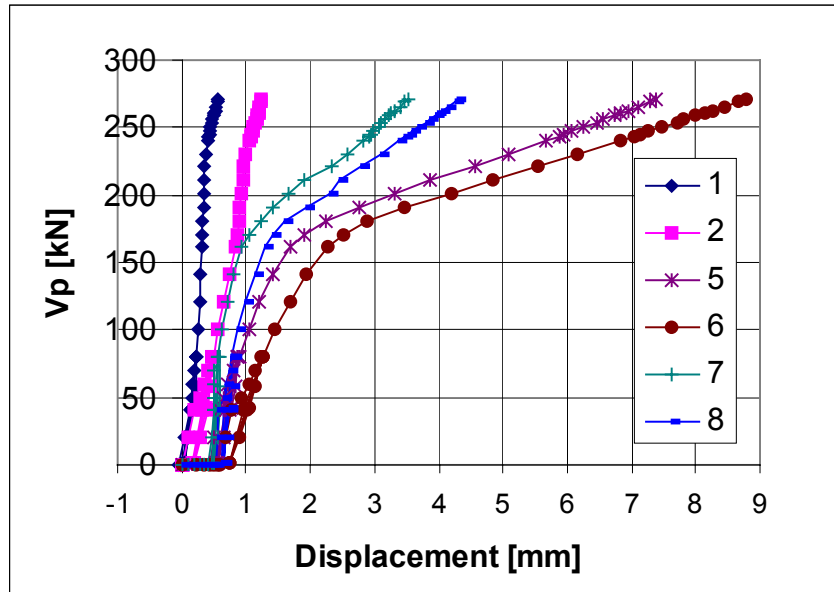
Fig. 51. Vertical displacement of slab measured by transducers 1 – 2 and 5 – 8 in test N1.
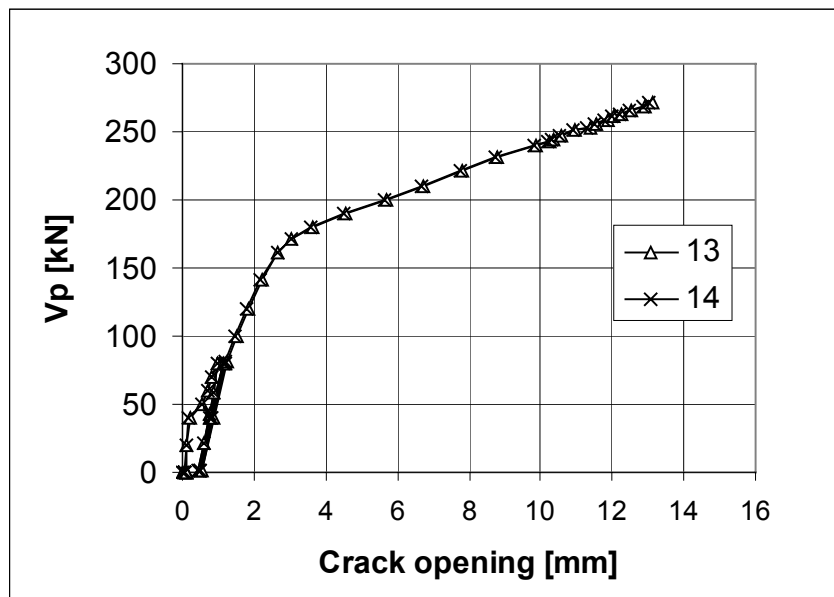
Fig. 52. Width of flexural crack at slab end next to the connection measured by transducers 13 and 14 in test N1.
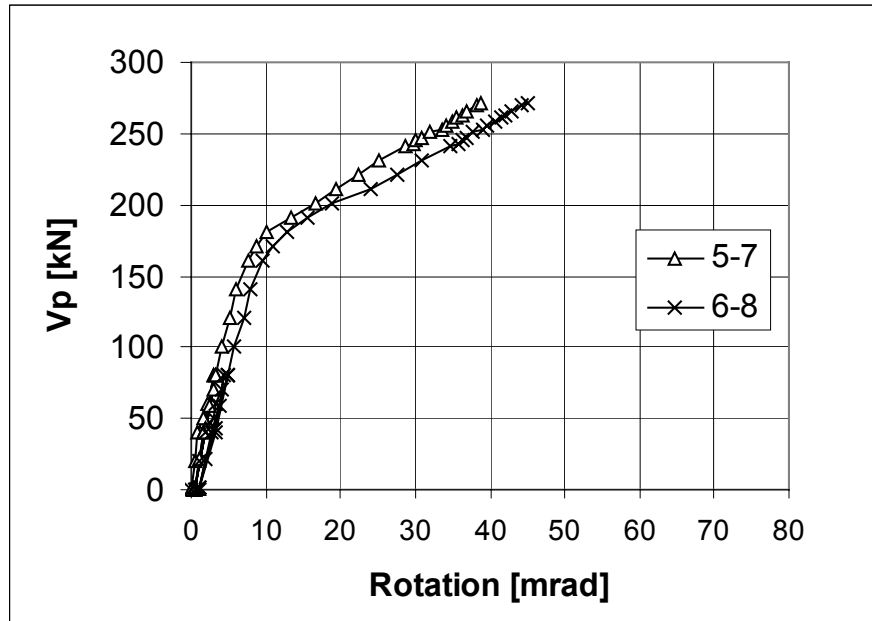
Fig. 53. Rotation of slab end next to the connection, calculated from displacements measured by transducers 5 - 8 in test N1.
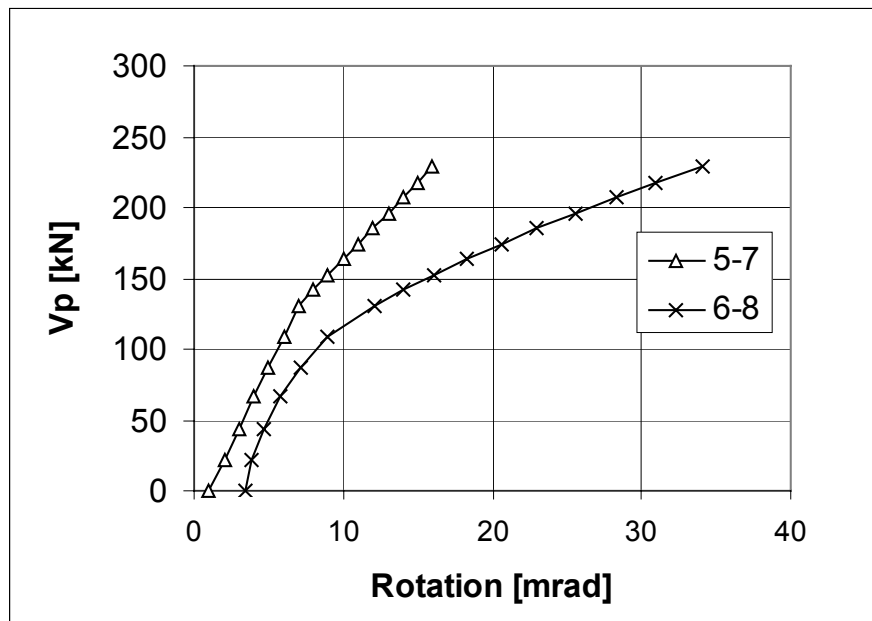
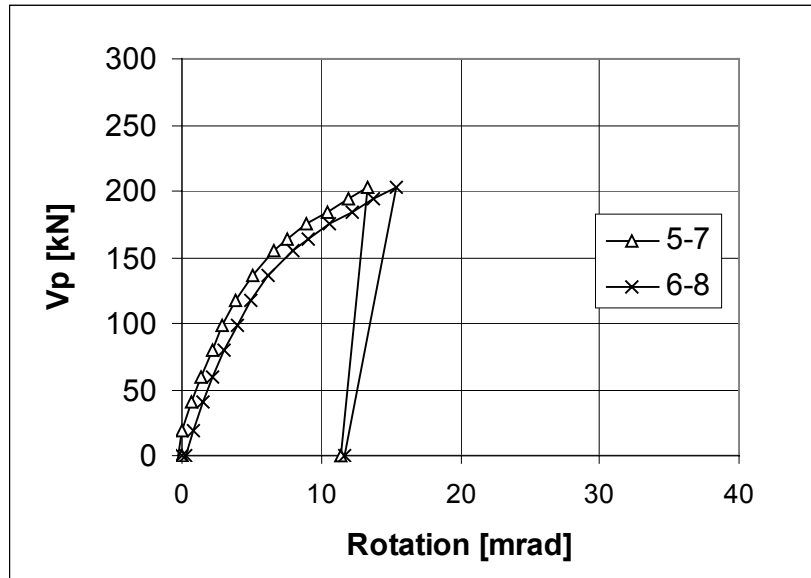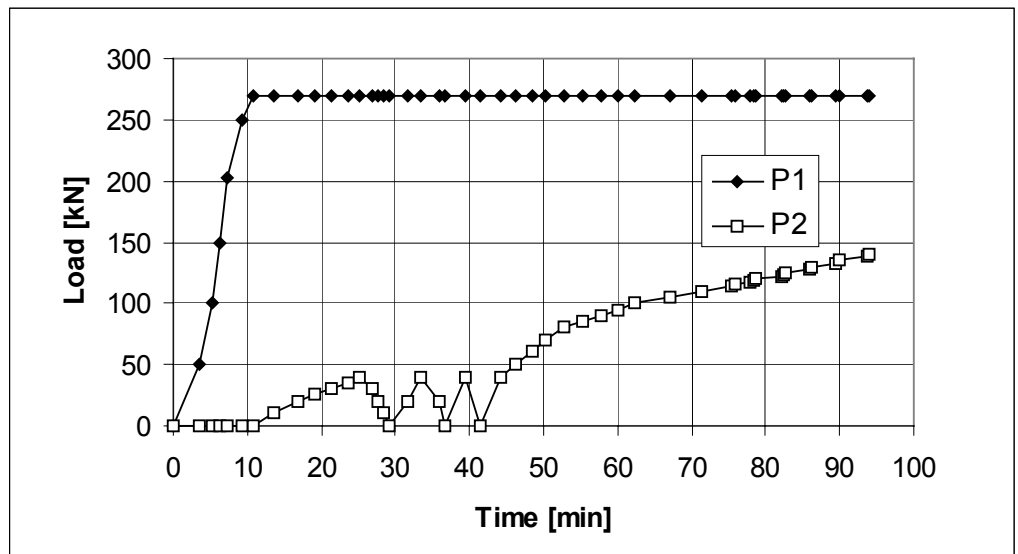**4.4.5 N2**
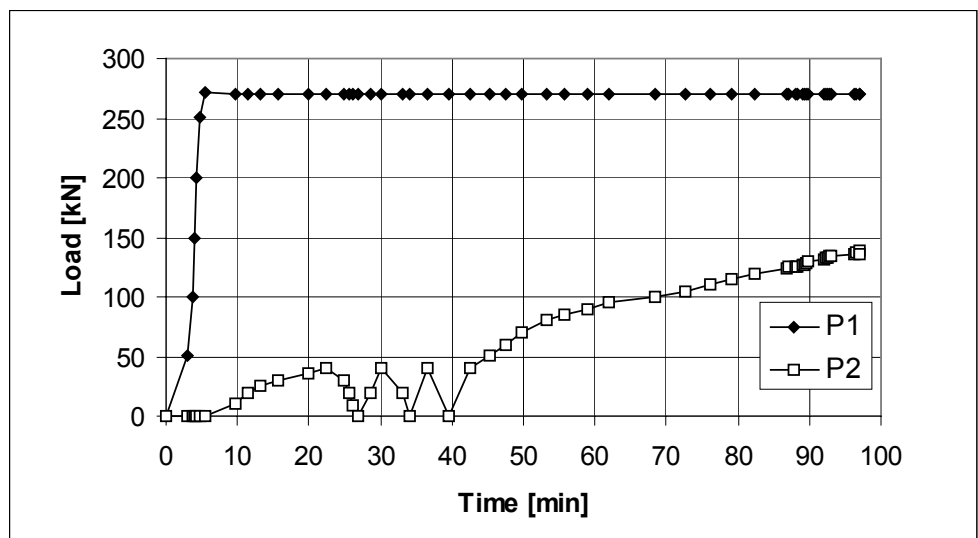
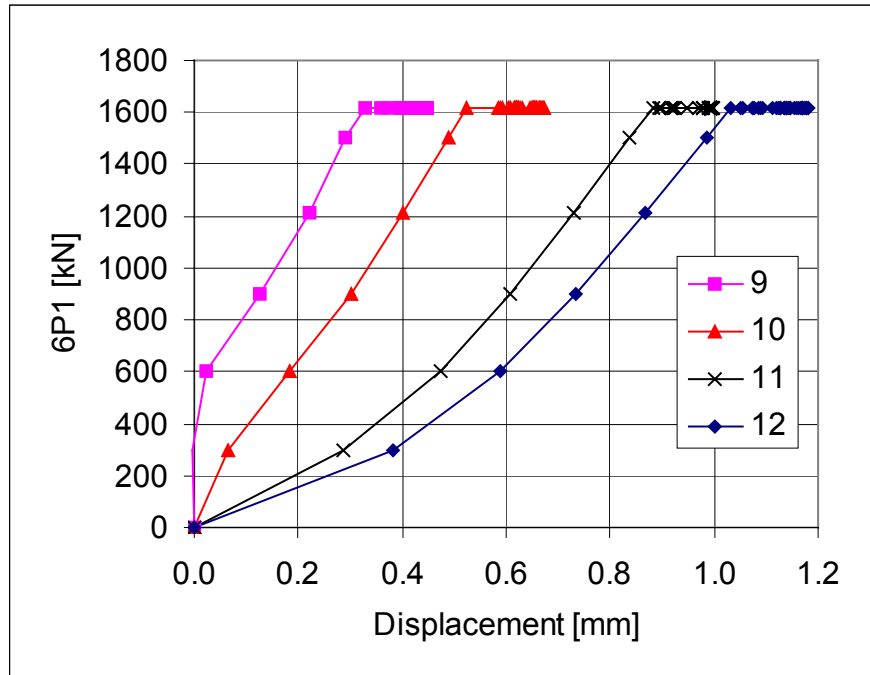*Fig. 54. Load – time relationship in test N2.*
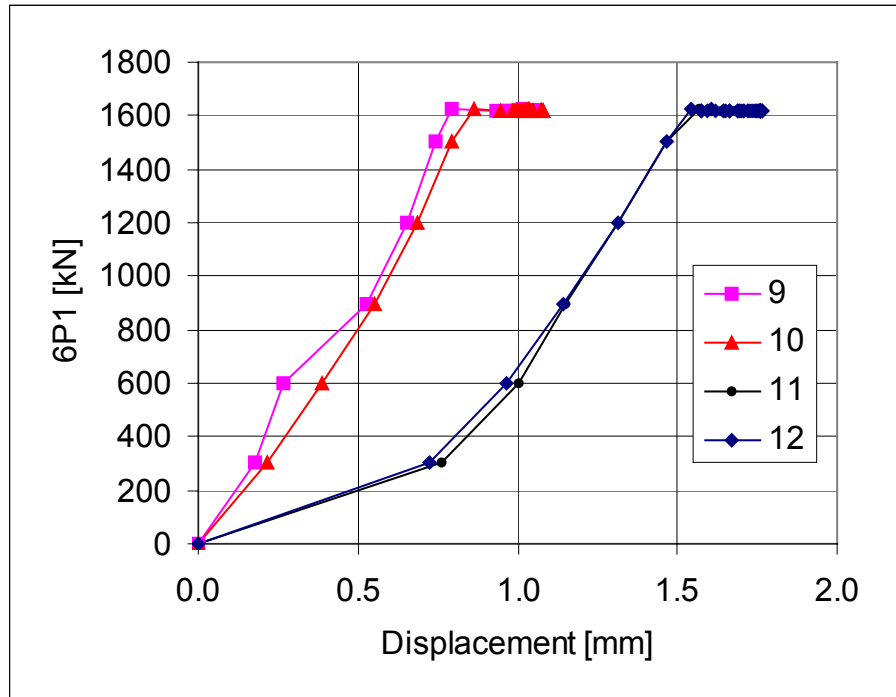
Fig. 55. Vertical displacement of connection measured by transducers 9 – 12 in test N2.
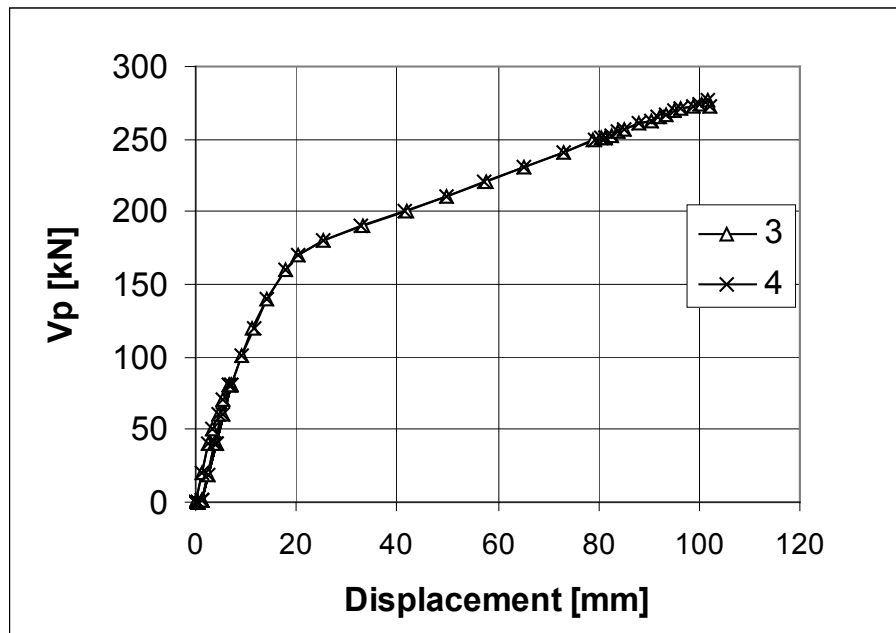
Fig. 56. Vertical displacement of mid-slab measured by transducers 3 and 4 in test N2.
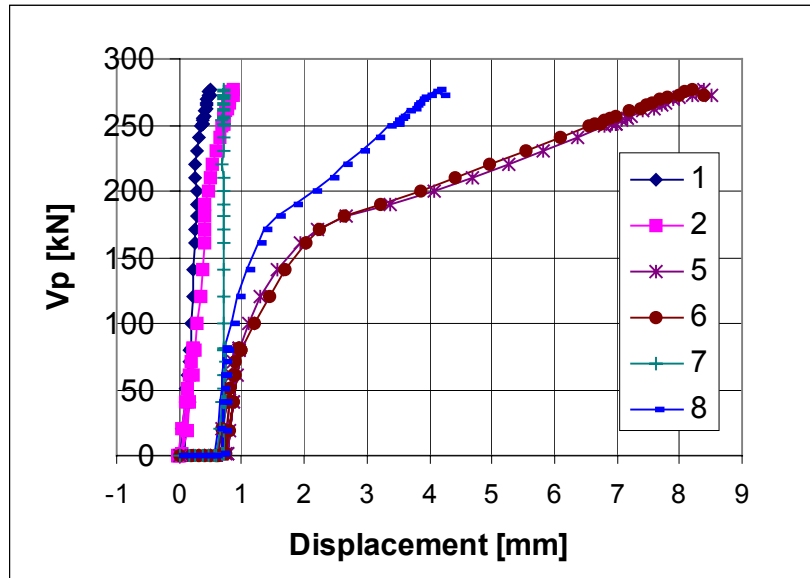
Fig. 57. Vertical displacement of slab measured by transducers 1 – 2 and 5 – 8 in test N2.
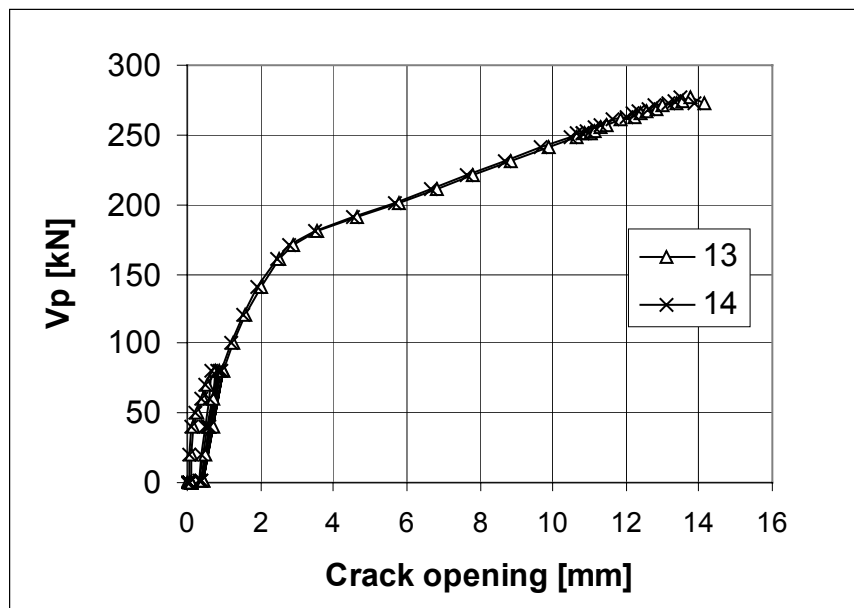
Fig. 58. Width of flexural crack at slab end next to the connection measured by transducers 13 and 14 in test N2.
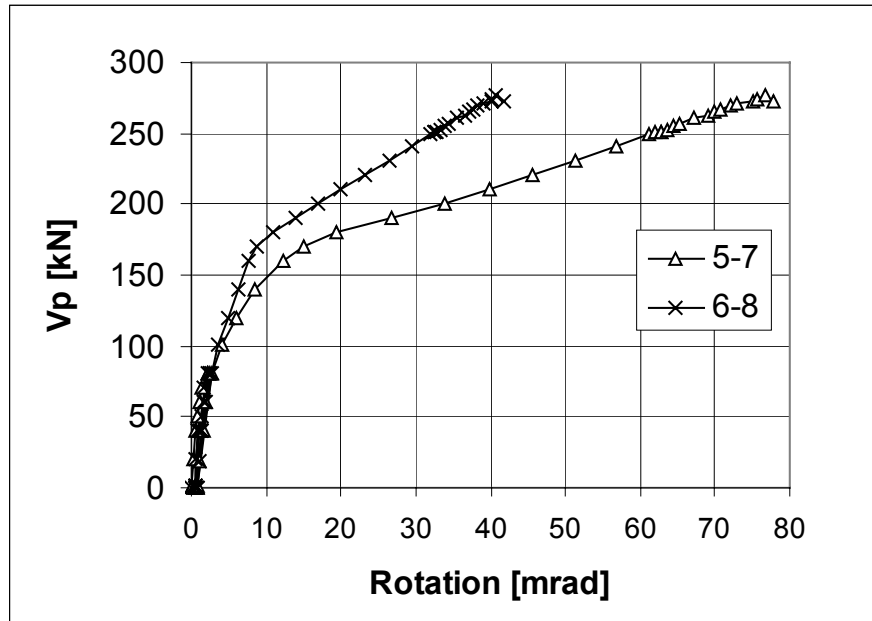
Fig. 59. Rotation of slab end next to the connection, calculated from displacements measured by transducers 5 - 8 in test N2.

4.4.6 N3
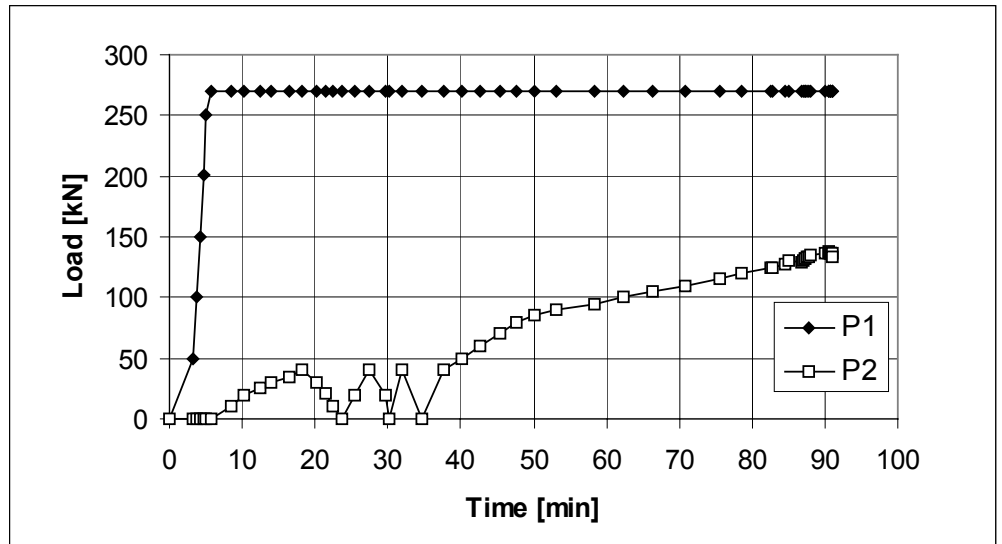
Fig. 60. Load – time relationship in test N3.
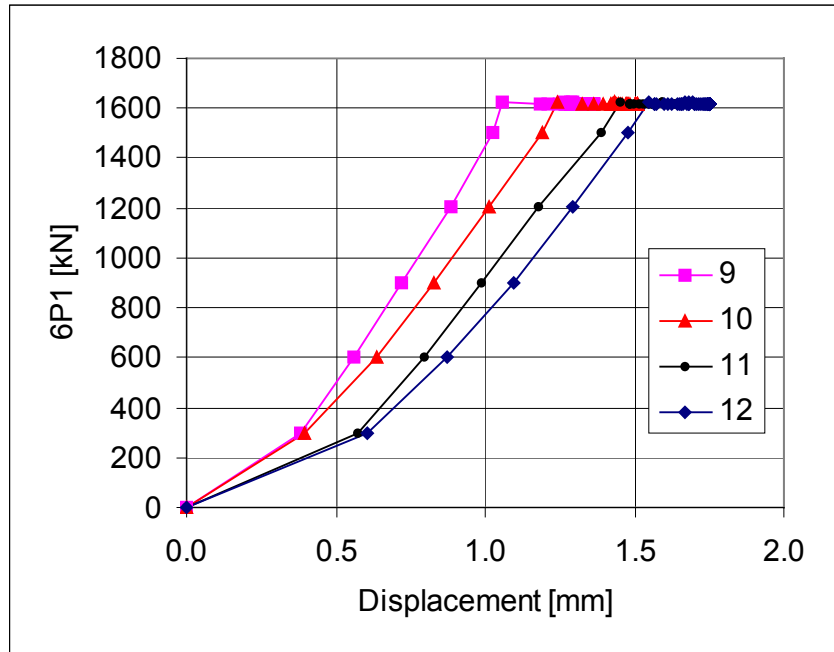
Fig. 61. Vertical displacement of connection measured by transducers 9 – 12 in test N3.
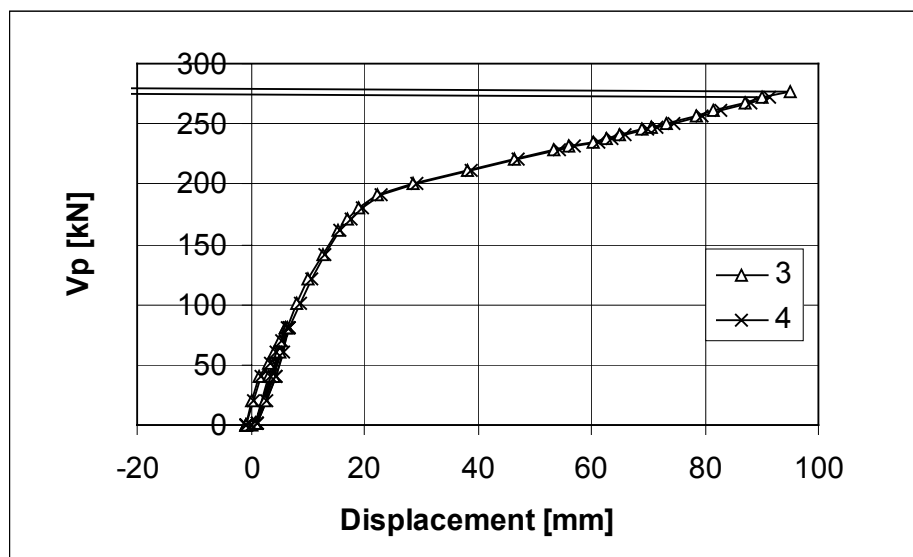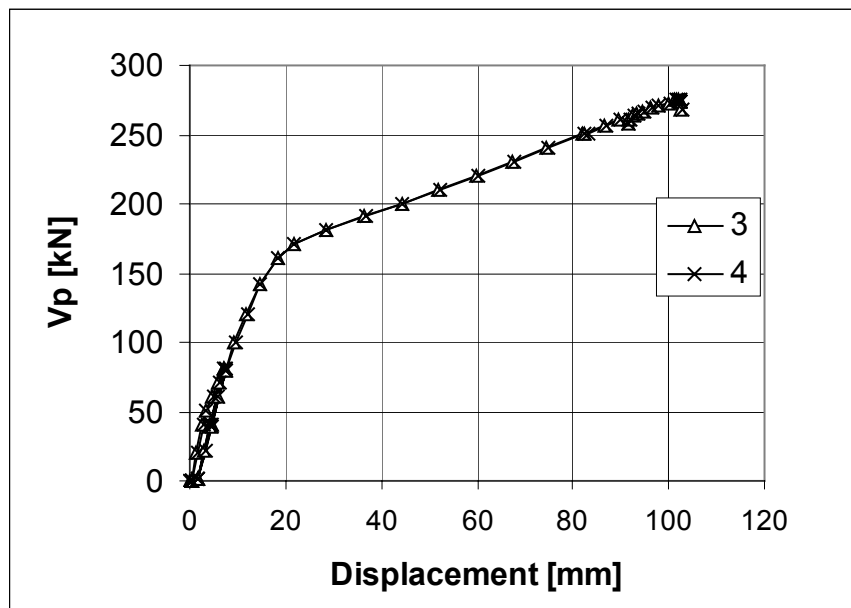

Fig. 62. Vertical displacement of mid-slab measured by transducers 3 and 4 in test N3.
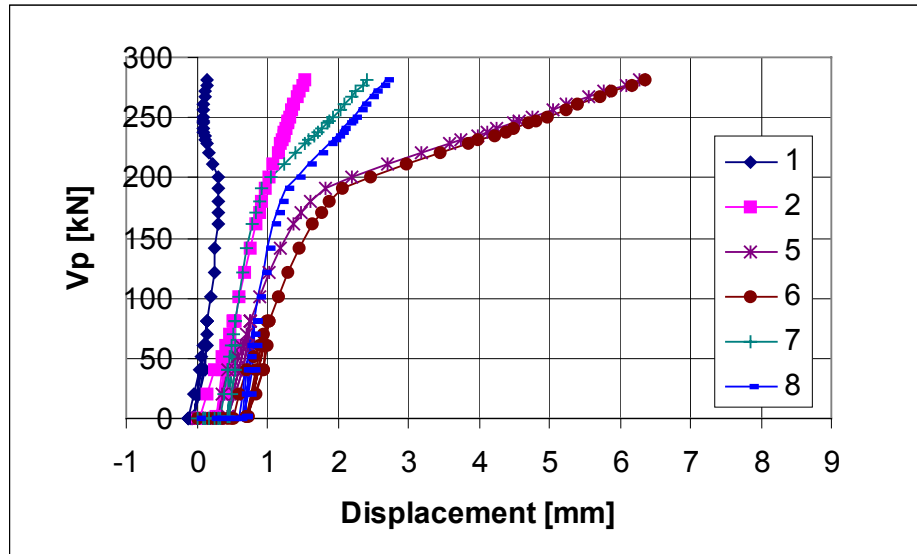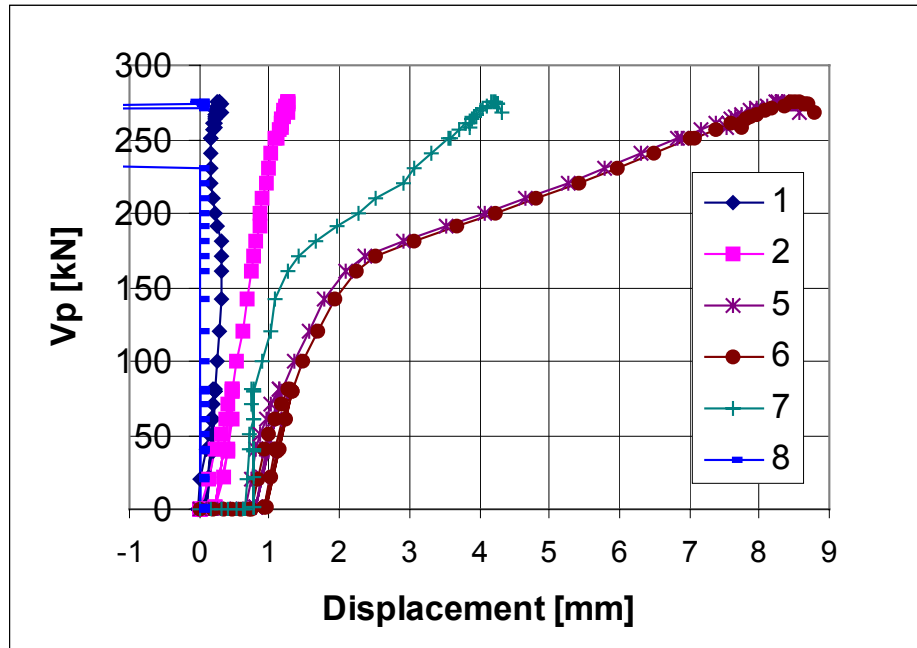
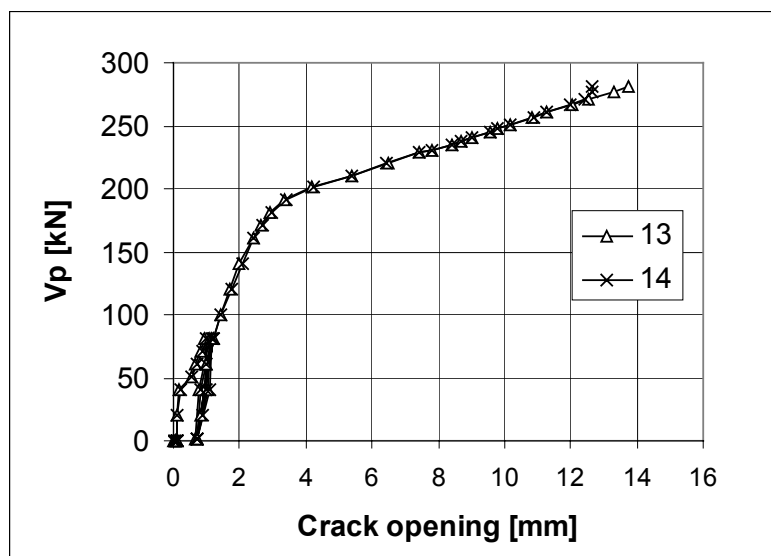*Fig. 63. Vertical displacement of slab measured by transducers 1 – 2 and 5 – 8 in test N3. Transducer 8 was out of action.*
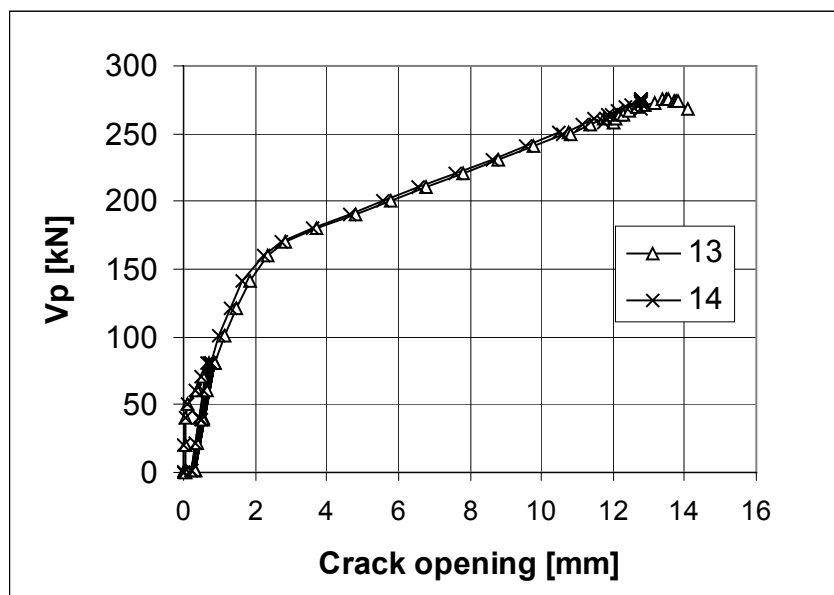
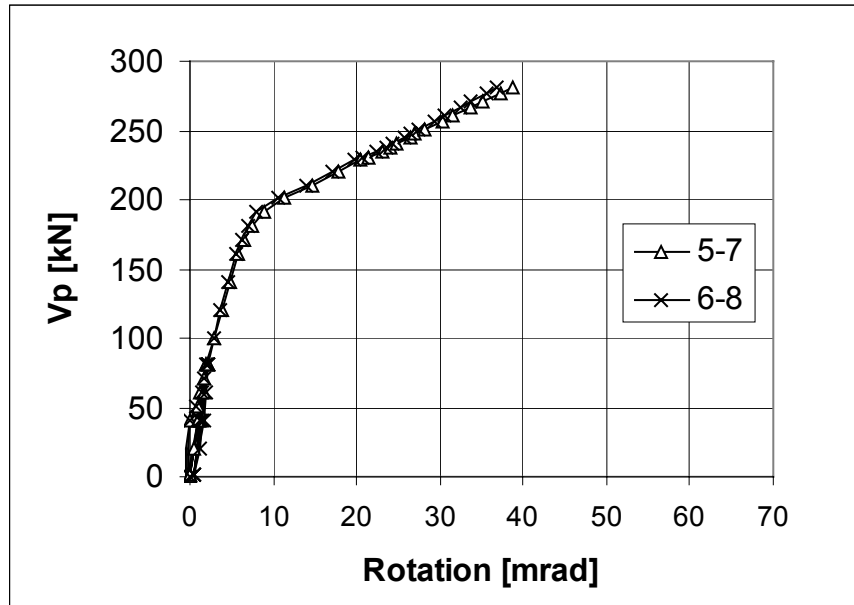*Fig. 64. Width of flexural crack at slab end next to the connection measured by transducers 13 and 14 in test N3.*
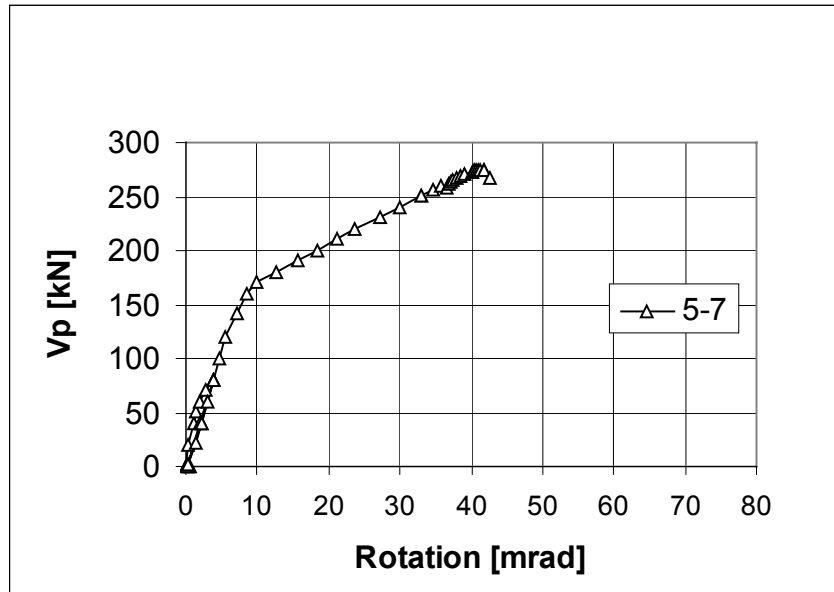
Fig. 65. Rotation of slab end next to the connection, calculated from displacements measured by transducers 5 and 7 in test N3.

5 STRENGTH OF CONCRETE

Twelve 50x50 mm cores were drilled, six from slab in test B2 and six from slab in test N2. The cores were covered by plastic until testing.

Six 150x150x150 mm^3 test cubes made of the same concrete as the upper beams WU, see Fig. 16, were kept in the same conditions as the beams.

Nine 150x150x150 mm^3 test cubes / casting lot were made of the grout. The cubes were kept in the same conditions as the slabs.

The results from the tests on the cores and cubes are given in App. E and summarized in Tables 4 and 5. The obtained strength for the concrete in the hollow core slabs was typical of normal production. The strength of the grout and that of the concrete in the concrete beams simulating wall elements were higher than the strength required for the specified grade K30, but not unusual for normal production.

Table 4. Date of grouting and testing of grout, number of 150 mm test cubes N and obtained mean compressive strength f_{cm}.

Load test		Phase I grouting April 2			Phase II grouting April 4		
Test	Date	Date of test	N	f_{cm} MPa	Date of test	N	f_{cm} MPa
B1	April 14	April 14	3	45.2	-		
B2	April 15	-			-		
B3	April 17	April 17	3	44.8	-		
N1	May 5	-			May 5	3	42.3
N2	May 6	-			May 6	3	42.2
N3	May 8	May 8	3	50.5	May 8	3	43.2

Table 5. Date of casting and testing of concrete in wall elements, number of 150 mm test cubes N and obtained mean compressive strength f_{cm}.

Load test		Wall element				
Test	Date	Date of casting	N	Date of test	f_{cm} MPa	
N1	May 5	March 10	2	May 5	41.8	
N2	May 6	March 11	2	May 6	38.5	
N3	May 8	March 12	2	May 8	36.3	

Table 6. Date of casting and testing of hollow core slabs, number of 50 mm cores N and obtained mean compressive strength $f_{cm,C50}$ and characteristic compressive strength $f_{ck,C50}$.

Load test		Slab element				
Test	Date	Date of casting	N	Date of test	f_{cm} MPa	$f_{ck,C50}$ MPa
B2	May 5	April 15	6	April 17	64.3	60.0
N2	May 6	March 7	6	May 8	64.8	66.2

6 REFERENCE TESTS

Two reference shear tests were carried out on the intact ends of slabs taken from tests B2 and N2. The test layout is illustrated in Fig. 66. The torsion was eliminated by placing the loaded slab end on a support that could freely rotate around an axis parallel to the slab. Before the loading was started, further rotation was prevented by locking two wedges as shown in photographs presented in App. C.
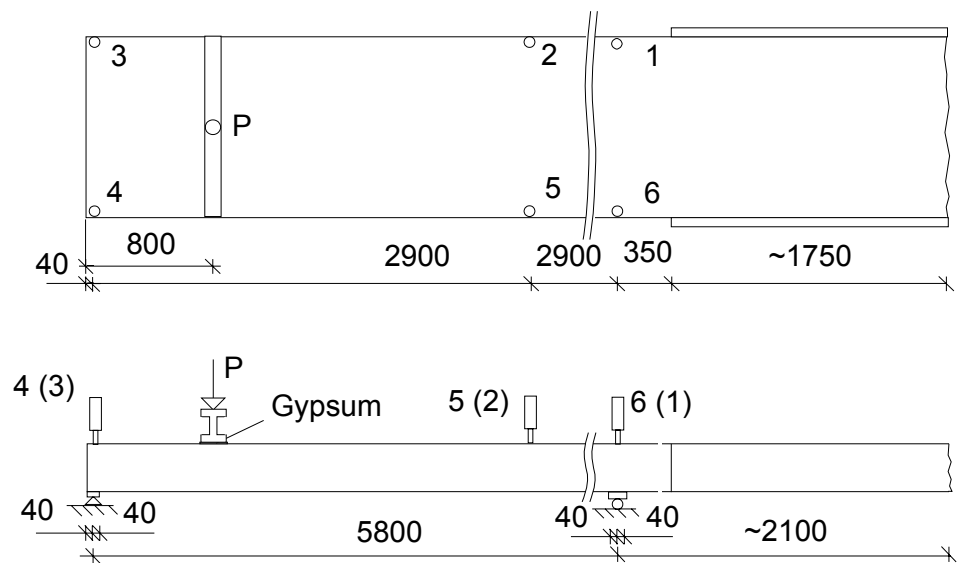
Fig. 66. Location of loads, supports and transducers 1 – 6 in reference tests.

The failure mode in both reference tests was shear tension failure, see App. C. The observed shear resistance (shear force next to the support) is given in Table 7. In Table 7 also the predicted resistances calculated according to Eurocode 2 (prEN 1992-1-1, Draft April 2002) are given for both test specimens. Neither the hollow core standard prEN 1168 nor Eurocode 2 give advice for transforming the core strength into 150 mm cylinder strength $f_{ck,C150}$. Here it has been assumed that
- the core strength gives directly the 150 mm cube strength and
- the cylinder strength is 85% of the cube strength.

Table 7. Characteristic core strength of slab concrete ($f_{ck,C50}$), corresponding cylinder strength ($f_{ck,C150}$), initial prestress of strands given by the slab producer (σ_{p0}), transfer length(l_{pt}), cross-sectional area (A), ratio of first and second moment of area (S/I) and sum of web widths (b_w).

	$f_{ck,C50}$ MPa	$f_{ck,C150}$ MPa	σ_{p0} MPa	l_{pt} mm	A mm2	S/I m^{-1}	b_w[1] mm
B2	60.0	51.0	1000	489	187400	0.00405	267
N2	66.2	56.3	1000	458	187400	0.00405	266

[1] For the inner webs the measured width given in App. D is used. For the outer webs the measured width at the depth of the lower slots is applied

Table 8. Observed shear resistance ($V_{u,obs}$), shear resistance predicted using mean tensile strength ($V_{u,pred,m}$) and characteristic tensile strength ($V_{u,pred,k}$).

Test	$V_{u,obs}$ kN	$V_{u,pred,m}$ kN	$V_{u,pred,k}$ kN
VB2	230	335	251
VN2	201	356	267

The observed resistances are 31 – 44% lower than the predicted ones calculated from the mean tensile strength and and even 8 – 25% lower than the predicted resistances calculated from the characteristic tensile strength. This inconsistency can partly be explained as follows. Firstly, there is a large scatter in the results because both the actual and the predicted resistance are sensitive to the tensile strength of the concrete. Secondly, the calculation method for the shear resistance given in Eurocode 2 and referred to in prEN 1168 gives values that for the considered slab type are tens of percent too optimistic. Nevertheless, the inconsistency is too great to be explained by these two facts only.

In test B1.I one of the outer webs of the slab failed when the simply supported slab end was subjected to a shear force of 201 kN while the other webs remained intact. This is a rare occasion for hollow core slabs loaded with symmetrical transverse line loads. After this local failure, the remaining webs, four out of five, could still carry a shear force of 212 kN. This suggests that there may have been some defects in the outer webs of the slabs. One explanation might be that the lower of the longitudinal slots along the outer webs had disturbed the compaction of the outer web. However, no visible weakness could been seen either on the outer face or on the cracked failure surface of the slabs.

7 ANALYSIS OF RESULTS

7.1 Calculated and observed cracking resistance next to the connection

A rough estimate of the tensile stresses and tensile strength at first cracking due to negative bending moment are given in Table 9. For tests N1 – N2 the stress calculated from measured loads is close to the estimated mean tensile strength. For tests B1 – B3 the consistency between the calculated stress and strength could be considerably improved by taking into account the cast-in-situ concrete when calculating the section modulus.

Table 9. Load at first flexural cracking (F_2), bending moment at support (M), Section modulus (W), tensile stress of top fibre (σ), rough estimation for characteristic cylinder strength (f_{ck}) and mean tensile strength (f_{ctm}).

Test	F_2 kN	M kNm	W 10^6mm^3	σ MPa	f_{ck}	f_{ctm} MPa
B1.I	25.1	102	15.6[1]	6.5	50	4.1
B2	25.6	86	15.6[1]	5.5	50	4.1
B3	30.6	103	15.6[1]	6.6	50	4.1
N1	19.6	66	21.9[2]	3.0	30	2.9
N2	18.6	62	21.9[2]	2.9	30	2.9
N3	19.6	66	21.9[2]	3.0	30	2.9

[1] Calculated assuming only hollow core slab effective
[2] Calculated assuming solid cross-section made of grout

7.2 Mechanisms explaining observed high shear resistance

In tests B1, B2 and B3 the slab end cracked almost vertically outside the support. Also in tests N1, N2 and N3 the upper end of the flexural crack was outside the wall but the lower end was inclined and ended above the neoprene strip as shown schematically in Fig. 67.
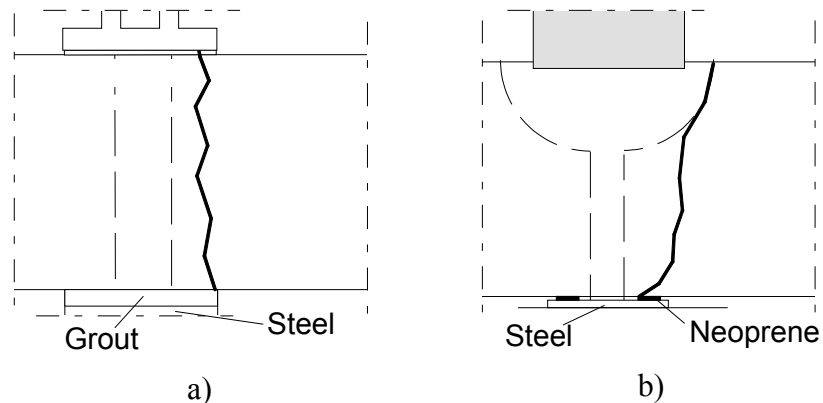
Fig. 67. Flexural crack after failure. a) Unnotched slabs end. b) Notched slab end.

The observed cracking modes and the width of the flexural crack next to the connection, greater than 10 mm, suggest that before the slab failed elsewhere, the load-carrying mechanisms next to the support have been shear in the compressed concrete zone below the crack tip and dowel action of the strands. With notched slab ends the neoprene strips may also have transferred a part of the support reaction. The role of aggregate interlocking may be smaller because the cracks were so wide at failure.

The slab ends were vertically compressed. In tests on unnotched slabs (B1, B2 and B3) the average compressive stress was 1.6 MN/ (0.2 m x 1.2 m) = 6.7 MPa in the connection. In these tests the compression made the crack grow outside the wall. In tests on notched slab (N1, N2 and N3) the slab ends were not supported by the neoprene strip only but also by the grout in the 3 mm deep and 25 mm wide space behind the neoprene and below the slab end. The grout filled the space until the inner edge of the neoprene, which was checked after the test, but its mechanical properties must have been poor.

7.3 Slab cracked due to unintended negative bending moment – design aspects

The width of the flexural crack at support depends not only on the load but also on the span. Hence, with shorter spans high shear forces may be present when the flexural cracks are narrower than in the present tests. With narrow flexural cracks next to the support the aggregate interlock and the shear resistance of the compressed lower part of the slab cross-section are effective. With increasing crack width the tie reinforcement is strained which increases the compression force in the compressed zone at the bottom until the tie reinforcement yields. The lower part of the slab section is compressed horizontally by a force equal to sum of the force in the tie reinforcement and

the effective prestressing force. At the outer edge of the support the prestressing force is small but not insignificant, especially when the slab is supported on a mortar bed and subjected to a high vertical compression.

In the present case the shear resistance at a plastic hinge is considered. A plastic hinge next to a support has some advantages over plastic hinges in the span. The pressure of the support prevents the strands from spalling the soffit of the slab on the supported side of the crack. On the other side of the crack the shear force presses the strands against the slab. In this way the shear resistance of the prestressing strands can considerably contribute to the shear resistance of the plastic hinge. The compression due to the negative bending moment also prevents the strands from slipping out of that piece of the slab which is between the compressed wall elements.

If the lower end of a flexural crack is clearly outside the outer edge of the support as shown in Fig. 68, left, the soffit will spall, see failure crack A in Fig. 68. If the crack is clearly inclined, there is a risk of a failure crack of type B shown in Fig. 68. Both of these cracking modes result in a considerably reduced shear resistance.

Failure crack A   Failure crack B
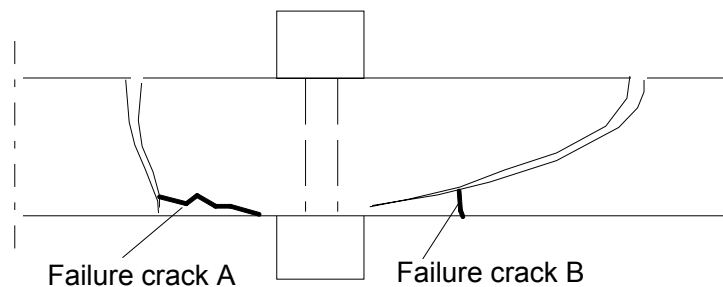
Fig. 68. Unfavourable cracking modes.

Structural means should be applied to make sure that cracks due to a negative bending moment do not exist too far from the support. Measures to be taken for this purpose are
-       Limiting the amount of tie reinforcement in such a way that the tensile stress of the top fibre due to the prestressing force and yield moment of tie reinforcement is too small to give rise to further flexural cracking after the first crack has appeared next to the support
-       Minimising the length of the core filling.

7.4 Proposed design method

The slab cross-section in the plane of the outer face of the wall is assumed to be cracked in flexure. The shear force of the slab shall not exceed the shear resistance at this section. The shear resistance in this section is the lesser of

$$V_{uv} = V_{u1} = 0{,}3k(1+50\rho)f_{ctd}b_w d + \beta_1 A_p \frac{F_{pub}}{P_{yd}} f_{pyd} \qquad (1)$$

or

$$V_{uv} = V_{u2} = \mu\left(A_s f_{yd} + \frac{x_1}{l_{bp}} P_\infty\right) \qquad (2)$$

where

k is $1.6 - d/(1\ m)$

d distance from fully anchored rebars parallel to the slabs (tie reinforcement), placed in connections between adjacent slabs, to the soffit of the slab

b_w sum of web widths in the hollow core cross-section without cast-in-situ concrete

A_s cross-sectional area of the aforementioned tie bars per width of one slab

f_{yd} design strength of the tie bars

ρ $A_s/(b_w d)$

f_{ctd} tensile strength of concrete in hollow core slab, design value

β_1 $= 0{,}9$,

A_p cross-sectional area of all lower strands in a hollow core slab

x_1 distance from slab end to the outer face of the supporting wall minus the horizontal width of the optional chamfering

F_{pub} anchorage capacity of lower strands at a distance of x_1 from slab end

f_{pyd} design strength of prestressing steel

P_{yd} $= A_p f_{pyd}$

μ friction coefficient $= 0{,}8$,

l_{bp} transfer length of the prestressing force in slab

P_∞ prestressing force in lower strands of slab after losses of prestress.

To be effective, the tie reinforcement shall be placed at the mid-depth of the cross-section or higher. Its cross-sectional area per one slab element shall not exceed

$$A_{s,max} = \left[\frac{f_{ctk} - (\sigma_{cp} + \sigma_{cg})}{df_{yk}}\right]W \qquad (3)$$

where σ_{cp} is the tensile stress in the top fibre of the slab due to fully transferred prestressing force at the age of first loading, σ_{cg} the stress in the top fibre of the slab due to self weight of the slab (characteristic value) at a distance of $0{,}5l_{bp}$ from slab end and W the section modulus (top fibre) of the hollow core slab. f_{ctk} and f_{yk} are the characteristic strength of the slab concrete and tie reinforcement, respectively.

If the slab end is notched, the notch and effective core filling shall not extend more than 60 mm and 80 mm outside the wall, respectively. In unnotched slabs the effective core filling shall not extend outside the wall.

The meaning of Eqs 1 – 3 is explained as follows:

1. The first term in Eq. 1 represents the shear resistance of a slab without shear reinforcement and the second term the dowel action of the strands in the compression zone.

2. Eq. 2 represents friction force in the compressed zone. This rule eliminates the risk of too small amount of tie reinforcement in deep slab cross-sections. This precaution is necessary because Eq. 1 has originally not been developed for a plastic hinge.

3. Eq. 3 reduces the risk of flexural cracking of the top fibre outside the connection.

4. The tie reinforcement needed for shear resistance shall be additional to the ordinary tie reinforcement specified by the design regulations whether there is clamping due to negative bending moment or not. The ordinary tie reinforcement should be placed below the mid-section of the slab.

7.5 Checking the proposed design method against test results and design practice

The proposed design method is applied to two test specimens: B2 and N2. The Finnish concrete code is applied when calculating l_{pt} (= 800 mm), F_{pu} and tensile strength of concrete. The cube strength f_{ck} (150 mm cubes) is obtained from core strength (50 mm cores) by multiplicating it by 1.1x0.85. For the reinforcing steel in tests B2 and N2 the measured strength values 536 MPa and 525 MPa are used, respectively. For the strands, the nominal 0.2% yield limit 1630 MPa is used.

The results are given in Table 10. They show that the resistance predicted by Eqs 1 and 3 is considerably lower than the resistance observed in the tests. The same is true also when the cast-in-situ concrete along the longitudinal edges is taken into account as a slab concrete increasing the total web width.

Table 10. Effective depth d, scaling factor k, cross-sectional area of rein-forcement A_s, sum of web widths b_w, characteristic cube strength f_{ck}, mean tensile strength f_{ctm}, distance from vertically cracked section to slab end x_1, anchorage capacity of all strands at the aforementioned section F_{pub}, shear resistances V_{uv1} and V_{uv2} obtained from Eqs 1 and 2, their minimum V_{uv} and observed lower limit $V_{uv,obs}$ for shear resistance at the aforementioned section. The italicized rows correspond to full width of cross-section.

	d mm	k	A_s mm^2	b_w mm	f_{ck} MPa	f_{ctm} MPa	x_1 mm	F_{pub} kN	V_{uv1} kN	V_{uv2} kN	V_{uv} kN	$V_{uv,obs}$ kN
B2	160	1.44	226	289[1]	66.0	4.90	60	63.4	179	152	152	302
B2	*160*	*1.44*	*226*	*369*	*66.0*	*4.90*	*60*	*63.4*	*206*	*152*	*152*	*302*
N2	250	1.35	101	287[1]	72.8	5.03	55	59.7	210	93	93	298
N2	*250*	*1.35*	*101*	*367*	*72.8*	*5.03*	*55*	*59.7*	*251*	*93*	*93*	*298*

[1] The lower longitudinal slot is not taken into account here because it was properly filled with cast-in-situ concrete, see App. D

Table 10 suggests that Eq. 2 would govern the design. This is not always the case as shown in Table 11 in which the design values have been applied to the strength of materials and to the prestressing force. The applied safety factors are
- 1.5 for the concrete
- 1.15 for the prestressing steel
- 1.10 for the reinforcing steel
- 0.9 for the prestressing force.

Table 11. Same parameters as in Table 10 but design values have been applied.

	b_w	f_{ctd}	F_{pub}	V_{uv1}	V_{uv2}	V_{uv}	$V_{uv,obs}$	$V_{uv,obs}/V_{uv}$
	mm	MPa	kN	kN	kN	kN	kN	kN
B2	289	2.18	27.4	79	132	79	302	3.8
N2	287	2.24	25.8	93	82	82	298	3.6

The obtained total safety factors 3.6 and 3.8 are high but justified because
- the number of tests was small
- only one slab cross-section was tested
- in the tests the cast-in-situ concrete outside the edges was considerably stronger than what can be guaranteed on site.

The effect of Eq. 3 on the design of slabs similar to those in the present tests is considered in Table 12. The following parameters, in addition to those given in Table 12, are used
- characteristic tensile strength of steel = 500 MPa
- cross-sectional area of slab = 187 400 mm^2
- section modulus = 1.56·10^7 mm^3
- distance from centroid of slab section to top surface of slab = 162 mm
- eccentricity of strands = 123 mm
- weight of slab per unit length, concrete in connections included, = 4.95 kN/m
- prestress at the age of first loading = 900 MPa.

Table 12. Characteristic strength of concrete (f_{ck}), characteristic tensile strength of concrete (f_{ctk}), stress of top fibre due to the self weight of slab at a distance of 400 mm from slab end (σ_g), stress of the top fibre due to fully transferred prestressing force (σ_p), maximum area of upper tie reinforcement per slab element (A_{smax}) and bar diameter corresponding to A_{smax} (ϕ) .

f_{ck}	f_{ctk}	d	σ_g	σ_p	A_{smax}	ϕ
MPa	MPa	mm	MPa	MPa	mm^2	mm
50	2.85	160	-0.431	2.33	185	>12
50	2.85	250	-0.431	2.33	118	>12
60	3.22	160	-0.431	2.33	257	>16
60	3.22	250	-0.431	2.33	164	>12

8 SUMMARY AND CONCLUSIONS

1. All tested slabs cracked due to the negative bending moment at an early stage of loading. One of these cracks, the one closest to the connection, increased in width while the others did not. At failure the crack width was greater than 10 mm.

2. Despite the wide flexural crack next to the connection, the failure took place elsewhere. In unnotched slabs the failure mode was shear tension failure. In two notched slabs the failure mode was anchorage or shear compression failure, and in one notched slabs a simultaneous shear tension failure and achorage – shear compression failure.

3. In two reference shear tests the observed resistances against shear tension failure were 230 and 201 kN. These values should be comparable to the *mean* theoretical resistance, but they are even 8 and 25% lower than the *characteristic* resistances calculated according to the product standard prEN 1168 and Eurocode 2. A part of this discrepancy can be explained by the well-known nonconservatism of the design formula in Eurocode 2 when applied to the slab types in the present tests. In addition, one of the outer webs failed in shear tension at the simply supported end of test specimen B1 when subjected to a shear force of 201 kN, but the remaining four webs could carry a shear force of 212 kN. This suggests that there may have been incomplete compaction in one or both of the outer webs.

4. The observed shear resistance in the clamped end was of the order of 300 kN, considerably higher than the resistance in the simply supported end. This is attributable to the cast-in-situ concrete simulating the grout in longitudinal connections. The cast-in-situ concrete enhanced effectively the resistance against shear tension failure, but contributed less to the resistance against flexural cracking and anchorage failure. Even though the positive effect of the connection concrete in real floors is smaller than in the test, the negative effect of the vertical cracking remains small or vanishes in ordinary floors in absence of axial forces in the slabs. It is likely that the cast-in-situ concrete outside the slab edges had a smaller effect on the resistance at the vertically cracked section than in more remote cross-sections.

5. The shear resistance for unnotched slabs was 4% higher than that observed for notched slabs. In addition, in all tests on notched slabs the soffit cracked in flexure in the shear span, but in tests on unnotched slabs no such crack was observed. This suggests that the bond between the strands and concrete was weaker in notched slabs. According to the test plan, a 60 mm strip of the unnotched slab end was in heavy compression. On the other hand, only a 25 mm strip of a notched slab end was supported by grout and a 30 mm strip by neoprene. Furthermore, the 3 mm deep and 25 mm wide space under the slab end could not be properly filled with grout having maximum aggregate size equal to 8 mm. The slight difference in negative bending moment at failure (5 kNm lower for the notched slabs) also favoured the greater resistance against flexural cracking in unnotched slabs.

6.   The notched slab end and neoprene bearing could not prevent vertical cracking of slab end as intended. The opposite was true in previous tests of Delvaux [2] in which notched slab ends were supported on mortar bearing. In the tests of Delvaux the highest vertical load on the connection was only 420 kN, i.e. 26% of the vertical load in the present tests. If a low vertical load results in a favourable inclined cracking of the slab end (only the upper corner of the slab end is cracked), two questions arise:

- How to estimate for the vertical load a threshold value below which only the upper corner of the slab is cut off by inclined flexural cracking?
- If such a value is known, how to apply it in the design when the real clamping with vertical tie bars between wall elements, grouted vertical connections between elements etc. (passive clamping) cannot be modelled using vertical normal force in the wall element (active clamping) only?

7.   A design method assuming a vertical flexural crack in the slab next to the wall surface is proposed. This method gives a total safety factor of the order of $3.6 - 3.8$ when compared with the present test results. Such a high safety factor is necessary because tests have been performed without any axial force in the slab on one slab type, one span and one prestressing force only.

Espoo, 28.11.2003

Heli Koukkari   *Matti Pajari*
Heli Koukkari   Matti Pajari
Deputy Group Manager   Senior Research Scientist

This is an electronic copy of the original research report.

APPENDICES
A   Photographs, unnotched slabs
B   Photographs, notched slabs
C   Photographs, reference tests
D   Nominal and measured properties of slab elements
E   Measured material properties of concrete and steel
F   Horizontal load due to nonvertical loads

REFERENCES

1   Technical Research Centre of Finland (VTT). Experimental research on wall-slab connections. Research report RTE77/02. Espoo 2002. 26 p. + App. 62 p. Not published.
2   Delvaux, C. Restrained hollow core floors, shear resistance. CBR, Department Development Service Studies and Research on Prefabrication. August 1976. Translated by AVA 10.6.2001. 13 p. + App. 12 p. Not published.

DISTRIBUTION   Customer   Original
                      VTT   Original

PHOTOGRAPHS, UNNOTCHED SLABS

The numbers on the surface of the slabs refer to the actuator load. They tell the load which made the crack grew until the indicated position. The lines with capital A refer to cracks observed before loading.

Fig. 1. Joint before grouting.

Fig. 2. Edge of slab before grouting.

Fig. 3. End of test specimen before grouting.

Fig. 4. Top surface after grouting.

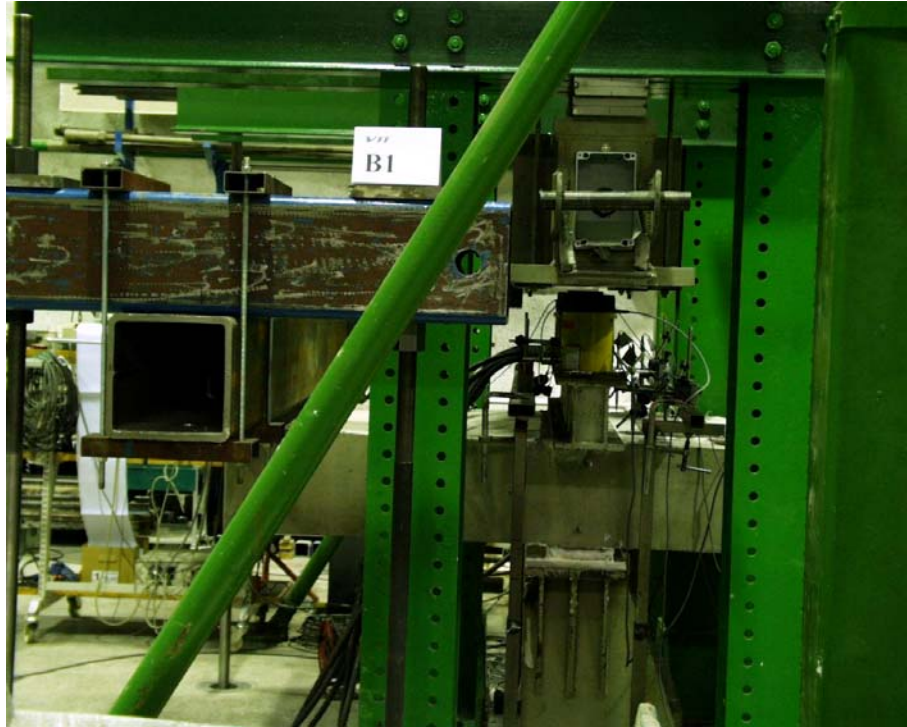*Fig. 5.   Steel plate and mortar below jointed slab ends .*

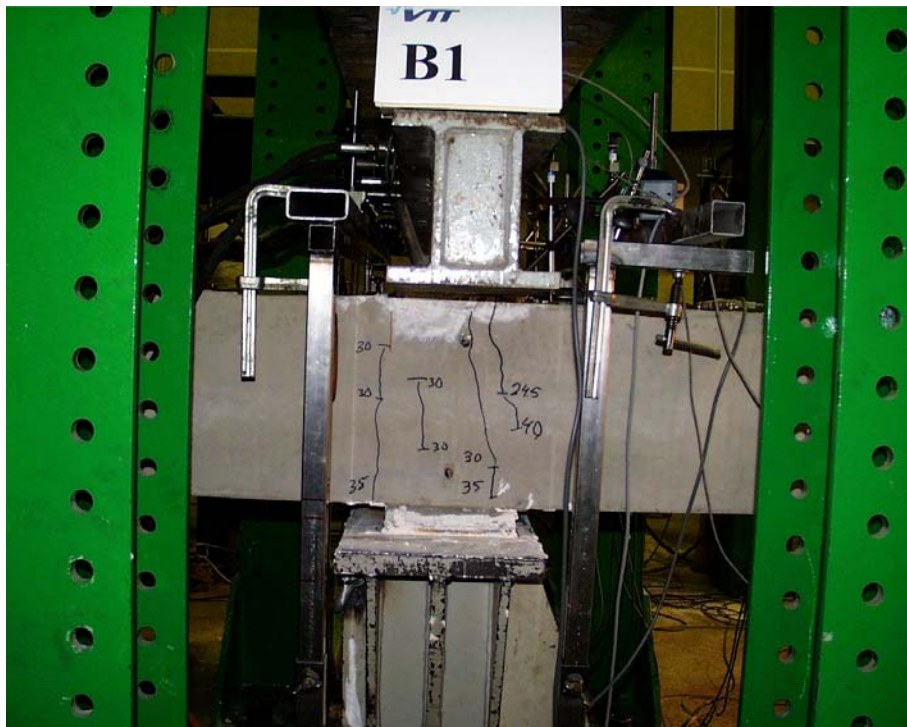*Fig. 6.   B1.I. Overview on test layout.*

Fig. 7.   B1.I. Overview on loads above the joint and next to it.

Fig. 8.   B1.I. Arrangements at non-jointed end of slab.

Fig. 9.   B1.III. Arrangements at jointed end.

Fig. 10. B1.I, North edge. First cracks.
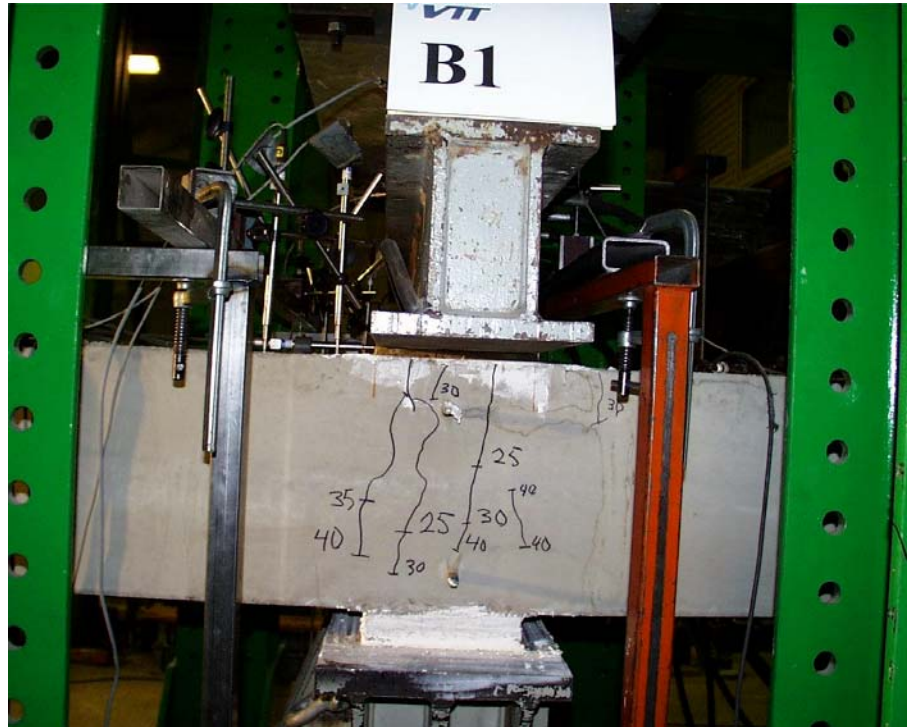
Fig. 11.   B1.I, South edge. First cracks.
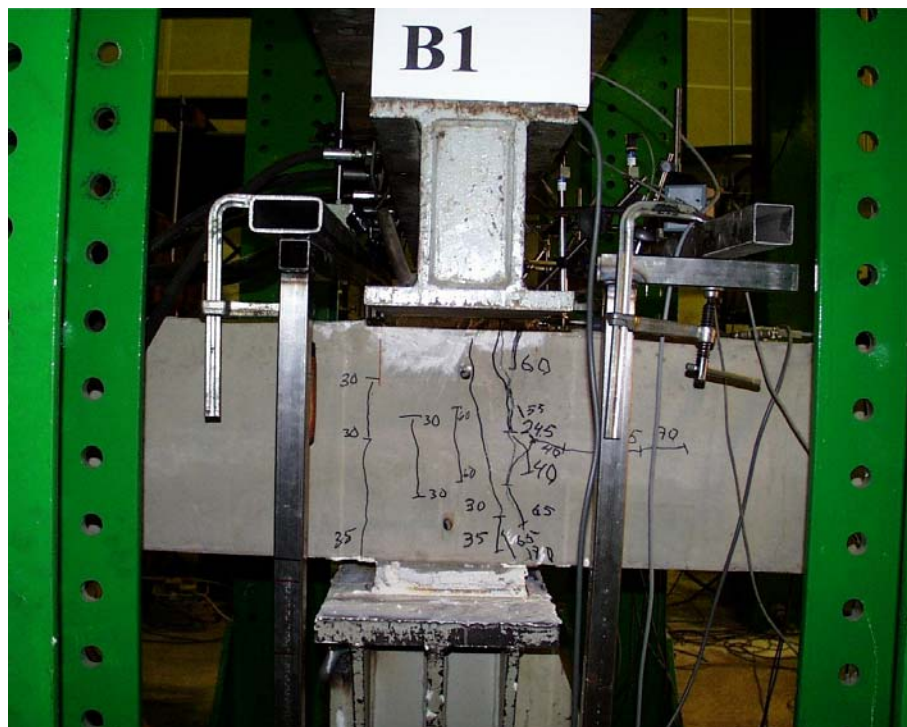
Fig. 12.   B1.III, North edge. Cracks before failure.
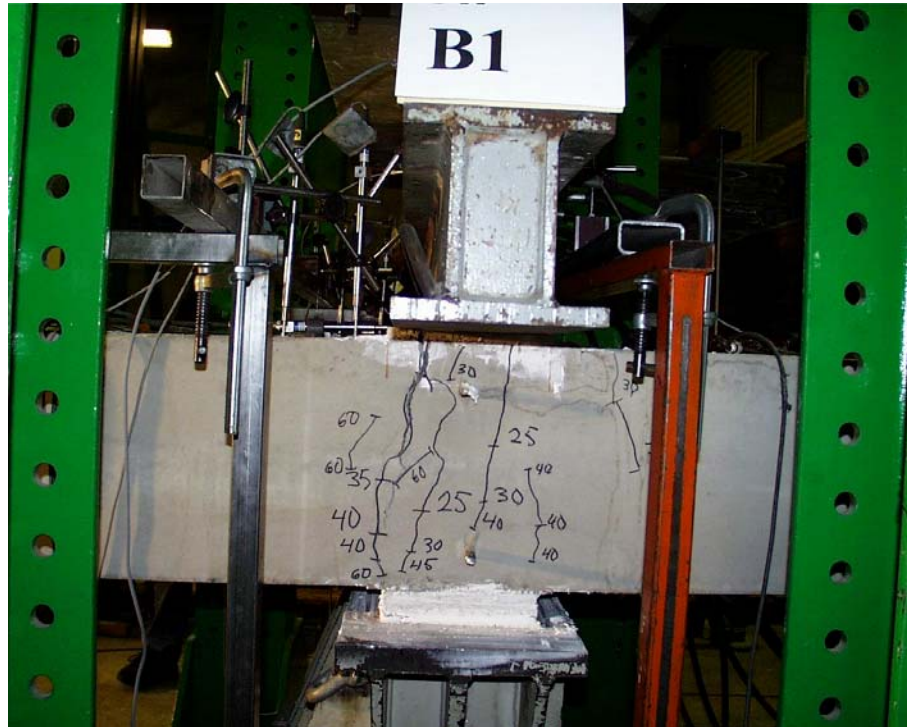
Fig. 13. B1.III, South edge. Cracks before failure.

Fig. 14. B1.III, North edge. Arrangements at simply supported end after failure in test B1.II.

Fig. 15. B1.III. North edge after failure.

Fig. 16. B1.III. North edge after failure.

Fig. 17.   B1.III. South edge after failure.

Fig. 18.   B1.III. South edge after failure.

Fig. 19.   B1.III. Top surface after failure.

Fig. 20.   B1.III. Top surface after failure. Note that the slab end is cracked, not the joint concrete.

Fig. 21. B1.III. Flexural crack after flame cutting the strands and tie bars.
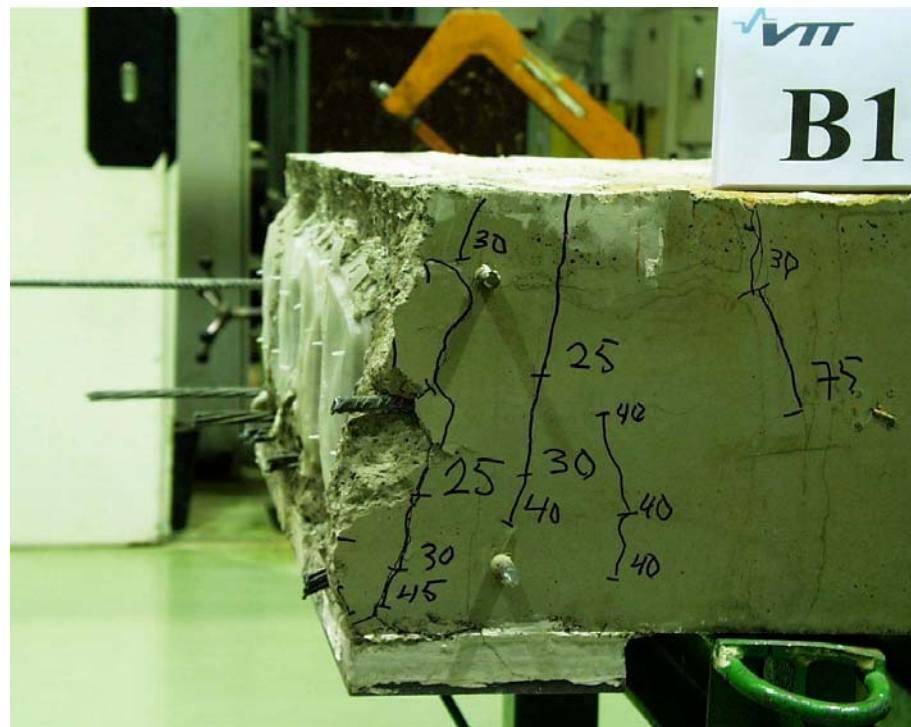
Fig. 22. B1.III. Flexural crack after flame cutting the strands and tie bars..

Fig. 23. B2. Overview on arrangements.
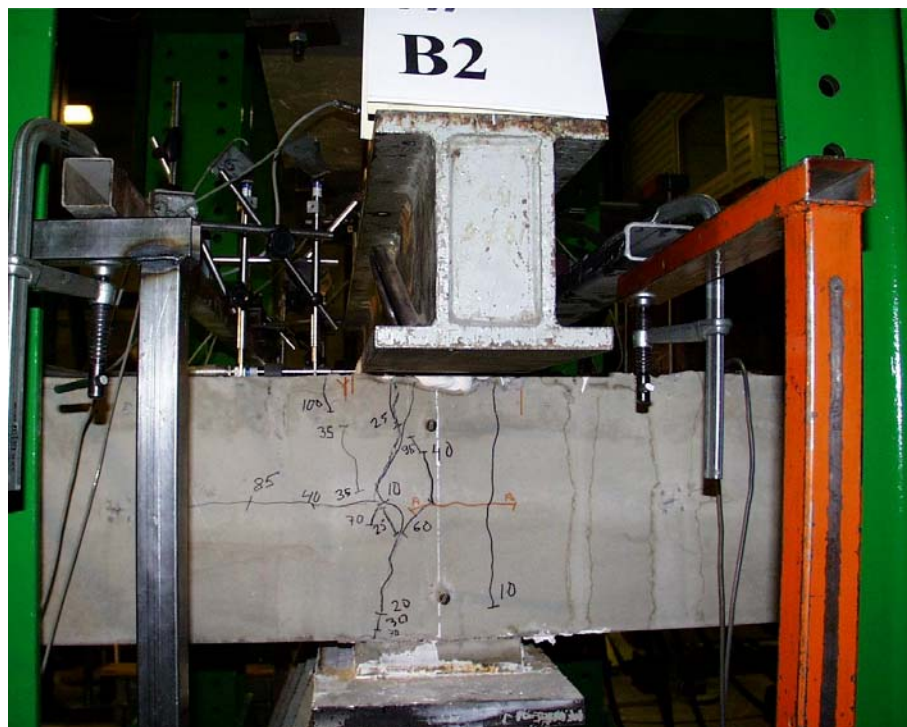
Fig. 24. B2, South edge. First cracks.

Fig. 25. B2, North edge. First cracks.
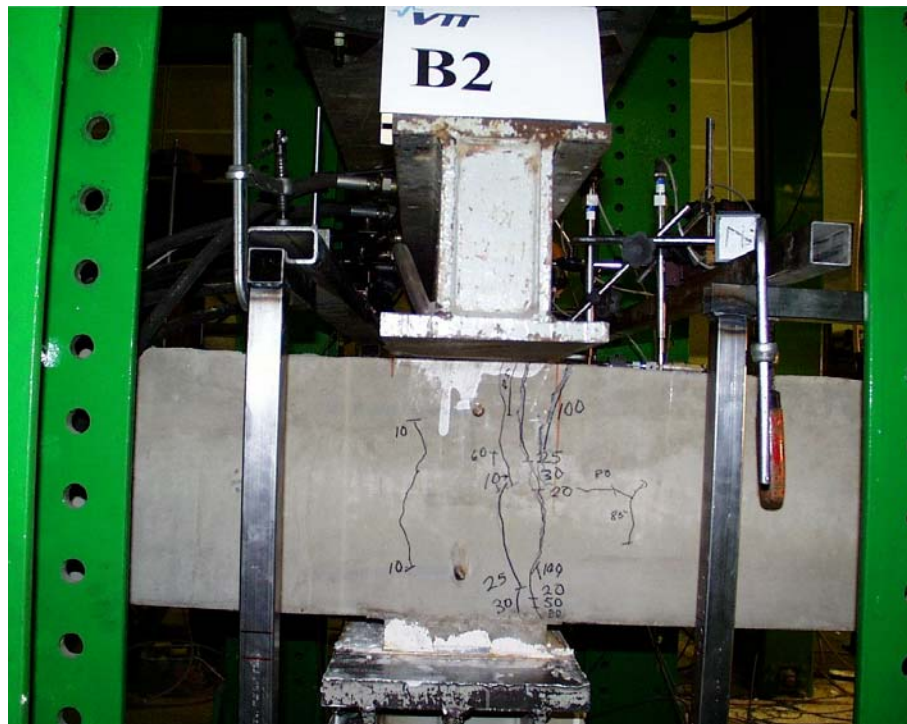
Fig. 26. B2, North edge. Cracks before failure.
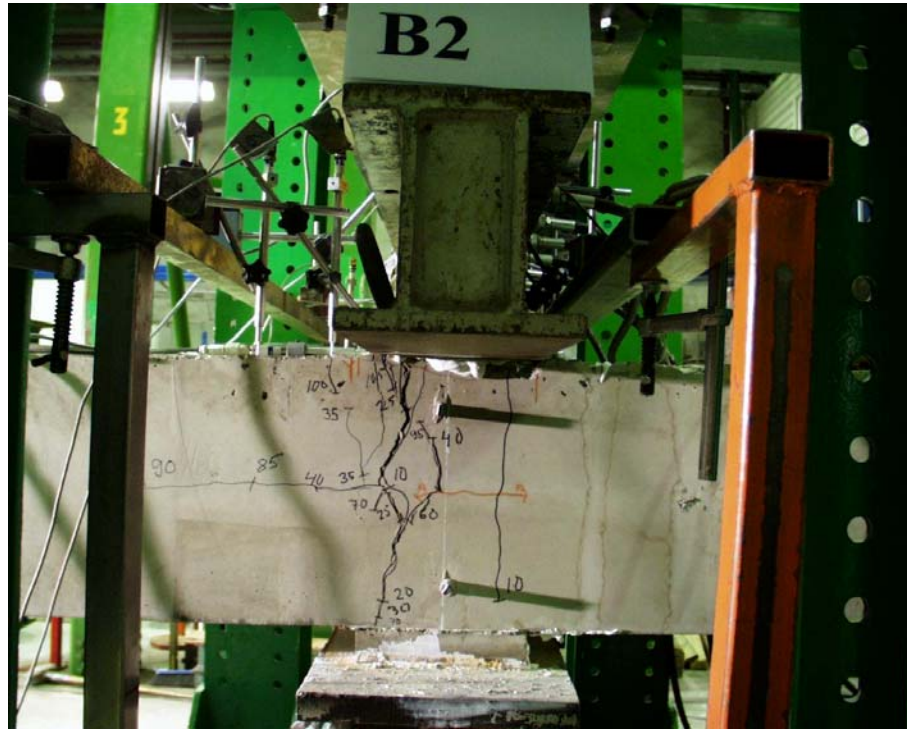
Fig. 27. B2, South edge. Cracks before failure.

Fig. 28. B2. North edge after failure.
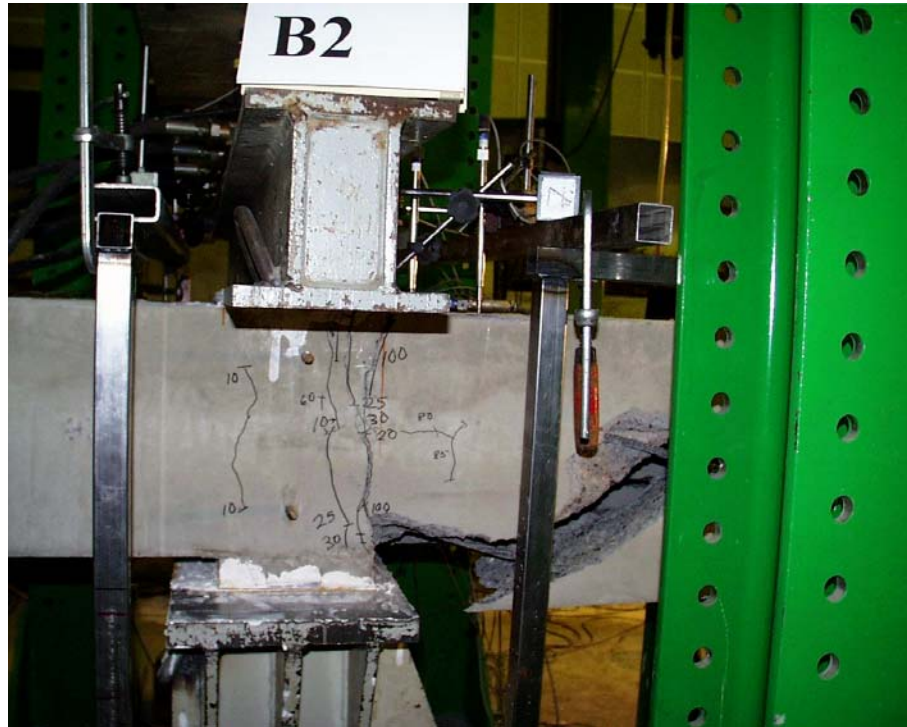
Fig. 29. B2. North edge after failure.

Fig. 30. B2. South edge after failure.

Fig. 31. B2. South edge after failure.

Fig. 32. B2. Flexural cracks.

Fig. 33. B2. Top surface after failure.

Fig. 34. B2. Flexural crack after flame cutting the strands and the tie bars.

Fig. 35. B2. Flexural crack after flame cutting the strands and the tie bars.
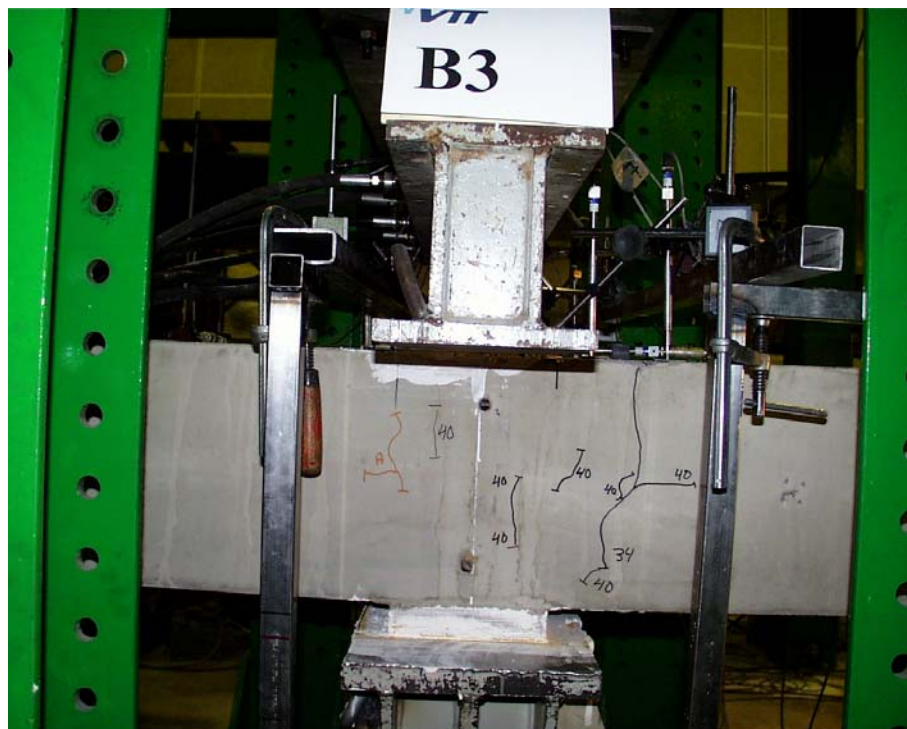
Fig. 36. B3, North edge. First cracks.

Fig. 37. B3, South edge. First cracks.
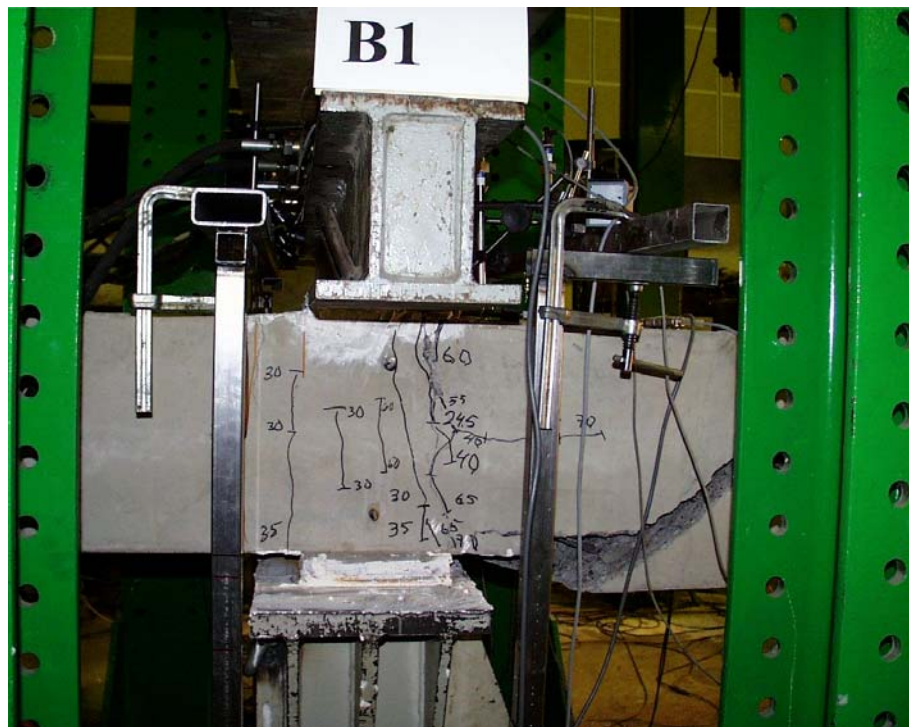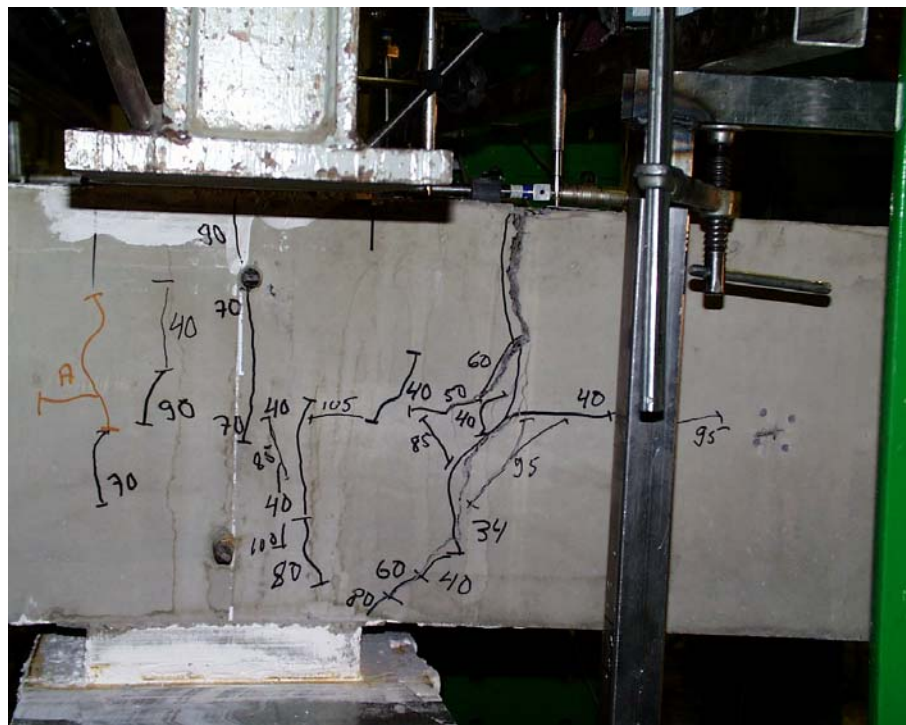

Fig. 38. B3, North edge. Cracks before failure.
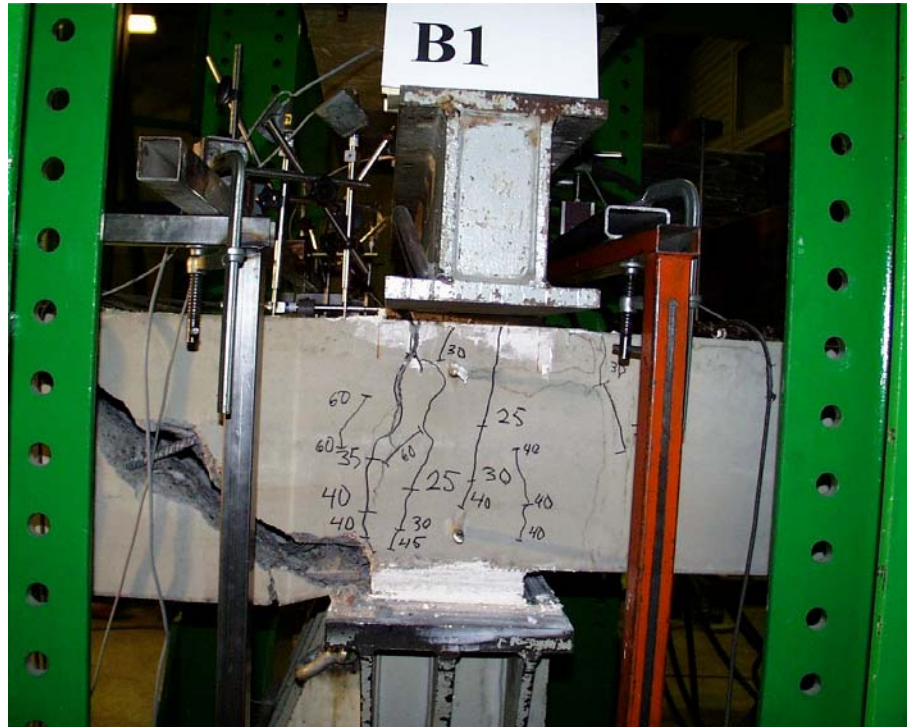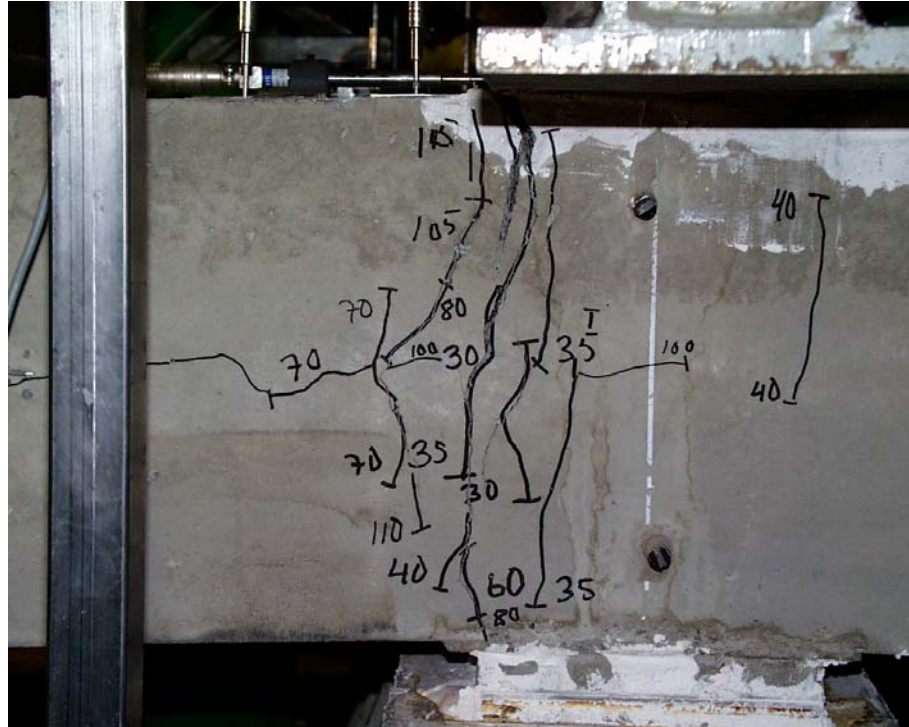
Fig. 39. B3, South edge. Cracks before failure.

Fig. 40. B3. North edge after failure.

Fig. 41. B3. North edge after failure.

Fig. 42. B3. South edge after failure.

Fig. 43. B3. South edge after failure.

Fig. 44. B3. Top surface after failure.
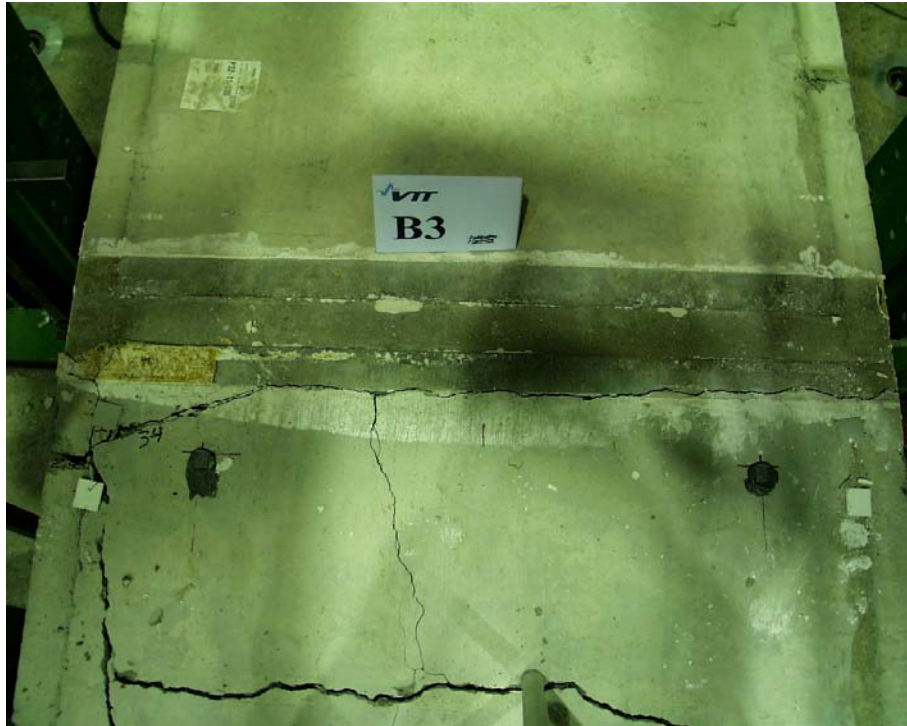
Fig. 45. B3. South edge after failure.

Fig. 46. B3. Shear crack after flame cutting the strands and tie bars.

Fig. 47. B3. Detail of shear crack.

Fig. 48. B3. Detail of flexural crack.

Fig. 49. B3. Detail of flexural crack.
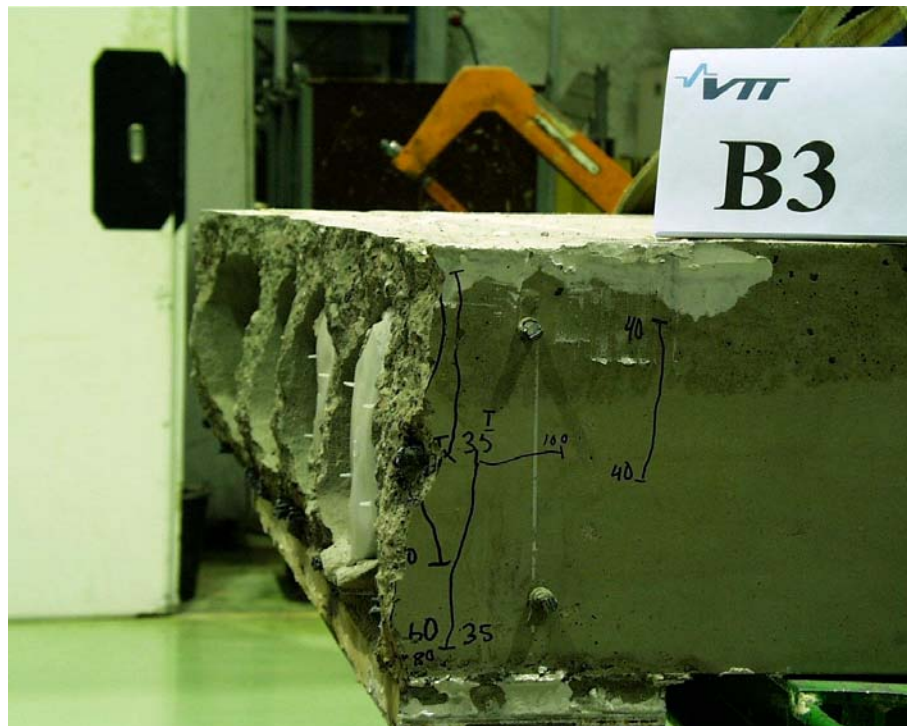
Fig. 50. B3. Side view on flexural crack.

PHOTOGRAPHS, NOTCHED SLABS

The numbers on the surface of the slabs refer to the actuator load. They tell the load which made the crack grew until the indicated position. The lines with capital A refer to cracks observed before loading.
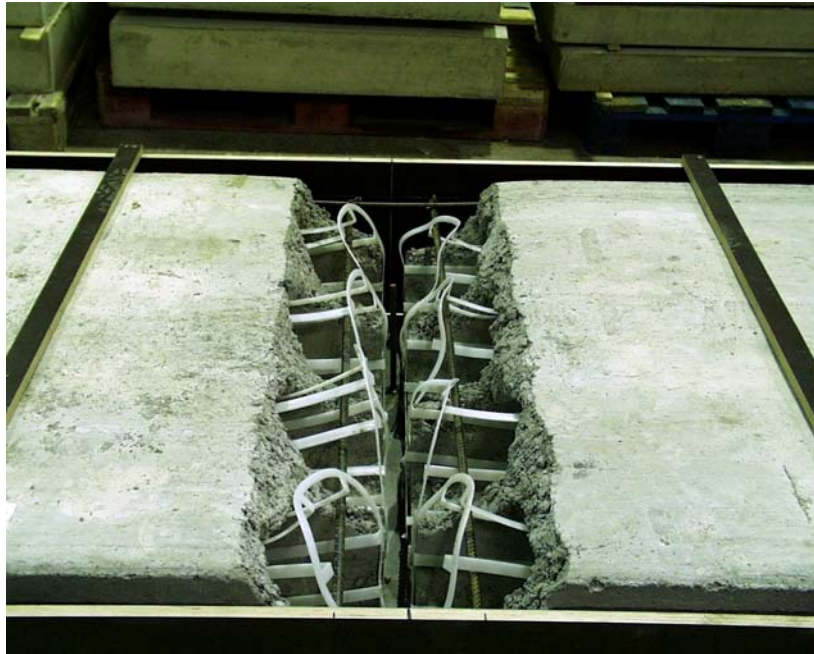
Fig. 1. N1. Joint before grouting.

Fig. 2. N1. Joint before grouting.

Fig. 3. N1. Joint after grouting of lower part of joint.

Fig. 4. N1. Preparations for grouting of upper part of joint.

Fig. 5. N1. Grout coming from the opposite side of the wall element.

Fig. 6. N1. Grouting completed.
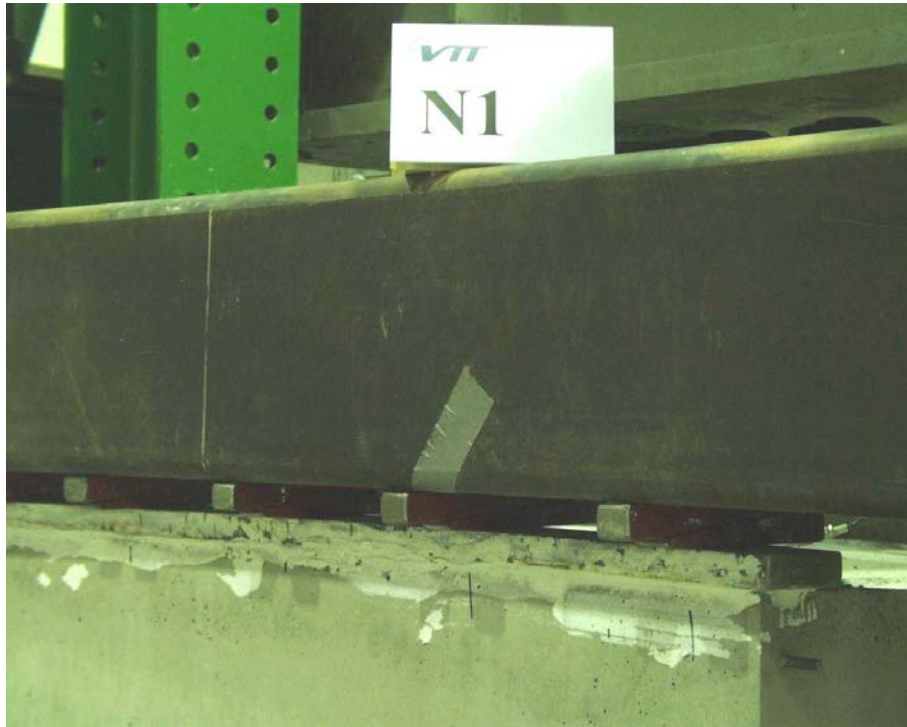
*Fig. 7. N1. Wedges to prevent the uplift of the short slab element.*
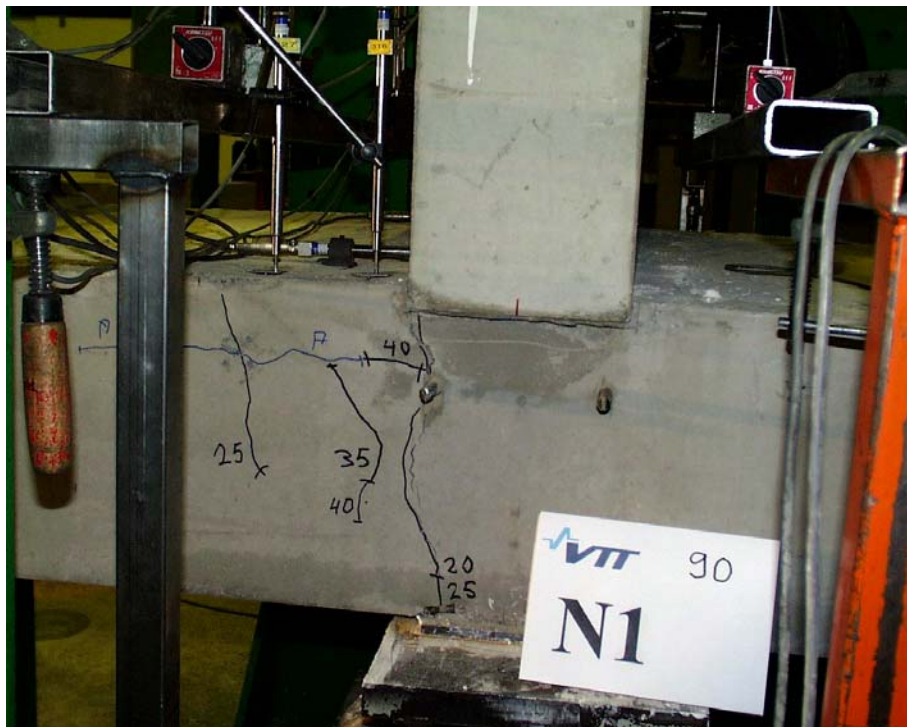
Fig. 8. N1, South edge. First cracks.

Fig. 9. N1, North edge. First cracks.

Fig. 10. N1, North edge. Cracks before failure.
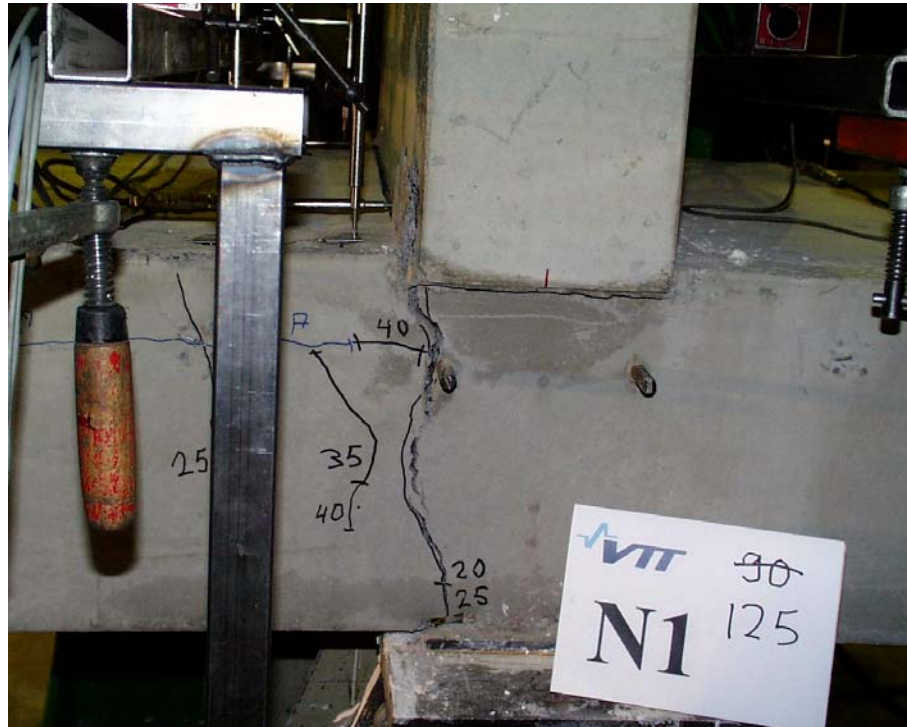
Fig. 11. N1, North edge. Cracks before failure.

Fig. 12. N1, South edge. Flexural crack before failure.

Fig. 13. N1. North edge after failure.

Fig. 14. N1. North edge after failure.

Fig. 15. N1. South edge after failure.
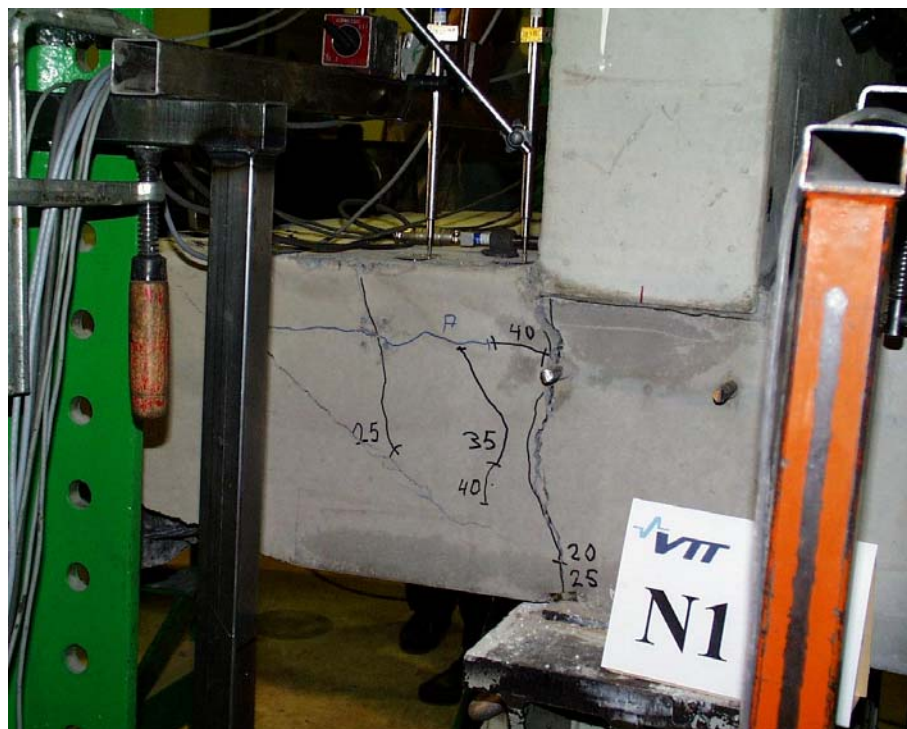
Fig. 16. N1. South edge after failure.

Fig. 17. N1. Soffit after failure.

Fig. 18. N1. Top surface after failure.

Fig. 19. N1. North edge after failure and removal of a loose piece of cast-in-situ concrete.

Fig. 20. N1. North edge after removing a loose corner of slab.

Fig. 21. N1. Joint after removing main part of slab element

Fig. 22. N1. Vertical crack.

Fig. 23. N1. Vertical crack.

Fig. 24. N2, North edge. Cracks before failure.

Fig. 25. N2, South edge. Cracks before failure.

Fig. 26. N2, North edge. Failure crack and flexural cracks.

Fig. 27. N2, North edge. Failure crack and flexural cracks.

Fig. 28. N2, North edge. Cracks next to the joint after failure.

Fig. 29. N2, South edge. Failure crack.

Fig. 30. N2, South edge. Cracks next to the joint after failure.

Fig. 31. N2. Soffit after failure.

Fig. 32. N2. Soffit after failure.

Fig. 33. N2. Flexural crack.

Fig. 34. N2. Flexural crack.

Fig. 35. N2. Flexural crack.

Fig. 36. N2. Flexural crack.

Fig. 37. N2. Soffit and cracked end of slab.
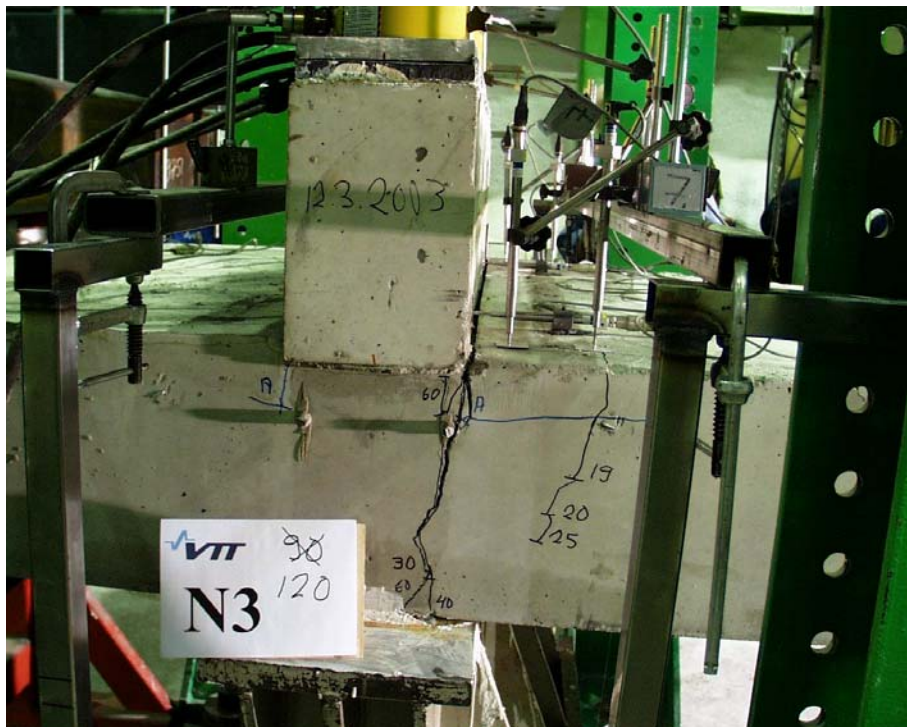
Fig. 38. N3, North edge. Cracks before failure.
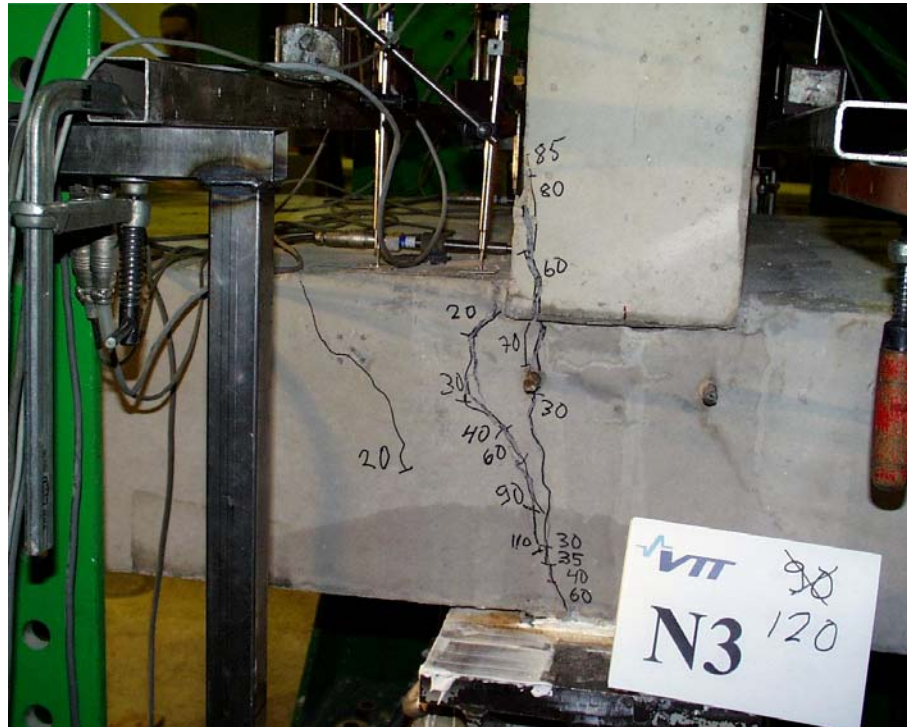
Fig. 39. N3, North edge. Cracks before failure.

Fig. 40. N3, North edge. Failure crack and flexural cracks.

Fig. 41. N3, North edge. Failure crack and flexural cracks.

Fig. 42.   N3, South edge. Failure crack and flexural cracks.

Fig. 43. N3, South edge. Failure crack.

Fig. 44. N3. Top surface after failure.
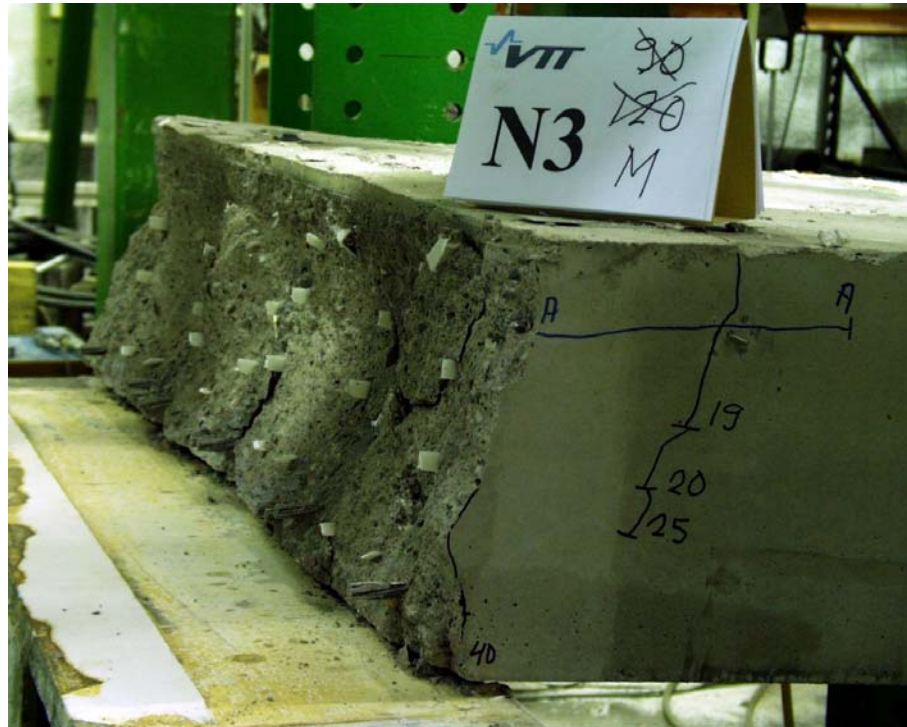
Fig. 45. N3. Flexural crack.

Fig. 46. N3. Flexural crack.
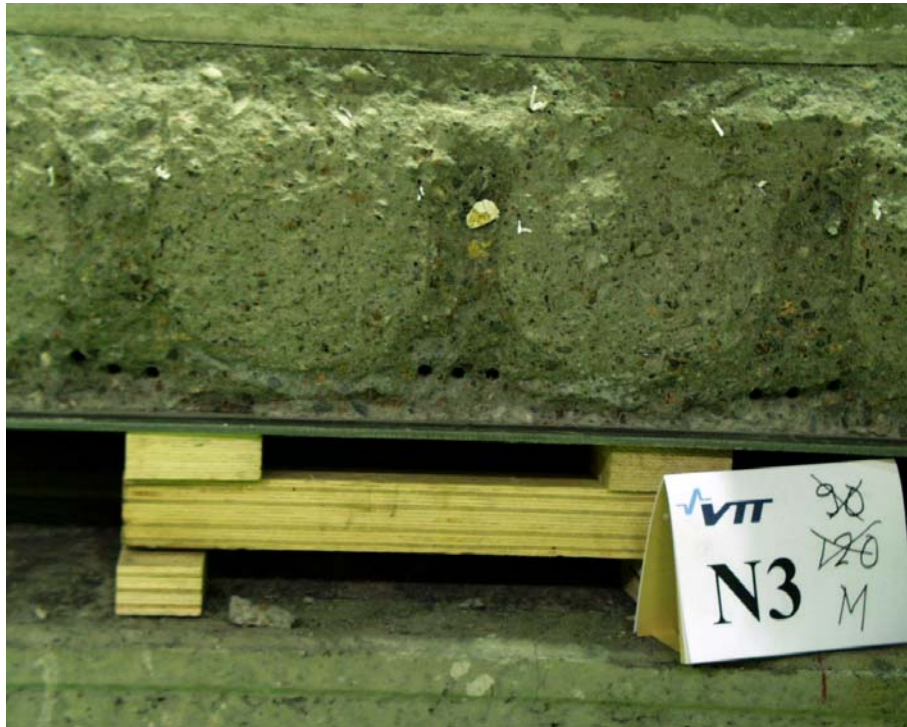
Fig. 47. N3. Detail of flexural crack.

Fig. 48. N3. Soffit.

PHOTOGRAPHS, REFERENCE TESTS

Fig. 1. VB2, North edge after failure.

Fig. 2. VB2, South edge after failure.

Fig. 3. VN2. North edge after failure.

Fig. 4. VN2. South edge after failure.

NOMINAL AND MEASURED PROPERTIES OF SLAB ELEMENTS

Nominal cross-section of slabs and size of end notches in tests N1, N2 and N3
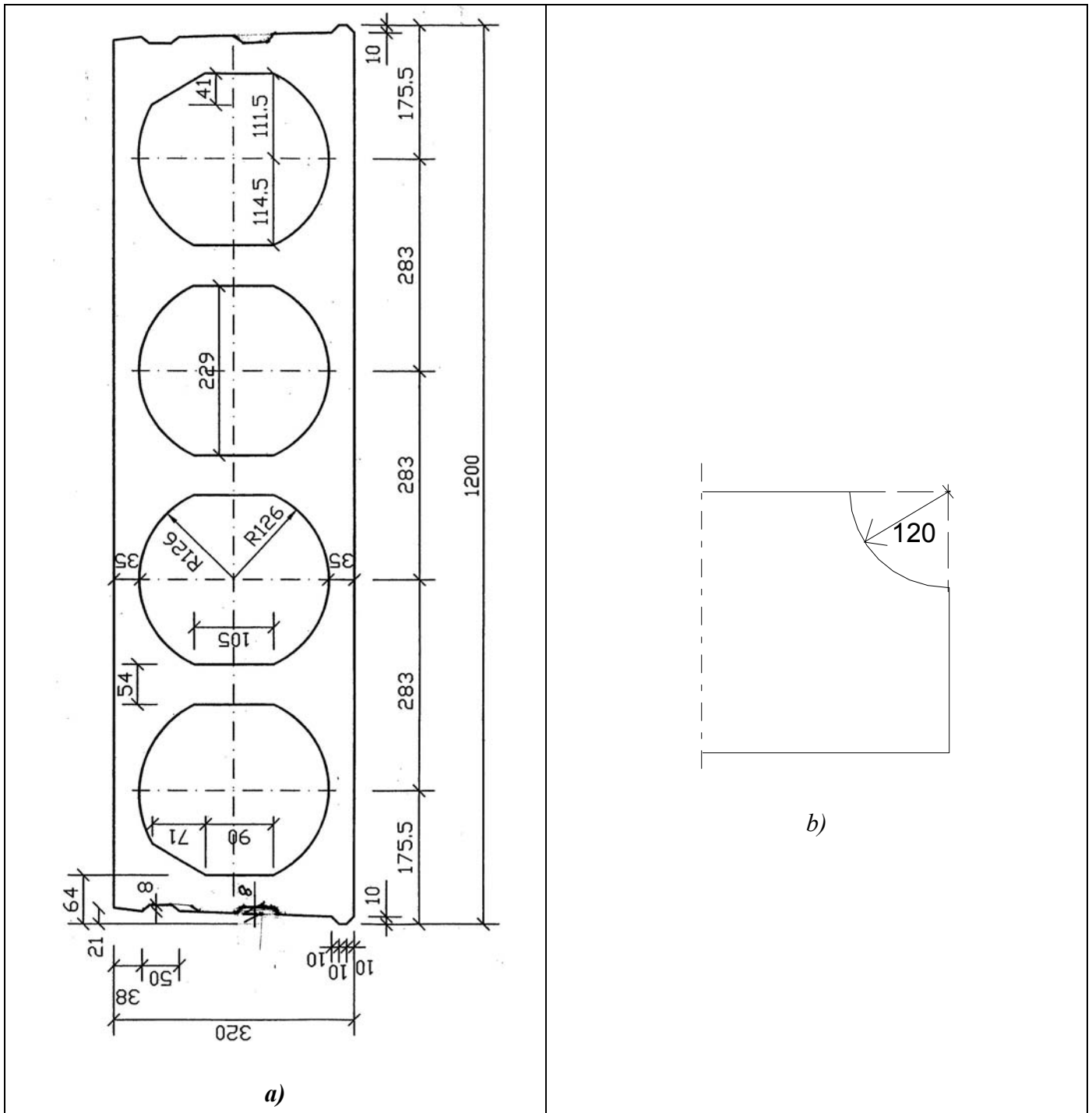
***Fig. 1** . a) Nominal cross-section. b) Nominal size of notches in tests N1, N2 and N3.*

MEASURED MATERIAL PROPERTIES OF CONCRETE AND STEEL

1 Concrete

The test cubes were kept in the same place and in the same conditions as the concrete elements or tests specimens. The cores drilled from the slabs were not allowed to dry before testing.

Table D1. Grouting, phase I (B1). Strength and density of 150 mm cubes cast on 2nd of April and tested on 14th of April 2003.

Specimen	Strength MPa	Density kg/m^3
1B	46.0	2280
2B	44.5	2250
3B	45.0	2270
Mean x	45.2	2267

Table 2. Grouting, phase I (B3). Strength and density of 150 mm cubes cast on 2nd of April and tested on 17th of April 2003.

Specimen	Strength MPa	Density kg/m^3
1N	45.5	2270
2N	45.5	2270
3N	43.5	2270
Mean x	44.8	2270

Table 3. B2, hollow core slab. Strength and density of 50 mm cores tested on 17th of April 2003. The slabs were cast on 7th of March 2003.

Specimen	Strength MPa	Density kg/m^3
B21	67.0	2400
B22	64.0	2430
B23	65.5	2380
B24	60.5	2450
B25	66.5	2430
B26	62.0	2430
Mean x	64.3	2420
Standard deviation s	2.6	
Characteristic strength $f_{ck,C50} = x - 1.65s$	60.0	

Table 4. Grouting, phase II (N2). Strength and density of 150 mm cubes cast on 4th of April and tested on 6th of May 2003.

Specimen	Strength MPa	Density kg/m^3
4N	42.0	2240
5N	42.5	2250
6N	42.0	2240
Mean x	42.2	2242

Table 5. Grouting, phase I. Strength and density of 150 mm cubes cast on 2nd of April and tested on 8th of May 2003.

Specimen	Strength MPa	Density kg/m^3
7B	49.0	2270
8B	52.0	2280
9B	50.5	2250
Mean x	50.5	2267

Table 6. Grouting, phase II (N1). Strength and density of 150 mm cubes cast on 4th of April and tested on 5th of May 2003.

Specimen	Strength MPa	Density kg/m^3
1N	42.5	2270
2N	41.5	2260
3N	43.0	2280
Mean x	42.3	2270

Table 7. Grouting, phase II (N2). Strength and density of 150 mm cubes cast on 4th of April and tested on 6th of May 2003.

Specimen	Strength MPa	Density kg/m^3
4N	42.0	2240
5N	42.5	2250
6N	42.0	2240
Mean x	42.2	2242

Table 8. Grouting, phase II (N3). Strength and density of 150 mm cubes cast on 4th of April and tested on 8th of May 2003.

Specimen	Strength MPa	Density kg/m^3
7N	44.0	2270
8N	42.0	2240
9N	43.5	2250
Mean *x*	43.2	2253

Table 9. N1, wall element RTP1. Strength and density of 150 mm cubes cast on 10th of March and tested on 5th of May 2003.

Specimen	Strength MPa	Density kg/m^3
RT1	41.5	2270
RT2	42.0	2280
Mean	41.8	2275

Table D10. N2, wall element RTP2. Strength and density of 150 mm cubes cast on 11th of March and tested on 6th of May 2003.

Specimen	Strength MPa	Density kg/m^3
RT3	39.0	2240
RT4	38.0	2230
Mean	38.5	2235

Table D11. N3, wall element RTP3. Strength and density of 150 mm cubes cast on 12th of March and tested on 8th of May 2003.

Specimen	Strength MPa	Density kg/m^3
RT5	36.0	2230
RT6	36.5	2250
Mean	36.3	2240

Table D12. N2, hollow core slab. Strength and density of 50 mm cores tested on 8th of May 2003. The slabs were cast on 7th of March 2003.

Specimen	Strength MPa	Density kg/m^3
N21	66.5	2390
N22	68.0	2420
N23	67.5	2420
N24	68.0	2420
N25	70.0	2430
N26	69.0	2440
Mean x	64.8	2420
Standard deviation s	1.2	
Characteristic strength $f_{ck,C50} = x - 1.65s$	66.2	

2 Reinforcing steel in tie reinforcement

Table D1. Tests on steel according to standard SFS-EN 10002-1.Diameter of steel bar d, upper yield strength R_{eH}, tensile strength R_m and elongation after fracture A_{10}.

	Steel grade	d mm	R_{eH} MPa	R_m MPa	A_{10} %
N1, N2, N3	A500HW	8	525	638	18.3
B1, B2, B3	A500HW	12	536	662	17.3

Measured length, mass and cross-sectional geometry of slabs

B1

Strands:11 ϕ 12,5   Length: 7995 mm
Prestress: 1000 MPa   Mass: 3870 kg

END 1 /EDGE 1   END 1 / EDGE 2

END 2 / EDGE 1   END 2 / EDGE 2

Fig. 2. B1.

B2

Strands: 11 φ 12,5   Length: 7995 mm
Prestress: 1000 MPa   Mass: 3880 kg

END 1 / EDGE 1   END 1 / EDGE 2

END 2 / EDGE 1   END 2 / EDGE 2
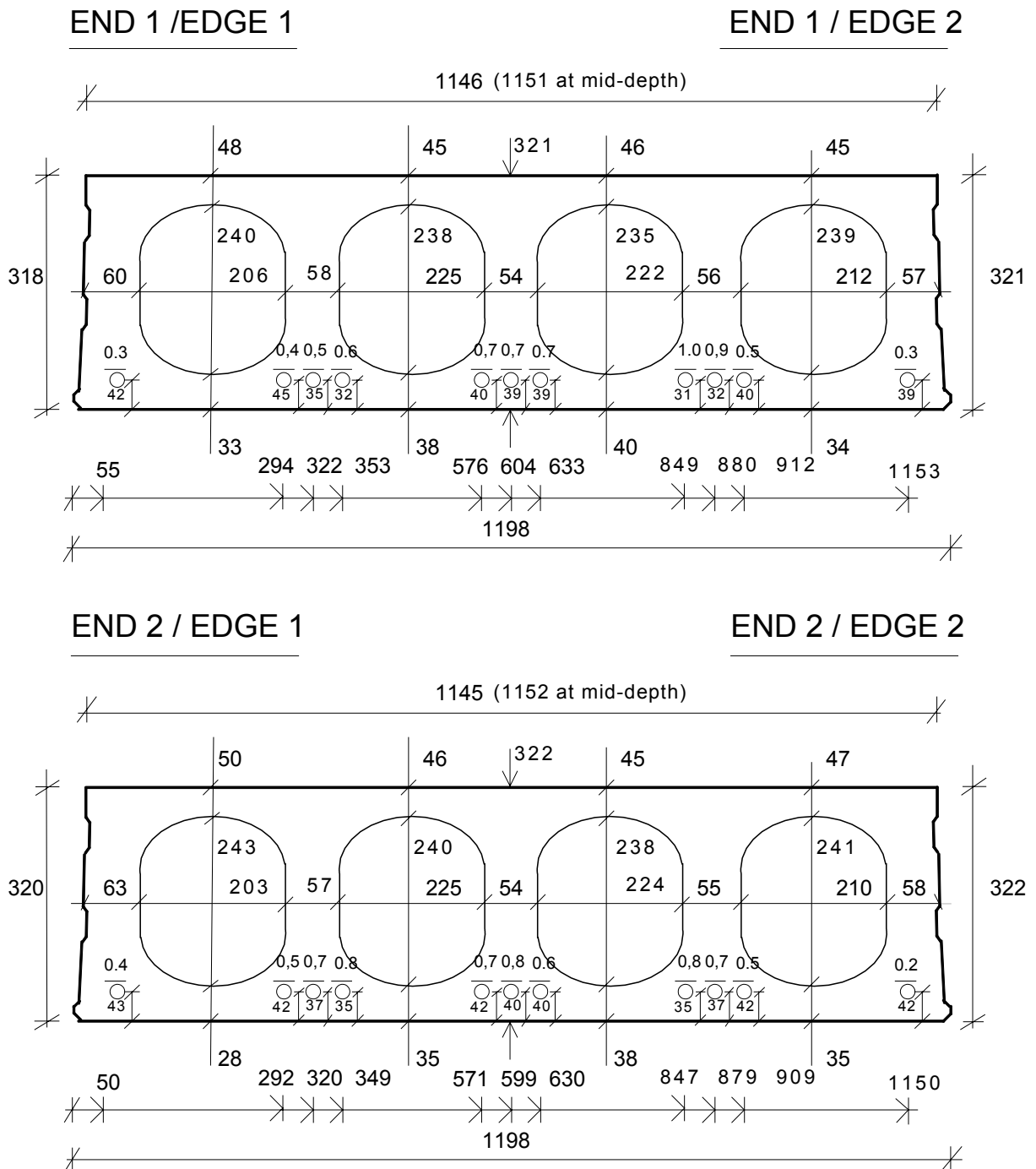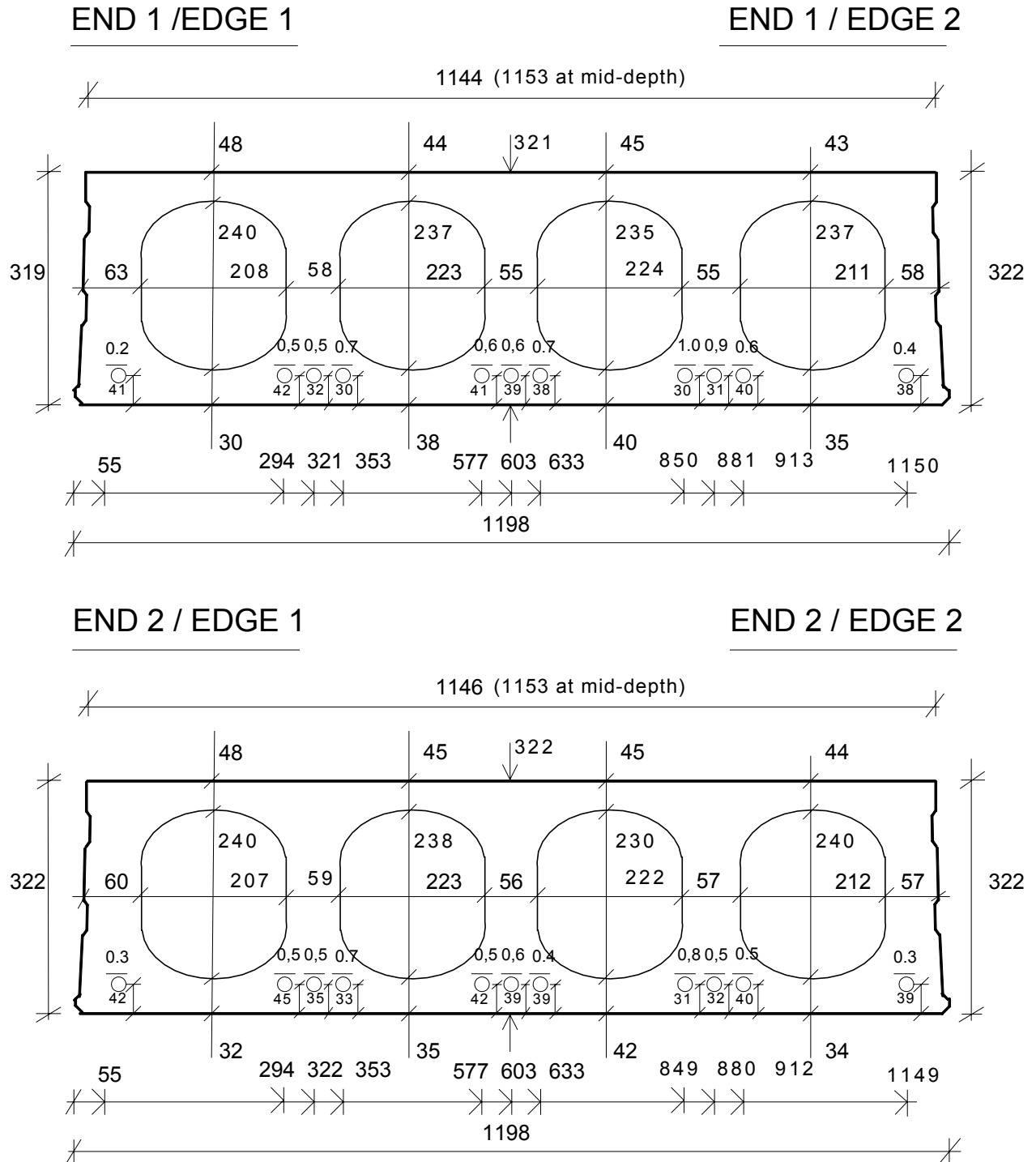
Fig. 3. B2.

B3

Strands: 11 ϕ 12,5
Prestress: 1000 MPa

Length: 7997 mm
Mass: 3890 kg

END 1 /EDGE 1   END 1 / EDGE 2

END 2 / EDGE 1   END 2 / EDGE 2
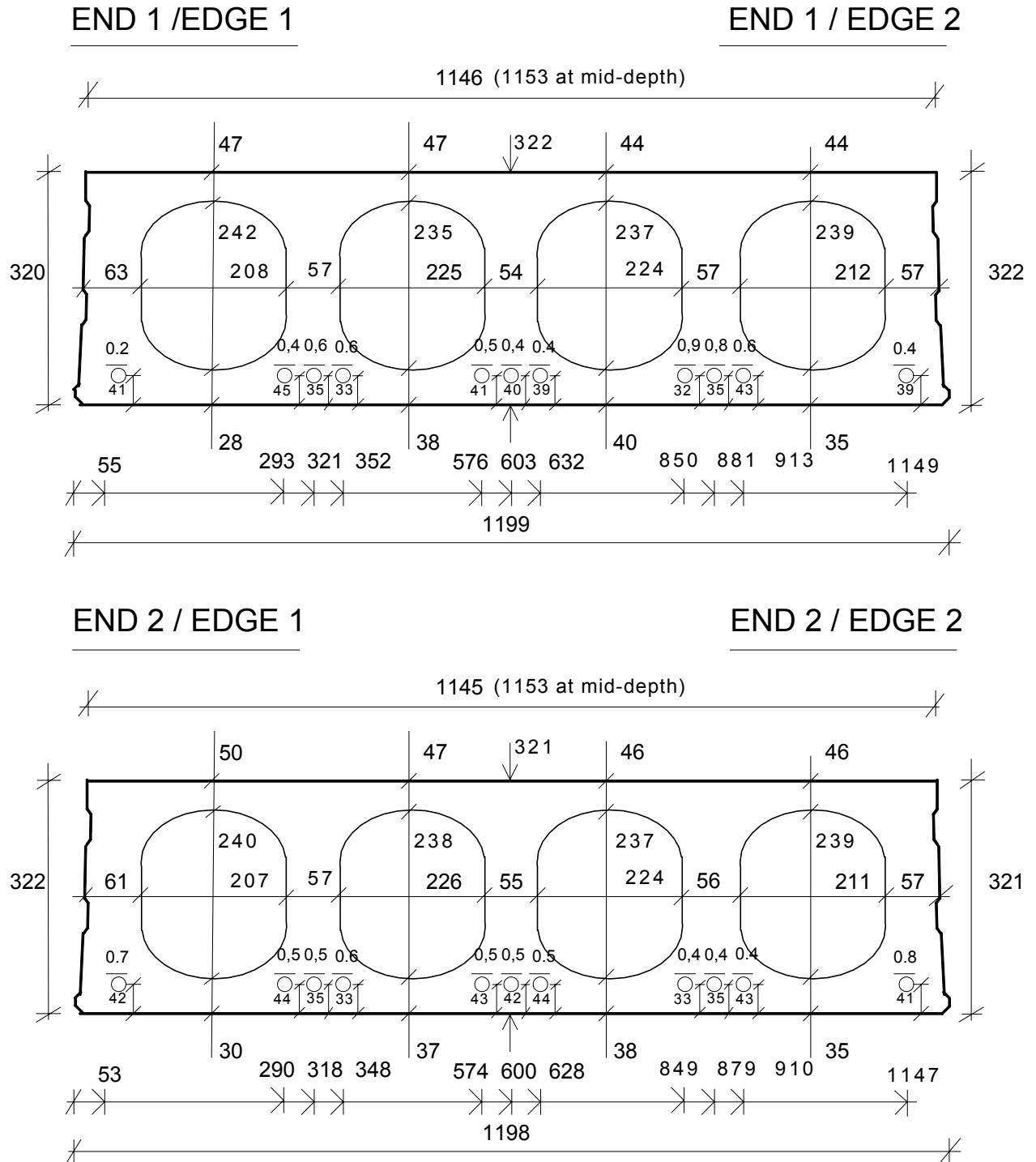
Fig. 4. B3.

N1

Strands: 11 ϕ 12,5   Length: 7984 mm
Prestress: 1000 MPa   Mass: 3860 kg
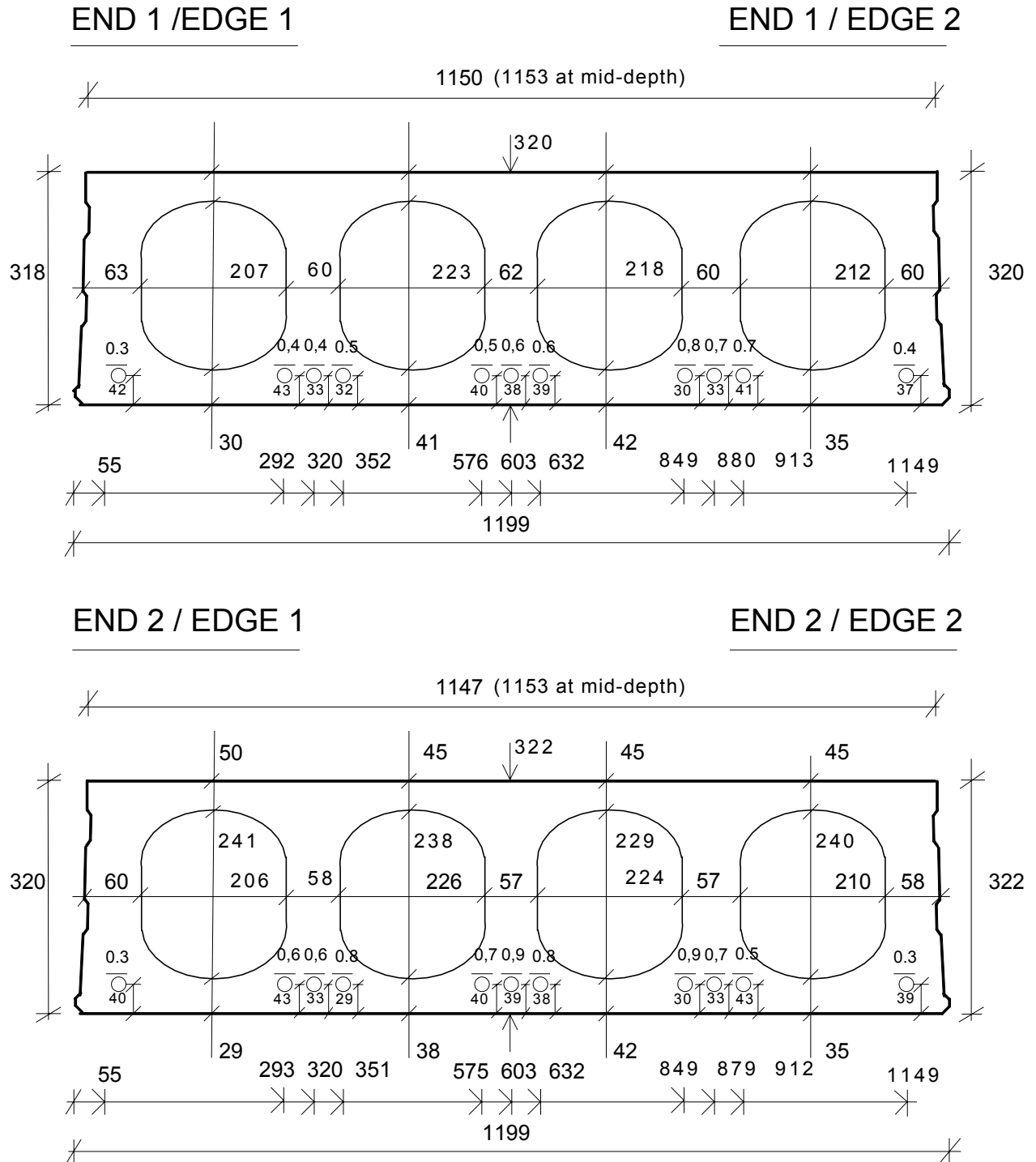
Fig. 5. N1.

N2

Strands: 11 φ 12,5
Prestress: 1000 MPa

Length: 7991 mm
Mass: 3830 kg

END 1 / EDGE 1   END 1 / EDGE 2

END 2 / EDGE 1   END 2 / EDGE 2
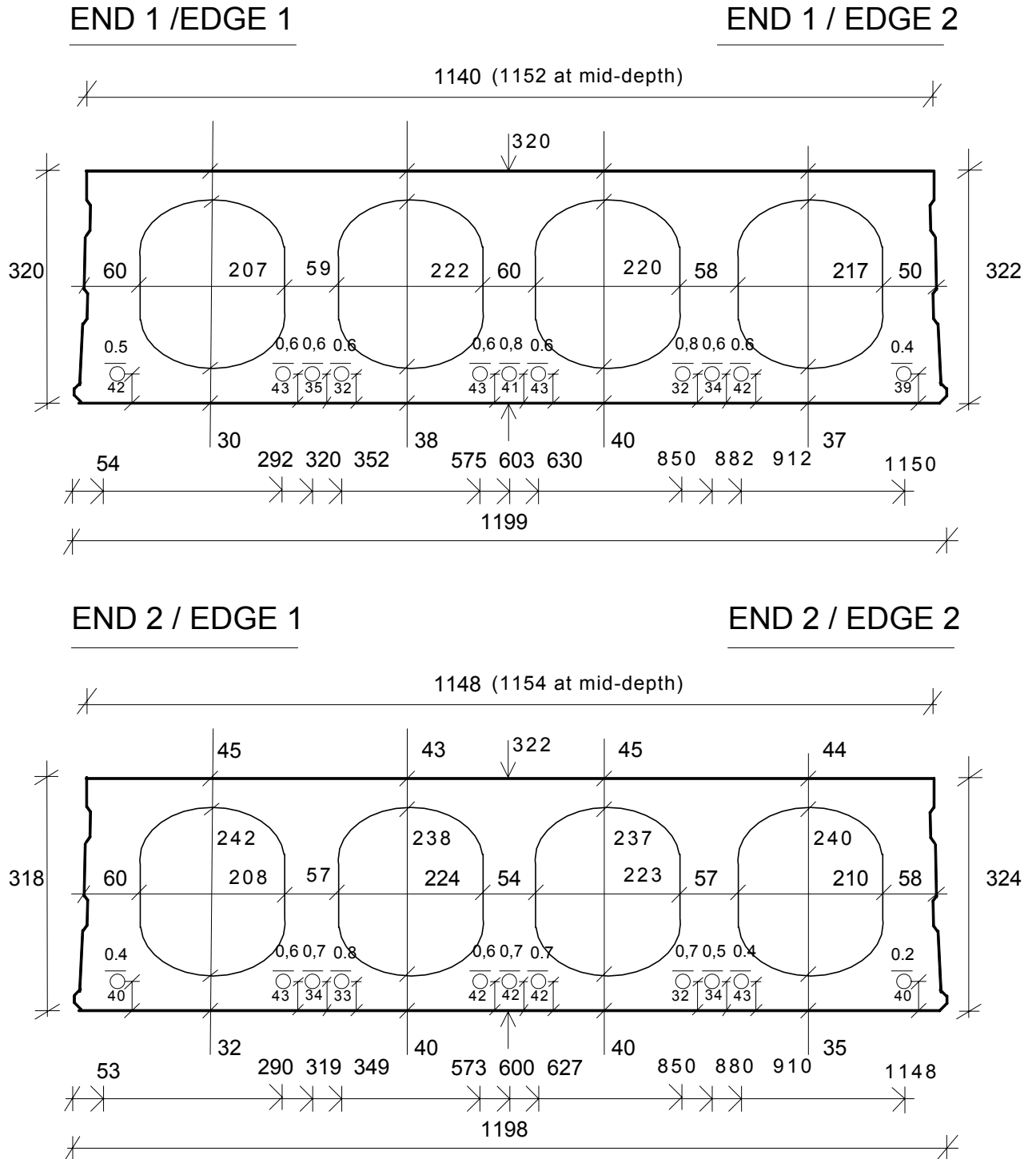
Fig. 6. N2.

N3

Strands: 11 φ 12,5
Prestress: 1000 MPa

Length: 8004 mm
Mass: 3900 kg

END 1 /EDGE 1

END 1 / EDGE 2
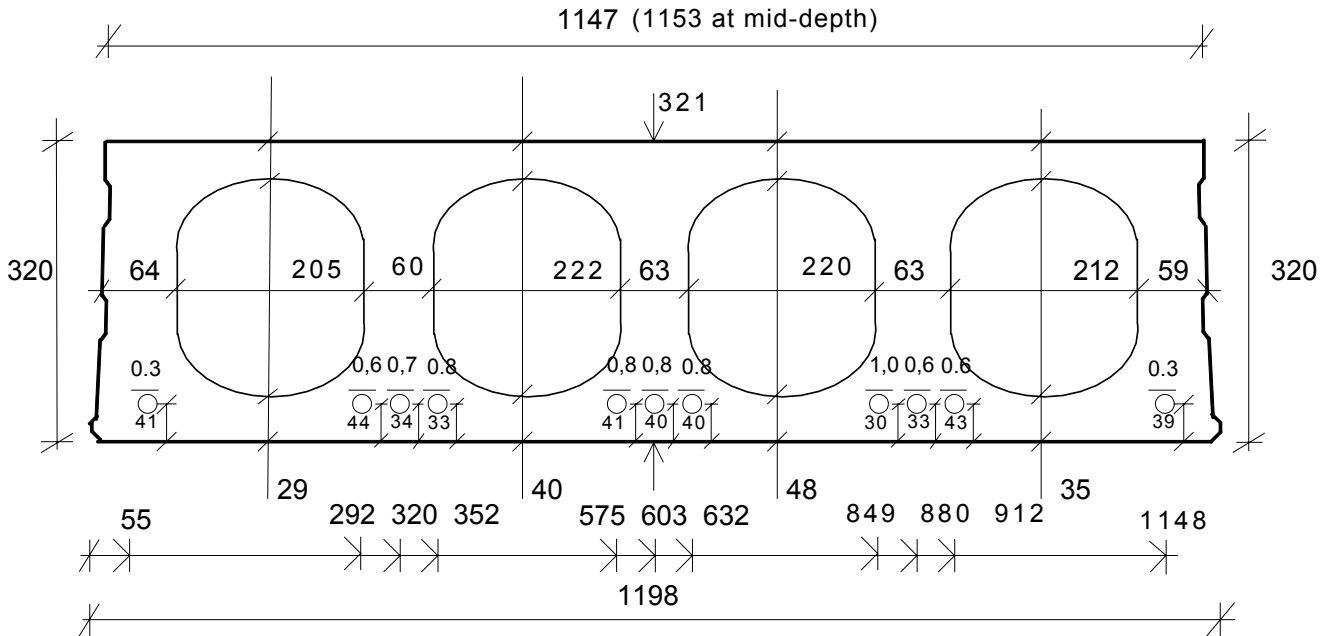
END 2 / EDGE 1

END 2 / EDGE 2

Fig. 7. N3.

MEASURED MATERIAL PROPERTIES OF CONCRETE AND STEEL

1 Concrete

The test cubes were kept in the same place and in the same conditions as the concrete elements or tests specimens. The cores drilled from the slabs were not allowed to dry before testing.

Table D1. Grouting, phase I (B1). Strength and density of 150 mm cubes cast on 2nd of April and tested on 14th of April 2003.

Specimen	Strength MPa	Density kg/m^3
1B	46.0	2280
2B	44.5	2250
3B	45.0	2270
Mean x	45.2	2267

Table 2. Grouting, phase I (B3). Strength and density of 150 mm cubes cast on 2nd of April and tested on 17th of April 2003.

Specimen	Strength MPa	Density kg/m^3
1N	45.5	2270
2N	45.5	2270
3N	43.5	2270
Mean x	44.8	2270

Table 3. B2, hollow core slab. Strength and density of 50 mm cores tested on 17th of April 2003. The slabs were cast on 7th of March 2003.

Specimen	Strength MPa	Density kg/m^3
B21	67.0	2400
B22	64.0	2430
B23	65.5	2380
B24	60.5	2450
B25	66.5	2430
B26	62.0	2430
Mean x	64.3	2420
Standard deviation s	2.6	
Characteristic strength $f_{ck,C50} = x - 1.65s$	60.0	

Table 4. Grouting, phase II (N2). Strength and density of 150 mm cubes cast on 4th of April and tested on 6th of May 2003.

Specimen	Strength MPa	Density kg/m^3
4N	42.0	2240
5N	42.5	2250
6N	42.0	2240
Mean x	42.2	2242

Table 5. Grouting, phase I. Strength and density of 150 mm cubes cast on 2nd of April and tested on 8th of May 2003.

Specimen	Strength MPa	Density kg/m^3
7B	49.0	2270
8B	52.0	2280
9B	50.5	2250
Mean x	50.5	2267

Table 6. Grouting, phase II (N1). Strength and density of 150 mm cubes cast on 4th of April and tested on 5th of May 2003.

Specimen	Strength MPa	Density kg/m^3
1N	42.5	2270
2N	41.5	2260
3N	43.0	2280
Mean x	42.3	2270

Table 7. Grouting, phase II (N2). Strength and density of 150 mm cubes cast on 4th of April and tested on 6th of May 2003.

Specimen	Strength MPa	Density kg/m^3
4N	42.0	2240
5N	42.5	2250
6N	42.0	2240
Mean x	42.2	2242

Table 8. Grouting, phase II (N3). Strength and density of 150 mm cubes cast on 4th of April and tested on 8th of May 2003.

Specimen	Strength MPa	Density kg/m³
7N	44.0	2270
8N	42.0	2240
9N	43.5	2250
Mean *x*	43.2	2253

Table 9. N1, wall element RTP1. Strength and density of 150 mm cubes cast on 10th of March and tested on 5th of May 2003.

Specimen	Strength MPa	Density kg/m³
RT1	41.5	2270
RT2	42.0	2280
Mean	41.8	2275

Table D10. N2, wall element RTP2. Strength and density of 150 mm cubes cast on 11th of March and tested on 6th of May 2003.

Specimen	Strength MPa	Density kg/m³
RT3	39.0	2240
RT4	38.0	2230
Mean	38.5	2235

Table D11. N3, wall element RTP3. Strength and density of 150 mm cubes cast on 12th of March and tested on 8th of May 2003.

Specimen	Strength MPa	Density kg/m³
RT5	36.0	2230
RT6	36.5	2250
Mean	36.3	2240

Table D12. N2, hollow core slab. Strength and density of 50 mm cores tested on 8th of May 2003. The slabs were cast on 7th of March 2003.

Specimen	Strength MPa	Density kg/m^3
N21	66.5	2390
N22	68.0	2420
N23	67.5	2420
N24	68.0	2420
N25	70.0	2430
N26	69.0	2440
Mean x	64.8	2420
Standard deviation s	1.2	
Characteristic strength $f_{ck,C50} = x - 1.65s$	66.2	

2 Reinforcing steel in tie reinforcement

Table D1. Tests on steel according to standard SFS-EN 10002-1.Diameter of steel bar d, upper yield strength R_{eH}, tensile strength R_m and elongation after fracture A_{10}.

	Steel grade	d mm	R_{eH} MPa	R_m MPa	A_{10} %
N1, N2, N3	A500HW	8	525	638	18.3
B1, B2, B3	A500HW	12	536	662	17.3

HORIZONTAL LOAD DUE TO NONVERTICAL LOADS

In test B1.I the actuators were vertical when the loading was started. In other tests the actuators were slightly inclined before loading as illustrated in Fig. 1. The aim was to stabilize the assembly of spreader beams.
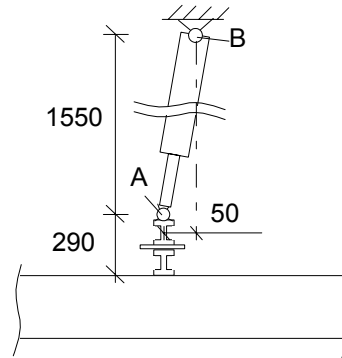

Fig. 1. Upper end of actuator 50 mm offset before loading in tests B1.II, B1.III, B2, B3, N1, N2 and N3.

The arrangements in tests B2, B3, N1, N2 and N3 are illustrated in Fig. 2. Since there are two forces pushing the slab to the left and only one to the right, there is a compressive horizontal force H in the slab between the joint and the first load $P_{2,1}$. H is reduced by the deflection of the slab, because the slab moves to the right and because the lower end of two actuators of three act on a point (point A in Fig.2) which moves to the right due to the curvature of the slab.
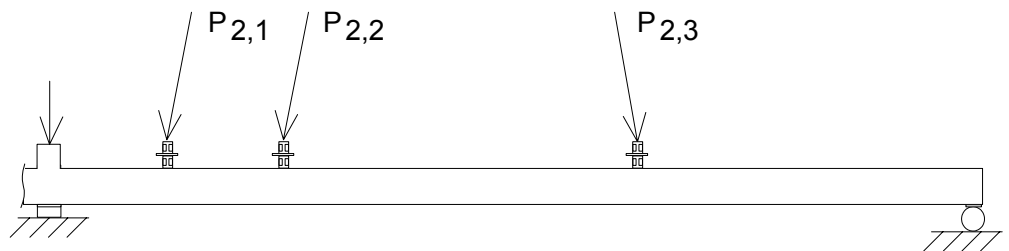
Fig. 2. Inclined loads in tests B2, B3, N1, N2 and N3.

In the following, *left* means towards the jointed slab end and *right* to the opposiste direction. The horizontal force H in the slab between the jointed slab end and the nearest load is estimated under the following assumptions
- The centroidal axis of the slab is at mid-depth of the cross-section
- The slope of the slab end is the measured crack width w divided by (320 +20) mm, i. e. $v'(0) = w/340$ mm
- The motion of the centroidal axisof the slab, u_0, is calculated from $u_0 = (160/340)w$
- The relative slope v'_1 of the slab is calculated assuming constant stiffness for the slab and three equal vertical loads in the same position as in tests B2 – N3

- The absolute slope $v'(x)$ at a distance x from the joint is obtained from $v'(x) = v'(0)v'_1(x)/v'_1(0)$
- The displacement of point A to the right from its original position is $u = u_0 + (450\ mm)v'(x)$.

The relative slope is shown in Fig. 3 and the calculated horizontal forces at failure in Table 1. The sum of the horizontal forces affecting the joint is less than 1.0 kN. Such a compressive force is 0.8% and 1.9% of the nominal yield force of tie reinforcement in tests B1 - B3 and N1 - N3, respectively. It has a negligible effect on the observed shear resistance.

In test B1.III the horizontal force H was of the same order as in tests B2, B3, N1, N2 and N3. In tests B1.II there were two actuators inclined to the left and two inclined to the right. The resulting horizontal force on the joint must have been negligible or tension which is on the conservative side.
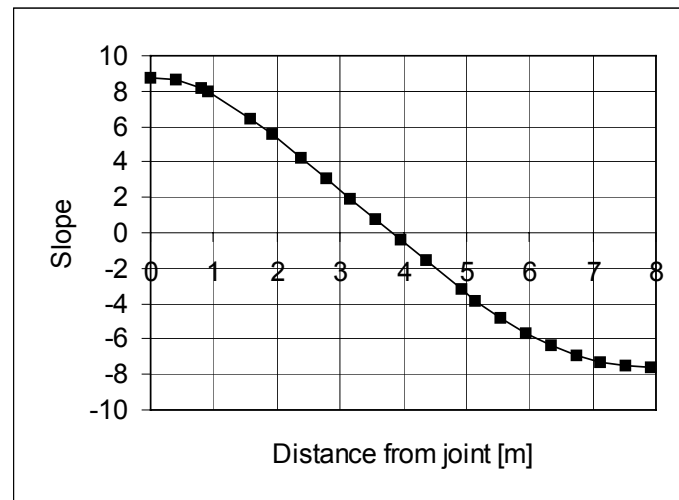

Fig. 3. Calculated relative slope of slab in tests B2, B3, N1, N2 and N3.

Table 1. Failure load ($P_{2,u}$), crack width (w), horizontal motion of centroidal axis of slab(u_0), horizontal motion due to curvature of slab end (u(0)), and below loads $P_{2,1}$ ... $P_{2,3}$ (u_1,u_2,u_3), horizontal forces (H_1 ... H_3) due to nonverticality of loads $P_{2,1}$ ... $P_{2,3}$, respectively, and sum of horizontal forces (H).

	$P_{2,u}$ kN	w mm	u_0 mm	u(0) mm	u_1 mm	u_2 mm	u_3 mm	H_1 kN	H_2 kN	H_3 kN	H_{1+2+3}[1] kN
B2	140.2	13.2	6.2	17.5	22.0	17.3	-0.07	-2.53	-2.96	4.53	-0.96
B3	145.1	14.0	6.6	18.5	23.3	18.3	-0.08	-2.50	-2.97	4.69	-0.77
N1	135.2	13.1	6.2	17.3	21.8	17.1	-0.07	-2.46	-2.87	4.37	-0.96
N2	138.1	14.0	6.6	18.5	23.3	18.3	-0.08	-2.38	-2.82	4.46	-0.74
N3	137.3	13.4	6.3	17.7	22.3	17.5	-0.08	-2.45	-2.88	4.44	-0.89

[1] *Negative value means compression*

TESTING OF INDENTED PRESTRESSING STRAND D 12,5 MM, LEFT-HAND LAY.

Date of testing: 5th of November, 2003.

Table 1.   Dimensions and masses (EN ISO 15630-3).

Test piece	Diameter D_0 mm	Diameter of wires		Mass m_l kg/m	Cross-sectional area S_m mm^2	Lay length mm
		centre wire d_1 mm	outer wires d_2-d_7 mm			
D 12,5	12,50	4,21	4,10	0,734	93,5	183

1) $S_m = m_l/\rho$, $\rho = 0{,}00785$ g/mm^3.

Table 2.   Dimensions of indentation (EN ISO 15630-3).

Test piece	Wire 1)	Side	Indentation					
			Spacing c mm	Gap between indentations b mm		Depth a_{max} mm		
D 12,5	wire 1	1	6,0	3,0	3,0	0,02	0,01	0,03
		2	6,0	2,0	2,0	0,03	0,02	0,03
		3	6,0	3,0	3,0	0,06	0,03	0,07
	wire 2	1	6,0	3,0	3,0	0,02	0,02	0,02
		2	6,0	2,3	2,2	0,03	0,02	0,03
		3	6,1	3,0	2,9	0,05	0,05	0,05
Average			6,0	2,7		0,03		

1) Two of the six outer wires were randomly selected for the indentation measurements. The wires had indentations on three sides around the circumference.